NUMERICAL ANALYSIS AND MODELLING OF GEOGRID REINFORCED ROAD EMBANKMENT USING FINITE ELEMENT BASED SOFTWARE: IN THE CASE OF DUKEM

By

Abdulselam Usman Tufa

A Thesis Submitted to
The department of Civil Engineering,
School of Civil Engineering and Architecture

Presented in Partial Fulfillment of the Requirement for the Degree of Master's in Civil Engineering (Specialization in Geotechnical Engineering)

Office of Graduate Studies
Adama Science and Technology University

Adama, Ethiopia

FEBRUARY, 2021

NUMERICAL ANALYSIS AND MODELLING OF GEOGRID REINFORCED ROAD EMBANKMENT USING FINITE ELEMENT BASED SOFTWARE: IN THE CASE OF DUKEM

By: Abdulselam Usman

Advisor: Argaw Asha (PhD)

A Thesis Submitted to

The department of Civil Engineering

School of Civil Engineering and Architecture

Presented in Partial Fulfillment of the Requirement for the Degree of Master's in Civil Engineering (Specialization in Geotechnical Engineering)

Office of Graduate Studies

Adama Science and Technology University

Adama, Ethiopia

FEBRUARY, 2021

Approval of Board of Examiners

We, the undersigned, members of the Board of Examiners of the final open defense by Abdulselam Usman have read and evaluated his thesis entitled "Numerical Analysis and Modelling of Geogrid Reinforced Road Embankment using Finite Element based Software: In case Dukem." and examined the candidate. This is, therefore, to certify that the thesis has been accepted in partial fulfillment of the requirement of the Degree of Masters in Civil Engineering (specialization in Geotechnical Engineering).

Name	**Signature**	**Date**
Abdulselam Usman Name of student	________________	____________________
Argaw Asha (PhD) Advisor	________________	____________________
____________________ External examiner	________________	____________________
____________________ Internal examiner	________________	____________________
____________________ Chair person	________________	____________________
____________________ Head of department	________________	____________________
____________________ School dean	________________	____________________
____________________ Post graduate dean	________________	____________________

Declaration

I hereby declare that this MSc Thesis is my original work and has not been presented for a degree in any other university, and all sources of material used for this thesis have been duly acknowledged.

Name: Abdulselam Usman

Signature: ___________

This MSc Thesis has been submitted for examination with my approval as thesis advisor.

Name: Argaw Asha (PhD)

Signature: ___________

Date of submission: ………..

ACKNOWLEDGEMENT

I want thank the almighty GOD for all the blessings I have received and the strength he gave me through my life time, during my research work and other activity . I would like to express my sincere appreciation and deep gratitude to my advisor, Dr. ARGAW ASHA, who devoted time and effort to this research project. I am extremely grateful for all his support, encouragement and advice throughout my studies. I would also like to extend a special thanks to my co-advisor Mr. BIRHANE GEBIRU for his highly practical advice and valuable contributions to many technical problems. Most of all, I appreciate his friendship and I would like to acknowledge ASTU for facilitating this program

Finally, my last and most important acknowledgement goes to my wife; Makiya Jamel for their highly practical advice and valuable contributions to every aspect of my life. I am forever indebted to you for the never-ending support provided to me and all the sacrifices made.

Table of Contents

ACKNOWLEDGEMENT v
LIST OF TABLES ix
LIST OF FIGURES x
LIST OF ACRONYMS, ABBREVATONS AND SYMBOL xii
ABSTRACT xiv
CHAPTER ONE 1
INTRODUCTION 1
1.1. Background of the study 1
1.2. Statement of the Problem 2
1.3. Objective of the study 3
1.3.1. General objective 3
1.3.2. Specific objective 3
1.4. Scope of the Study 3
1.5. Significance of the Study 3
1.6. Organization of Thesis 4
1.7 Limitation of Thesis 4
CHAPTER TWO 5
LITERATURE REVIEWS 5
2.1. Introduction 5
2.2. Ground Improvement Techniques 5
2.2.1. Methods for ground improvement techniques for pavement 6
2.2.2. Ground Reinforcement 6
2.3. Road Embankment 10
2.3.1. Embankments on soft ground 11
2.4.2. Road embankment Design Considerations 12
2.4.3. Settlement Analysis 13
2.4.4. Stability of road embankment 15
2.4.5. Base reinforcement 17
2.4. Geogrid Reinforced Bases in Flexible Pavements 18
2.4.1. Reinforcement Mechanisms of Reinforced Geogrid Base Reinforced Pavement 20

2.5. Numerical Analyses of Geosynthetic Reinforced Pavement 23
2.6. Summary of Literature Findings 26
CHAPTER THREE 28
MATERIALS AND METHODOLOGY 28
3.1. Introduction 28
3.2. Description of study area 28
3.2.1. Location 28
3.2.2. Geology 30
3.3. Development of material parameter 31
3.3.1. Sub-grade soil 31
3.3.2. Embankment 34
3.3.3. Asphalt concrete (AC) Layer 36
3.3.4. Geogrid 36
3.4. Model development 38
3.4.1. Preliminary checks to ensure accurate numerical analysis 38
3.4.2. Mesh sensitivity analysis 42
3.4.3. Modeling of geogrid-soil interface 44
3.5. Numerical simulation of geogrid reinforced road embankment 45
3.5.1. Geometric modeling 45
3.5.2. The theoretical framework of numerical simulation 45
3.5.3. FEM Matrix 48
CHAPTER FOUR 49
RESULTS OF FEA AND DISCUSSION 49
4.1. Introduction 49
4.2. Detail Results of Finite Element Analysis 49
4.3. Parametric study 59
4.4. Validation of Finite Element Analysis 68
4.5. Discussion 69
CHAPTER FIVE 71
CONCLUSIONS AND RECOMMENDATIONS 71
5.1. Conclusions 71
5.2. Recommendations 72

REFERENCES 73
APPENDICES 77
Appendix A: Data Collection and Correlation 77
Appendix B: PLAXIS 2D Foundation Input 79
Appendix C: PLAXIS 2D Foundation Output 80

LIST OF TABLES

Table 2. 1: Summary of finite element studies of reinforced pavements 27
Table 3. 1: Summary of Sub-grade Soil Laboratory Test Results 32
Table 3. 2: Summary of subgrade and embankment materials 36
Table 3. 3: Geogrid material properties (after Jie Gu, 2011). 37
Table 3. 4: Influence of the distance to boundary upon the Vertical displacement of a 7 m road cross-section.. 41
Table 3. 5: Influence of the distance to boundary upon the horizontal displacement of a 7 m road cross-section.. 41
Table 3. 6: Influence of the distance to boundary upon the effective stress of a 7 m road cross-section 41
Table 3. 7: Influence of the mesh sensitivity on the vertical displacement at points A, B and C 44
Table 3. 8: Influence of the mesh sensitivity on the horizontal displacement at points A, B and C 44
Table 3. 9: Influence of the mesh sensitivity on the extreme effective stress 44
Table 4. 1: The results of FEA of a road embankment at slope of 1:1.5. 50
Table 4. 2: The results of FEA of a road embankment at slope of 1:2. 53
Table 4. 3: The results of FEA of a road embankment at slope of 1:3. 56

LIST OF FIGURES

Figure 2. 1: Illustration of embankment stability and failure mechanisms.................................. 17
Figure 2. 2: Section layout of geogrid reinforced bases in flexible pavements............................ 20
Figure 2. 3: Schematic illustration of lateral restraint mechanism (Perkins 2001)....................... 21
Figure 2. 4: Schematic illustration of improved bearing capacity (Perkins 2001) 22
Figure 2. 5: Schematic illustration of tension membrane mechanism (Perkins 2001) 23
Figure 3. 1: Satellite map of study area 29
Figure 3. 2: Google map of study area... 29
Figure 3. 3: Geology of Dukem areas and esp. study area 30
Figure 3. 4: CBR Distribution of Subgrade Samples along the route.. 33
Figure 3. 5: Layout of traffic loading as per ERA manual 2013. 37
Figure 3. 6: Layout of soil profile.. 39
Figure 3. 7: Flowchart outlining preliminary analysis checks for mesh density 43
Figure 3. 8: The layout of road embankment.. 45
Figure 3. 9: Schematic illustration of FEM matrix 48
Figure 4. 1: PLAXIS 2D output view (Sample) of horizontal displacement [mm] of unreinforced road embankment at slope of 1:1.5. 51
Figure 4. 2: PLAXIS 2D output of horizontal displacement [mm] at slope of 1:1.5.................... 51
Figure 4. 3: PLAXIS 2D output of vertical displacement [mm] at slope of 1:1.5. 52
Figure 4. 4: PLAXIS 2D output of effective stress [kN/m^2] at slope of 1:1.5. 52
Figure 4. 5: PLAXIS 2D output view (Sample) of vertical displacement [mm] of single layer reinforced road embankment at slope of 1:2.. 54
Figure 4. 6: PLAXIS 2D output of horizontal displacement [mm] at slope of 1:2....................... 54
Figure 4. 7: PLAXIS 2D output of vertical displacement [mm] at slope of 1:2. 55
Figure 4. 8: PLAXIS 2D output of effective stress [kN/m^2] at slope of 1:2. 55
Figure 4. 9: PLAXIS 2D output view (Sample) of effective stress [kN//m^2] of double layer reinforced road embankment at slope of 1:3.. 57
Figure 4. 10: PLAXIS 2D output of horizontal displacement [mm] at slope of 1:3..................... 57
Figure 4. 11: PLAXIS 2D output of vertical displacement [mm] at slope of 1:3. 58
Figure 4. 12: PLAXIS 2D output of effective stress [kN/m^2] at slope of 1:3.............................. 58

Figure 4. 13: Horizontal displacement Vs Side slope for *single-layered* at (i) “bottom”, (ii) “middle” and (iii) “top” reinforcement 60
Figure 4. 14: Horizontal displacement Vs Side slope for *double-layered* at (i) “bottom”, (ii) “middle” and (iii) “top” reinforcement 60
Figure 4. 15: Vertical displacement Vs Side slope for *single-layered* at (i) “bottom”, (ii) “middle” and (iii) “top” reinforcement 61
Figure 4. 16: Vertical displacement Vs Side slope for *double-layered* at (i) “bottom”, (ii) “middle” and (iii) “top” reinforcement 61
Figure 4. 17: Effective stress Vs Side slope for *single-layered* at (i) “bottom”, (ii) “middle” and (iii) “top” reinforcement 62
Figure 4. 18: Effective stress Vs Side slope for *double-layered* at (i) “bottom”, (ii) “middle” and (iii) “top” reinforcement 62
Figure 4. 19: Horizontal displacement Vs Reinforcement for *single-layered* and *double-layered* reinforcement 64
Figure 4. 20: Vertical displacement Vs Reinforcement for (i) *single-layered* and (ii) *double-layered* reinforcement 64
Figure 4. 21: Effective stress Vs Reinforcement for (i) *single-layered* and (ii) *double-layered* reinforcement 65
Figure 4. 22: Reinforcement Vs (i) *Horizontal displacement*, (ii) *Vertical displacement* and (ii) *Effective stress* 67
Figure 4. 23: the comparison between the finite element analyses and the laboratory model tests for (i) Unreinforced embankment soil (ii) Geogrid-reinforced embankment soil 68

LIST OF ACRONYMS, ABBREVATONS AND SYMBOL

2D	Two-dimensional;
3D	Three-dimensional;
AASHTO	American Association of State Highway and Transportation Officials;
AC	Asphalt Concrete;
CBR	California Bearing Ratio;
E	Easting;
ERA	Ethiopian Road Authority;
ESAL	Equivalent Single Axle Load;
FEA	Finite Element Analysis;
GG-I	Geogrid type I;
GG-II	Geogrid type II;
GG-III	Geogrid type III;
H	Horizontal;
HDPE	High Density Poly Ethylene;
LL	Liquid Limit;
MC	Mohr Coulomb;
MD	Machine Direction;
MDD	Maximum Dry Density;
N	Northing;
OMC	Optimum Moisture Content;
PET	Poly Ethylene Terephthalate;
PL	Plasticity Limit;
PLAXIS	Plane strain and axial symmetry;
PVC	Polyvinyl chloride;
TBR	Traffic Benefit Ratio;
V	Vertical;
XDM	Cross-Machine Direction;
α_r	Area ratio;
β	Settlement reduction factor;

γ	Bulk unit weight;
γ_{sat}	Saturated unit weight;
υ	Poisson's ratio;
ϕ	Angle of internal friction; and
ψ	Angle of dilatancy.

ABSTRACT

Road embankments and other constructions on natural weak clay are still a challenge in geotechnical engineering work. Problems due to deformation are very common on embankments and cause failure, which results in either large settlement or sliding due to inadequate shear strength. In order to mitigate the problem of poor ground bulk excavation and borrow fill was conservative previously. However, this way of mitigation leads to temporary destruction of infrastructure like water distribution line, electric cable, telecom fiber line and etc. Consequently, a cost of time delay, unserviceability period, and cost of maintenance is high. Hence, a mechanistic design procedure for reinforced pavement structures should be developed, which requires a better understanding and characterization of the geogrid-reinforced mechanisms. Thus, the present study aimed to address these issues by developing improved model for analysis and design of geogrid-reinforced road embankment laid on weak clay under cyclic working traffic loads in the case of Dukam town. It is intended in quantifying the structural contribution by geogrid reinforcement and incorporating it into the design methodology. PLAXIS 2D plane strain v8.6 is used for this research in conjunction with the Mohr-Coulomb model, which is adopted for the parent soil and embankment and Linear Elastic Model for the AC pavement and Geogrid reinforcement. The influence of key design parameters such as the effect of side slope, reinforcement position, number of layers and type of geogrid applied upon the performance of geogrid reinforced road embankment was investigated through a total of 67 numerical analyses including preliminary checks to ensure accurate numerical analysis. The modeling has shown that the performance of geogrid reinforced road embankment for efficient combination with respect to lateral deformation is that the horizontal displacement of reinforced embankment was reduced around one-third of unreinforced one (i.e. reduction factor is 36%). It was demonstrated that there is also a significant reduction in settlement when the ground is reinforced with the convenient combination of geogrid reinforcement factors. The vertical displacement of the reinforced embankment was reduced by 42% of untreated one. Relying on the parametric study the geogrid reinforced road embankment with side slope of 1:2, a single layered type III geogrid placed at the bottom of the embankment is selected and recommended as the most efficient combination of the rest all.

Key words: *Ground reinforcement*, *Geogrid, Settlement, PLAXIS 2D, Mohr-coulomb model*

CHAPTER ONE

INTRODUCTION

1.1. Background of the study

Ethiopia is developing country, where population increase at higher rate, needs to allocate huge amount of resources for construction works to meet the growing demand for shelter and other related facilities such as road networks. This effort should be accompanied by strict and professionally ethical quality assurance and supervision of construction. With the expansion of urban areas, increasing the necessity of occupation, sites that were not historically occupied are now being increasingly occupied. This situation concerns the technical means to find alternative solutions for mitigation of structural problems caused in the buildings and embankments by soil settlements.

Geotechnical engineers face several challenges when constructing embankments over soft soils. These include potential bearing failure, intolerable settlement, and global or local instability (Mim and Ping, 2008). When constructing an embankment over soft subsoil of low strength and high compressibility, the engineering tasks are to prevent the failure of the embankment and to control the subsoil deformation. Several methods have been developed for economically and safely constructing embankments on soft subsoil. Placing a layer of reinforcement at the base of the embankment is one of the methods (Chai et al., 2002).

A wide variety of geosynthetics with different properties has been developed to meet highly specific requirements corresponding to a range of different uses. Geosynthetics materials perform five principal functions in civil engineering applications: separation, reinforcement, filtration, and drainage and moisture barrier. Geogrid can notably improve the construction height, decrease the horizontal displacements and asymmetrical settlement of the soft soil, and increase dissipation speed of pore water pressure. (Indraratna et al. 2007)

This research has developed a better understanding on predicting the performance of geogrid reinforced embankment on soft soil in the case of Dukam town. A soil data was acquired from laboratory test and the soil profile and material parameters has been correlated to use as an input. The investigation tool used for numerical modeling was PLAXIS 2D finite element based software. A series of 2D numerical analysis was conducted to analyze the settlement and deformation, as important criteria in embankment. Investigation concerning the key parameters that mainly influence the performance of geogrid-reinforced road embankment was discussed by a researcher through an intensive literature review based on the analyses result.

1.2. Statement of the Problem

Road embankments and other constructions on natural soft clay are still a challenge in geotechnical engineering work. The use of various soil improvement methods to stabilise the soft clay need to be carried out in order to increase the bearing capacity and reduce the settlement. (Bakhtiar, 2012)

Problems due to deformation are very common on embankments and cause failure which results in either large settlement or sliding due to inadequate shear strength. Normal fill can comprise of mix of different soils like silty sand, clayey sand or silty clay etc., which are commonly found embankment material at various locations. Due to climatic variations, swelling or shrinkage related soil movements commonly occur in the soils underneath the infrastructures such as pavements, embankments and light to medium loaded residential & commercial buildings. (Sabahat Khan, 2014)

In pavements, the soil movement results in settlements, surface cracking and thereby creating difficult driving conditions and also costly rehabilitation and maintenance for the highways in dukem. In order to mitigate the problem of poor ground bulk excavation and borrow fill was conservative previously. However, this way of mitigation leads to temporary destruction of infrastructure like water distribution line, electric cable, telecom fiber line and etc. Consequently, a cost of time delay, unserviceability period, and cost of maintenance is high. Geosynthetic material (i.e. geogrid) was used as reinforcement to overcome the soil movement related problem. (Indraratna et al. 2007)

Thus, in order to overcome these limitations, a mechanistic design procedure for reinforced pavement structures should be developed, which requires a better understanding and characterization of the geogrid-reinforced mechanisms. In particular, more research is needed in quantifying the structural contribution by geogrid reinforcement and incorporating it into the design methodology. As a part of this process, factors that affect the performance of geogrid reinforced pavement structures has been determined and evaluated. That is why the present study aimed to address these issues by developing improved model for analysis and design of geogrid-reinforced bases in flexible paved road embankment under cyclic working traffic loads.

1.3. Objective of the study

1.3.1. General objective

The aim of this thesis is numerical analysis of geogrid reinforced road embankment on soft soil using finite element based software in the case of Dukam

1.3.2. Specific objective

- To determine deformation and settlement of embankment without reinforcement and when reinforced with geogrid
- To investigate the influence of different parameters like side slope, geogrid application layer and type of geogrid and number of reinforcement layer on the performance of embankment laid on soft soil
- To obtain optimum geogrid application on the embankments.

1.4. Scope of the Study

The scope of the study limited to numerical analysis most effective reinforcement type for the specified soil by determining the deformation of embankment and changing embankment parameters (side slope, geogrid application layer and type of geogrid and number of reinforcement layer). PLAXIS 2D was used for this study in conjunction with the advanced Mohr-Coulomb model

1.5. Significance of the Study

It is expected that this work may contribute a lot of importance:

- Develop a better understanding of the behavior of reinforced road embankment weak soils.
- Verify the previous analysis done abroad and enhance the confidence of the designers (esp. Geotechnical Engineers) to apply this preferable alternative in Ethiopia.
- Contribute as reference for other future work.

1.6. Organization of Thesis

The content of this thesis is organized in to five chapters:

Chapter 1 provides general introduction with the research objectives, scope and significance of the study. Chapter 2 outlines a full detailed literature review of the geogrid reinforced road embankment, including historical development, construction methods and previous research works.

Chapter 3 presents study area description, material parameters soil profile adopted for modeling, preliminary checks for sensitivity analyses and generation of finite element analyses using PLAXIS 2D plane strain code.

In Chapter 4 analysis of results, validation of FEA and discussion is presented. Parametric study regarding the influence of key design parameters is also furnished.

The last chapter, Chapter 5, discusses the conclusions derived from this study and limitations in the analyses and recommendations for future work.

1.7. Limitation of Thesis

The effects of some key design parameters have been addressed in detail. But there are still other influential points to be touched especially width ratio effects, variability of material stiffness and strength characteristics, and effect of pavement structures.

The material parameter for soil profile was tested only for basic property the other property such as strength characteristics and stiffness characteristics is correlated from basic property and used as software input.

CHAPTER TWO

LITERATURE REVIEWS

2.1. Introduction

The road network in Ethiopia provides the dominant mode of freight and passenger transport and thus plays a vital role in the economy of the country. The network comprises a huge national asset that requires adherence to appropriate standards for design, construction and maintenance in order to provide a high level of service. When the length of the road network is increasing, appropriate choice of methods to preserve this investment becomes increasingly important.(ERA)

Kiran and Mohan (2016) suggest that of transportation like road, railway, airways etc. however the most mode of transportation is usually road or highways. In the method of road development, the alignment of road could have to be compelled to be mounted through the soils that cannot bear the traffic loads. There are numerous techniques of ground improvement techniques like soil stabilization, stabilizing trenches, vertical sand drains, capillary cut-off, soil nailing, Vibro-compaction, Vibro-floatation, use of geo-textiles, Vibro-replacement, stone columns, dynamic compaction etc.

2.2. Ground Improvement Techniques

The construction sites are inflated (increased) currently days. Thus engineers are have not any alternative left except to use soft and weak soils around by improving their strength by means that of modern ground improvement techniques for construction. The ground improvement techniques are stone columns, dynamic compaction, Vibro compaction, soil reinforcement, vertical drains, and replacement of soil, in-situ densification, Vibro piers, grouting, pre-loadings and stabilization using admixtures. The aim of those techniques is to extend the bearing capacity of soil, improve the soil properties and reduce the settlement. Ground improvement by reinforcing the soil is achieved by using fibers of glass, steel, varied polymers within the type of grids or strips and geosynthetics. Geosynthetics may be impermeable or permeable in nature counting on composition and its structure. The geosynthetics materials are often used for various applications. It is often used as protection, reinforcement, separation, filtration, containment and confinement of soil to extend the strength of soil. Depending upon the requirements of site condition the Geocell reinforcement also used (Kiran and Mohan, 2016).

2.2.1. Methods for ground improvement techniques for pavement

Now a day there is some many ground improvement techniques employed for the pavement construction. Some of them are soil stabilization, vertical drains, stabilization trenches, capillary cut-off, soil nailing, vibro compaction, dynamic compaction etc. (Kiran and Mohan, 2016).

(Kiran and Mohan, 2016). Stated that Soil stabilization is a general term for any chemical, physical, organic, or joined strategy for changing a characteristic soil (natural soil) to meet a designing reason or engineering properties. Upgrades incorporate expanding the weight bearing abilities and execution of in-situ sub-soils, sands, and other waste materials keeping in mind the end goal to strengthen pavement or road surfaces.

The methods of soil stabilization are mechanical stabilization, additive stabilization, stabilization with portland cement, stabilization with lime, stabilization with bitumen, stabilization by geogrid, reinforced earth using bio-enzymes.

2.2.2. Ground Reinforcement

Reinforced soil is a composite construction material formed by combining soil and reinforcement. This material possesses high compressive and tensile strength similar, in principle, to the reinforced cement concrete. It can be obtained by either incorporating continuous reinforcement inclusions (for example, strip, bar, sheet, mat or net) within a soil mass in a definite pattern or mixing discrete fibers randomly with a soil fill before placement. The term ‘reinforced soil’ generally refers to the former one, although it may more appropriately be called ‘systematically reinforced soil’, whereas latter one is called ‘randomly distributed/oriented fiber-reinforced soil’ or simply ‘fiber-reinforced soil’. (Kiran and Mohan, 2016).

The apparently simple mechanism of reinforced soil and the economy in cost and time have made it an instant success in geotechnical and highway engineering applications for temporary as well as permanent structures. Reinforcement, inextensible or extensible, has the main task of resisting the applied tensile stresses or preventing inadmissible deformations in geotechnical structures such as retaining walls, soil slopes, bridge abutments, foundation rafts, embankment etc. In this process, the reinforcement acts as a tensile member coupled to the soil/fill material by friction, adhesion, interlocking or confinement, and thus improves the stability of the soil mass. . (Kiran and Mohan, 2016).

Principles

Kiran and Mohan, (2016) concluded that Soil has an inherently low tensile strength but a high compressive strength. An objective of incorporating soil reinforcement is to absorb tensile loads or shear stresses within the structure. In absence of the reinforcement, structure my fail in shear or by excess of the deformation. When an axial load is applied to the reinforced soil, it generates an axial compressive strain and lateral tensile strain. If the reinforcement has an axial tensile stiffness greater than that of the soil, then lateral movements of the soil will only occur if soil can move relative to the reinforcement movement of the soil, relative to the reinforcement, will generate shear stresses at the soil/ reinforcement interface, these shear stresses are redistributed back into the soil in the form of internal confining stress. Due to this, the strain within the reinforced soil mass is less than the strain in unreinforced soil for the same amount of stresses, where $\delta hr < \delta h$. and $\delta vr < \delta v$, provided the surface of the reinforcement is sufficiently rough to prevent the relatively movement and the axial tensile stiffness of reinforcement is more than that of soil.

Soil reinforcement interaction

For soil reinforcement, interaction to be effective reinforcement is required to absorb strains, which would otherwise cause failure. In this context, an ultimate state of collapse in terms of interaction with the soil and reinforcement can be caused by rapture of reinforcement or failure of bond between soil and reinforcement. In serviceability, limit state occurs when deformation occurs beyond serviceable limit or strain within the reinforcement exceed prescribed limit. If the soil is cohesion less the bond resistance will be friction and will depend upon surface roughness and soil. If soil is cohesive the bond stress will be adhesive. In case of grid reinforcement the bond stress will be governed by the shear strength of the soil and roughness of the reinforcement.

Having absorbed load it is necessary for the reinforcement to sustain this load during the design life without rupture or without suffering time dependent deformation which might give rise to serviceability limit. To maximize the tensile load capacity the flexible reinforcement are install horizontally to coincide with the principle tensile strain. The axial forces absorbed by the reinforcement are statically determinate (Kiran and Mohan, 2016)

2.2.2.3. Material used for reinforcement

In most of the current civil engineering applications, the reinforcement generally consists of geosynthetic sheets or strips of galvanized steel, arranged horizontally or in the directions in which the soil is subject to the undesirable tensile strains (Abu-Farsakh et al 2009).

Geosynthetics

Geosynthetics are a rapidly emerging family of geomaterials used in a wide variety of civil engineering applications. Many polymers (plastics) common to everyday life are found in geosynthetics. The most common are polyolefin and polyester; although rubber, fiberglass, and natural materials are sometimes used. Geosynthetics may be used to function as a separator, filter, planar drain, reinforcement, cushion/protection, and/or as a liquid and gas barrier. (G. Look B. 2007)

Geogrids

Geogrids have an open, grid like configuration, i.e. they have large apertures and are invariably used in some form of reinforcement. Geogrids are commonly used to reinforce retaining walls, as well as sub- bases or sub soils below roads or structures. (G. Look B. 2007)

Geogrids are matrix like materials with large open spaces called apertures, which are typically 10 to 100mm between ribs that are called longitudinal and transvers respectively. The ribs themselves can be manufactured from a number of different materials, and the rib cross-over joining or junction-bonding methods can vary. The primary function of geogrids is clearly reinforcement.

Geogrid is also defined as a geosynthetic formed by a regular network of integrally connected elements and possess apertures greater than 6.35 mm (1⁄4 inch) to allow interlocking with surrounding soil, rock, earth, and other surrounding materials to primarily function as reinforcement.

The various types of geogrids used in the work which are either in the machine (MD), or cross-machine direction (XMD) as manufactured, Junction is the point where geogrid ribs are interconnected to provide structure and dimensional stability.

Geogrid is stiff or flexible polymer grid-like sheets with large apertures used primarily for stabilization and reinforcement of unstable or week soil. The general types of geogrid are unidirectional geogrid, bidirectional geogrid, extruded geogrid, bonded geogrid, woven geogrid. . (G. Look B. 2007) .

Effect of geogrid properties

According to Salahudeen (2016) The principle requirements of reinforcing materials are strength and stability (low tendency to creep), durability, ease of handling, a high coefficient of friction and or adherence with the soil, together with low cost and ready availability .The selection of fabric for a particular construction application must necessarily depend upon adequate and suitable fabric properties and characteristics.

Geogrid tests are unique in a number of aspects when compared with geotextiles. Properties relating to separation, filtration, drainage, and barrier applications are not included since geogrids always serve the primary function of reinforcement (Salahudeen ,2016)

The effective important properties of geogrids may be concerned in three main properties are physical properties, mechanical properties, endurance properties.

Many of the physical properties of geogrids including the weight (mass), type of structure, rib dimensions, junction type, aperture size, and thickness can be measured directly and are relatively straightforward. Other properties that are of interest are mass per unit area, which varies over a tremendous range from 200 to 1000 g/m2, and percent open area, which varies from 40 to 95%. (Salahudeen ,2016)

The mechanical properties of geogrids including the geogrid stiffness, the peak tensile strength, modulus of elasticity, upper yield strength, lower yield strength, tensile strength, non-proportional extension strength, total extension strength, fracture elongation, elongation at maximum load and total elongation. (Salahudeen ,2016)

The strength of the geogrids varies between 20 and 250 kN/m, and they are used in both road constructions and reinforced slopes. Geogrids can be divided into two groups. Stiff geogrids, mostly high-density polyethylene(HDPE) with a monolithic mesh structure. Flexible geogrids, mostly polyethylene terephthalate (PET) with poly vinyl chloride (PVC) or acrylic coating with mechanically connected longitudinal and transverse elements.

The main design requirements for the use of geogrids in soil structures result from the geotechnical design. This includes the calculation of different failure modes resulting in requirements for: axial tensile design strength of the geogrid and maximum strain requirements in the geogrid. (Salahudeen ,2016)

Geogrids are single or multi-layer materials usually made from extruding and stretching high-density polyethylene or polypropylene or by weaving or knitting and coating high tenacity polyester yarns. The resulting grid structure possesses large openings (called apertures) that enhance interaction with the soil or aggregate. The high tensile strength and stiffness of geogrids make them especially effective as soil and aggregate reinforcement.(Salahudeen ,2016)

2.3. Road Embankment

Embankment is a very important part of every road and railway structure. It has to support the road pavement or railway structure and shall further distribute the forces, applied onto the pavement or railway structure, over the subsoil without exhibiting unacceptably large deformations. When constructing an embankment one should take into account a great number of variable properties of both the construction materials to be applied and the subsoil. The stability of the embankment determines the performance of the overlying road pavement or railway structure. As the embankment consists of soil, in road and railway engineering soil is an essential construction material.

The stability of the embankment is influenced by many factors. Some of these factors have to be accepted and the structural design of the road pavement or the railway structure has to include these factors. However, the negative effects of other factors can be limited through a solid structural design and an adequate construction of the road or railway.

The construction of an embankment on weak subsoil always leads to settlements. The magnitude of these settlements depends on the magnitude of the loading, i.e. the deadweight of the embankment, and the deformation characteristics of the subsoil. As both the magnitude of the loading and the deformation characteristics of the subsoil usually exhibit some variation, the settlements of the subsoil nearly always are no uniform.

The reason for the occurrence of settlements is clear. The extra deadweight load of the embankment must be borne by the grain skeleton of the subsoil, so by the normal stresses and shear stresses that develop in the contact points between the grains. When the shear stresses become too great a reorientation of the grain skeleton takes place, in such a way that the volume of the pores decreases and the number of contact points between the grains thus increases to such an extent that equilibrium is obtained. Settlements therefore are the consequence of a decrease of the pore content in the subsoil. These settlements are called the primary settlements. Except primary settlement also secondary settlements occur in the subsoil. These secondary settlements result from creep of the grains themselves due to the extra deadweight load of the embankment. These secondary settlements are also called secular effect. (Molenaar and Houben, 2003).

2.3.1. Embankments on soft ground

Embankments on soft ground also have a tendency to spread laterally because of horizontal earth pressures acting within the embankment. These earth pressures cause horizontal shear stresses at the base of the embankment that must be resisted by the shear strengths of foundation soils. Soft soils do not have adequate shear strength and failure may occur as a result. Hence, embankments on soft soils are ideally designed so that the increase in stress is relatively small, i.e. shallow embankments. Embankment fills over soft ground are frequently stronger and stiffer than their foundations. This leads to the possibility that an embankment will deform as the foundation fails under the weight of the embankment and the possibility of progressive failure because of stress–strain incompatibility between the embankment and its foundation. Because of this problem, peak strengths of the embankment and the foundation soils do not mobilize simultaneously. Often, stability analyses performed using peak strengths of soils would overestimate the factor of safety. (Abramson et al, 2002)

Where embankments are required to be built over soft ground, stability and settlement of the fill should be carefully evaluated. Some very soft and highly organic materials need to be tested in situ with vane shear apparatus, as retrieving undisturbed samples from these soils for laboratory testing is difficult. In addition, the level of groundwater should be determined and its fluctuation monitored. Attention should be given to the internal stability of the entire embankment foundation interface rather than the embankment or the foundation soils alone. Consideration should be given to removing the soft underlying layer and replacing it with free-draining material prior to the placement of the embankment. (Abramson et al, 2001).

2.4.2. Road embankment Design Considerations

The key geotechnical issues are stability and settlement characteristics of the foundation soils and the bearing capacity at the base. The impact of these considerations on stages of construction is also an issue that should be considered during design.

Embankments provide adequate support for roadways if the additional stress from traffic loads and pavement structures does not exceed the shear strength of the soils. Overstressing the embankment may result in slope failure. In addition to issues related to side slope stability, any anticipated settlement problem must also be considered. This settlement can be short term created as a result of the addition of increased load on the soil beneath the embankment (bearing failure during placement of the fill) or long-term due to consolidation.

The primary design issue is whether the existing foundation soil can support the new embankment loads without undergoing bearing failure, or excessive settlement. These conditions are most critical when soft cohesive soils are present below the embankment. Staged construction may need to be considered whereby the embankment is constructed in a number of stages and excess pore water pressures allowed to dissipate over a period of time before the next lift is constructed. Sometimes trial embankments are constructed at the beginning of the construction process to check assumptions made during the design. (ERA’s Geotechnical Design Manual, 2013).

The second type of load is the long-term operational loading. This loading occurs after the embankment is constructed to the final grade and excess pore-water pressures have dissipated. The long-term stability of embankment slopes should be analysed especially in fine grained soils. When foundation soils are cohesive and not heavily over-consolidated, potential settlement will be a design consideration. Consolidation settlement and secondary compression can continue for many years and, depending on the thickness of soils, the amount of settlement can be very high. Significant settlement can result in distress to the pavement at the top of the embankment, as well as differential settlement of the pavement at cut and fill transitions and bridge approaches.

Another load that may occur in embankments is seismic loading. This load is usually a rare occurrence but may be very important in areas like the rift valley of Ethiopia where earthquakes are much more common. The primary geotechnical concern during the design earthquake is the potential for liquefaction in foundation soils beneath the embankment. Liquefaction could lead to bearing failures, side slope failures and post-liquefaction settlement. The potential for side slope failure without liquefaction is also a design consideration. The duration of loading during a seismic event is usually short; however, pore-water pressures can redistribute after an earthquake leading to liquefaction-related failures that may occur several minutes after the main earthquake event.

Embankments under 5 m high in areas of stable ground and with slopes not greater than 1.5H:1V generally do not require a detailed geotechnical investigation and analysis. These embankments can be specified particularly when based on past experience in the same region and on engineering judgment. On the same basis, embankments over 5 m high and those constructed over soft ground will usually require a detailed geotechnical analysis. (ERA's Geotechnical Design Manual, 2013).

2.4.3. Settlement Analysis

Settlement is the amount of vertical deformation that occurs when a load is applied or an embankment is placed over compressible soils. The settlement may be due to the consolidation of the embankment itself as well as the underlying soils.

The total settlement in an embankment is a summation of three potential components: immediate settlement of the fill or the foundation soil, primary consolidation of the foundation soil, and secondary compression controlled by the composition and structure of the foundation soil skeleton. Settlement caused by lateral deformation of the foundation soil at the edges of an embankment is not considered here. (ERA's Geotechnical Design Manual - 2013).

Immediate settlement of the fill and the foundation soil occur during construction and will not usually have any impact on the future pavement. Therefore, the analysis of settlement for embankment design focuses on primary consolidation and secondary compression of the foundation soil.

Because primary consolidation and secondary compression can continue long after the embankment is constructed (post construction settlement), they represent the major settlement considerations for embankment design. Usually, post-construction settlement can damage structures located within the embankment, especially if these facilities are also supported by adjacent soils that do not settle appreciably, leading to differential settlements. Differential settlements that occur along the longitudinal axis of the embankment because of changes in consolidation properties of underlying clays can cause transverse cracking on the surface of the embankment. (ERA's Geotechnical Design Manual - 2013).

a) Primary consolidation

The settlement associated with the readjustment of soil particles due to migration of water out of the voids is known as primary consolidation. The amount of primary consolidation depends on the initial void ratio of the soil. The greater the initial void ratio, the more water that can be squeezed out, and the greater the primary consolidation. The rate at which primary consolidation occurs is also dependent on the rate at which the water is squeezed out of the soil voids.

The response of foundation soils to additional loads is also dependent upon their stress history. Usually, settlement happens when the weight of the embankment exceeds the previous stress history of the soils. Depending upon the magnitude of the existing effective pressure relative to the maximum past effective stress at a given depth, foundation soils can be classified as normally consolidated, over-consolidated, or under-consolidated. When the existing load is equal to the historical load, the soil is said to be normally consolidated. Pre-consolidation pressure in excess of the current vertical effective stress occurs in over-consolidated soils. Soils are considered to be under-consolidated when consolidation under the existing load is still occurring and will continue to occur until primary consolidation is complete, even if no additional load is applied.

Settlement computation starts with the soil profile being divided into layers, with each layer reflecting changes in soils properties. Thick layers with similar properties are also subdivided to improve the analysis since the settlement calculations are based on the stress conditions at the midpoint of the layer (i.e. it is preferable to evaluate a 6 m thick layer as two 3 m thick layers). The total settlement is the sum of the settlement from each of the compressible layers. . (ERA's Geotechnical Design Manual - 2013).

b) Secondary compression

The end of primary consolidation is considered as the amount of compression that occurs during the period of time required for excess pore-water pressure to dissipate because of an increase in effective stress. Secondary compression occurs when the soil continues to settle after the excess pore water pressures are dissipated to a negligible level, i.e. primary consolidation is essentially completed. It can take years for primary settlement to complete and secondary compression continues for decades. The occurrence of secondary compression is independent of the stress state and theoretically is a function only of the secondary compression index and time.

For many soils, contribution from secondary settlement is small. However, in soft soils and particularly in soils with a high peat or organic content, it can be large and difficult to predict.

Like the primary consolidation, detailed numerical procedures for estimating the amount of secondary compression are given in the literature. Generally, the contributions from the individual soil layers are summed to estimate the total settlement. Since secondary compression is not a function of the stress state in the soil but rather how the soil breaks down over time, techniques such as surcharging to pre-induce settlement are sometimes only partially effective at mitigating the effect of secondary compression. Often the owner must accept the risks and maintenance costs associated with secondary compression if a cost/benefit analysis indicates that mitigation techniques such as using lightweight fills or over-excavating are too costly. (ERA's Geotechnical Design Manual, 2013).

2.4.4. Stability of road embankment

In addition to settlement, the design of embankments should also consider side slope stability and bearing capacity. Stability problems in the form of rotational or sliding block failures most often occur when the embankment is built over soft soils such as low strength clays and silts, or when the foundation soil is overstressed during or immediately after construction. Failure can also occur if the fill materials are not compacted to specification. In addition, failures can also occur when the fill materials at the toe of the embankment are eroded. Dynamic forces from earthquakes, blasting or pile driving can also trigger failures of embankment slopes. Usually, short-term stability of embankments on cohesive soil is more critical than long-term stability, because the foundation soil will gain shear strength as the pore pressures dissipate. ERA's Geotechnical Design Manual, 2013).

An embankment slope may fail in following way

1) Rotational slip failure it may be circular slips are formed in homogenous, isotropic soil and non –circular slip formed with non-homogenise soil
2) Translation and compound slip occur if the underlying stratum possess significantly different property and strength. (Shyamal Kumar, 2009).

Prior to commencing a stability analysis, the following key issues need to be addressed:

- Is the site underlain by soft silt, clay or peat? If so, a staged stability analysis may be required.

Are there geometrical and site constraints which need embankment slopes steeper than 1.5H:1V? If so, a slope stability assessment may be needed to evaluate the various alternatives. Is the embankment temporary or permanent? Factors of safety for temporary fills may be lower than for permanent embankments, depending on the site conditions and the availability of materials. .(ERA's *Geotechnical Design Manual - 2013.*

Generally, experience and observations of failures of embankments constructed over relatively deep deposits of soft soils have shown that when failure occurs, the embankment settles, the adjacent ground rises and the failure surface follows a circular arc. A slip circle failure in embankments may be a base circle, a toe circle, or a slope circle. A base slip circle develops when there is a significant thickness of weak foundation soil. The base of the failure arc is tangent to the base of the weak layer, and the arc will have a significant portion of its length in the weak soil. A slip circle develops within the embankment and intersects with the slope. A toe slip circle develops in the embankment and intersects at the toe. This happens, sometimes, when the embankment material becomes saturated and failure occurs.

In general, at failure, the driving and resisting forces act as follows:

- The force driving movement consists of the embankment weight. The driving moment is the product of the weight of the embankment acting through its centre of gravity times the horizontal distance from the centre of gravity to the centre of rotation (Lw).
- The resisting force is the total shear strength acting along the slip plane. The resisting moment is the product of the resisting force times the radius of the circle (LS).

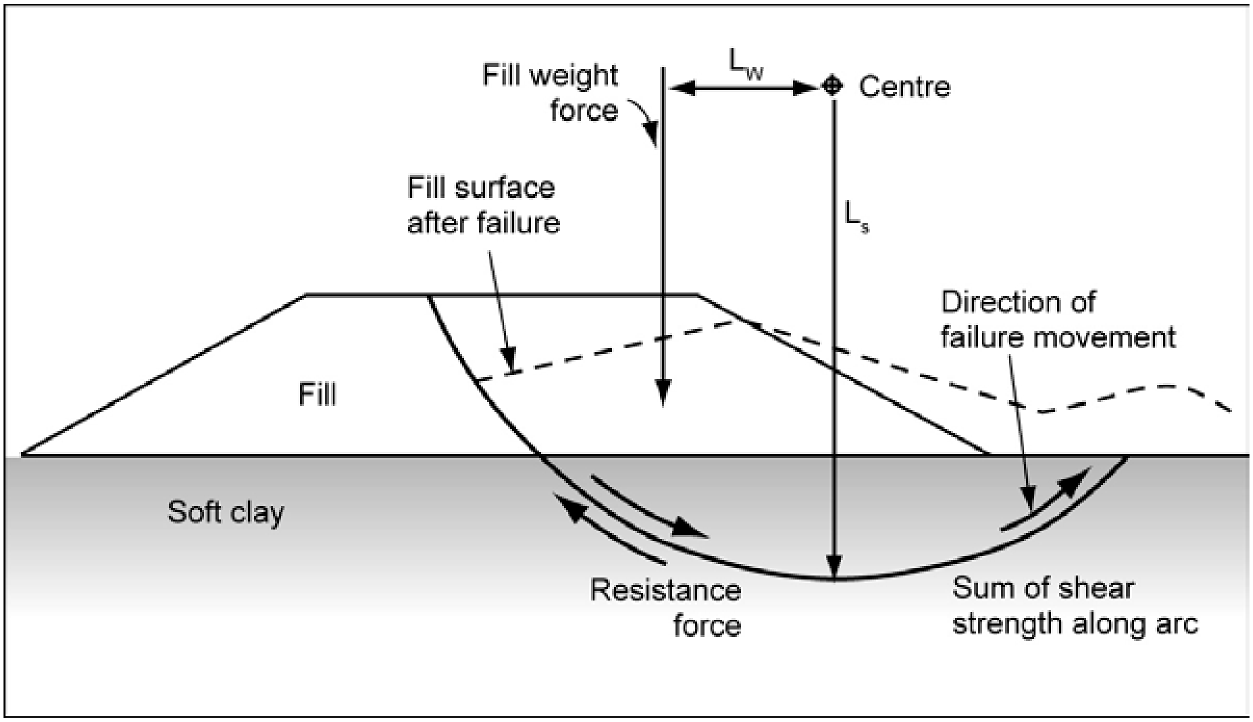

Figure 2. 1: Illustration of embankment stability and failure mechanisms. (ERA's Geotechnical Design Manual - 2013).

In general, for side slopes of any road embankment, a minimum design safety factor of 1.3 as determined by the ordinary method of slices is sufficient to maintain long-term stability. Embankments supporting or potentially impacting non-critical structures should have a minimum safety factor of 1.3. For slopes that would cause greater damage upon failure, such as slopes adjacent to bridge abutments, major retaining structures, and major roadways, the design safety factor should be increased in the range of 1.3 to 1.5. All bridge approach embankments and those supporting critical structures should have a safety factor of 1.5. Critical structures are those in which failure would result in property damage. If an embankment is provided with benches, these should be at least 1.5 m wide and not more than 6m apart vertically. If springs or seepages are found near the embankment, suitable drains should be provided to collect the flow. (ERA's Geotechnical Design Manual, 2013).

2.4.5. Base reinforcement

Base reinforcement may be used to increase the factor of safety against slope failure. Base reinforcement typically consists of placing a geotextile or geogrid at the base of an embankment prior to constructing the embankment. Base reinforcement is particularly effective where soft/weak soils are present below a planned embankment location. The base reinforcement can be designed for either temporary or permanent applications. Most base reinforcement applications are temporary, in that the reinforcement is needed only until the shear strength of the underlying soil has increased sufficiently as a result of consolidation under the weight of the embankment. Therefore, the base reinforcement does not need to meet the same design requirements as permanent base reinforcement regarding creep and durability.

The design of base reinforcement is similar to the design of a reinforced slope in that limit equilibrium slope stability methods are used to determine the strength required to obtain the desired safety factor. Base reinforcement materials should be placed in continuous longitudinal strips in the direction of main reinforcement. Joints between pieces of geotextile or geogrid in the strength direction (perpendicular to the slope) should be avoided. All seams in the geotextiles should be sewn and not lapped. Likewise, geogrids should be linked with pins and not simply overlapped. Where base reinforcement is used, the use of gravel borrow areas, instead of earth materials, may also be appropriate in order to increase the embankment shear strength. (ERA’s Geotechnical Design Manual, 2013).

2.4. Geogrid Reinforced Bases in Flexible Pavements

Kinney et al. (1998).explained that Pavement structures are built to support loads induced by traffic vehicle loading and to distribute them safely to the subgrade soil. A conventional flexible pavement structure consists of a surface layer of asphalt (AC) and a base course layer of granular materials built on top of a subgrade layer. Pavement design procedures are intended to find the most economical combination of AC and base layers’ thicknesses and material types, taking into account the properties of the subgrade and the traffic loading to be carried during the service life of the roadway.

The major structural function of a base layer is to provide a stable platform for the construction of the asphalt layer and to reduce the compressive stresses on top of the subgrade and the tensile stresses in the asphalt layer. The base layer should be able distribute the stresses applied to the pavement surface by traffic loading. These stresses must be reduced to levels that do not overstress the underlying subgrade soil.

The Base course layer can be the cause of pavement failures, due to inadequate capacity of support to upper layers or to being insufficiently stiff, such that they fail to transfer the load uniformly to the subgrade, leading to localized overloading of the subgrade, and resulting in excessive pavement rutting. These pavement failures usually necessitate complete pavement reconstruction, and not only remedial treatment of the pavement surface where the problem is visible. Therefore, when constructing a pavement structure on a weak subgrade soil layer, it may be required to increase the thickness of base layers, or use good quality base course material. However, the depletion of high quality aggregates is at a rapid pace as a consequence of the increasingly demands on highway systems. In addition, there are usually limitations on the thickness of the pavement structures. These problems provide a motivation for exploring alternatives to existing methods of building and rehabilitating roads. Geogrid reinforcement in base course layer offers one such alternative.

The use of geogrids reinforcement in roadway applications started in the 1970s. Since then, the technique of geogrid reinforcement has been increasingly used and many studies have been performed to investigate the behavior of geogrid reinforcement in roadway applications (e.g., Hass et al., 1988; Al-Qadi et al., 1994; Perkins, 1999, 2001, 2002; and Berg et al., 2000). The results of numerical studies reported in literature showed that geogrid reinforcement in pavement structures can extend the pavement's service life, reduce base course thickness for a given service life, delay rutting development and help construction of pavements over soft subgrades. (Al-Qadi et al. 1997, Cancelli and Montanelli 1999, Wasage et al. 2004, Montanelli et al. 1997, Moghaddas-Nejad and Small 1996, Kinney et al. 1998). The increase in service life of pavement structure is usually evaluated using the Traffic Benefit Ratio (TBR), which is defined as the ratio of the number of load cycles to achieve a particular rut depth in reinforced section to that of an unreinforced section of identical thickness, material properties, and loading characteristics. Meanwhile, the reduction in base thickness is usually evaluated using the Base Course Reduction (BCR) factor, which is defined as the ratio of reinforced base thickness divided by the unreinforced base thickness of same performance under a given traffic load level.

In providing reinforcement, the geosynthetic material structurally strengthens the pavement section by changing the response of the pavement to applied loading (Koerner, 2005). Geogrid reinforcement provided a more uniform load distribution through distributing the load to larger area and a deduction in the rut depth at the surface of the asphalt course (Wasage et al., 2004).

The amount of improvement in pavement performance with the inclusion of geogrid in base layer depends on many factors, including the strength of subgrade, geogrid properties, location of geogrid in pavement, thickness of base layer, etc (Hass et al. 1988, Webster 1993, Collin et al. 1996, Kinney et al. 1998, Cancelli and Montanelli 1999, Perkins 1999, Berg et al. 2000, Al-Qadi et al 2008).

Earlier studies (Anderson and Killeavy 1989, Barksdale et al, 1989 and Cancelli et al., 1996) have demonstrated that geogrids are superior to geotextiles when used as a reinforced member. So geogrids will be used as the only reinforcement for the study of reinforced bases in flexible pavements in this dissertation.

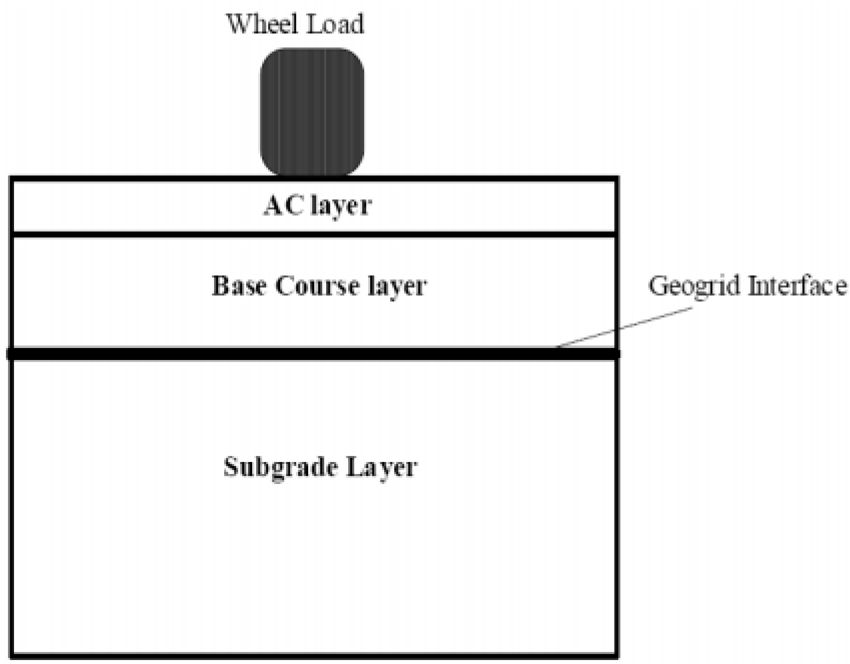

Figure 2. 2: Section layout of geogrid reinforced bases in flexible pavements**(Anderson and Killeavy 1989, Barksdale et al, 1989 and Cancelli et al., 1996)**

2.4.1. Reinforcement Mechanisms of Reinforced Geogrid Base Reinforced Pavement

The reinforcement mechanisms in geogrid base reinforced pavement sections include lateral restraint, increased bearing capacity and tension membrane effect.

Lateral Confinement Mechanism

The principle mechanism responsible for reinforcement in paved roadways is the base course lateral restraint and is schematically illustrated in Figure 2.3. Verticular loads applied to the roadway surface create a lateral spreading motion of the base course. Tensile lateral strains are created in the base below the applied load as the material moves down and out away from the load. The geosynthetic restrains the base thus reducing or restraining this lateral movement. The term lateral restraint involves several components of reinforcement including: (i) restraint of lateral movement of base aggregate (Perkins, 1999a); (ii) increase in stiffness of the base course aggregate layer (Bender and Barenberg, 1978), (iii) reduction of shear stress in the subgrade soil (Love et al., 1987), (iv) improved vertical stress distribution on the subgrade (Milligan et al., 1989). This mechanism of reinforced bases pavement is illustrated in Figure 2.3.

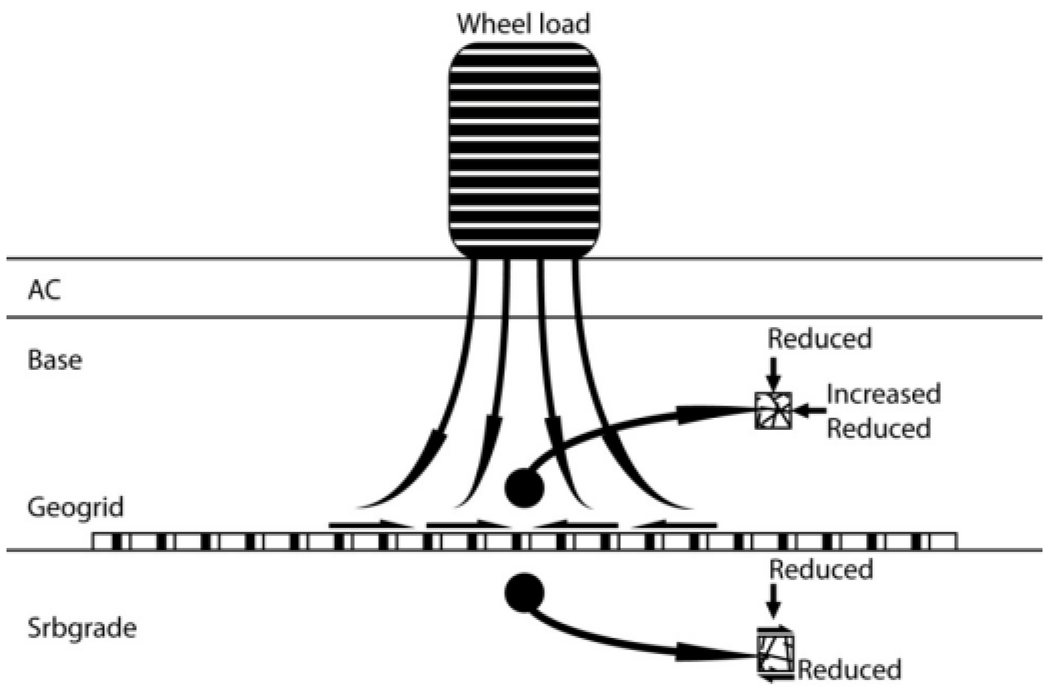

Figure 2. 3: Schematic illustration of lateral restraint mechanism (Perkins 2001)

Increase of the Bearing Capacity Mechanism

The improved bearing capacity is achieved by shifting the failure envelope of the pavement system from the relatively weak subgrade to the relatively stiff base layer as illustrated in Figure 2.4. Such that, the bearing failure model of subgrade may change from punching failure without reinforcement to general failure with ideal reinforcement. Binquet and Lee (1975) initially established this finding.

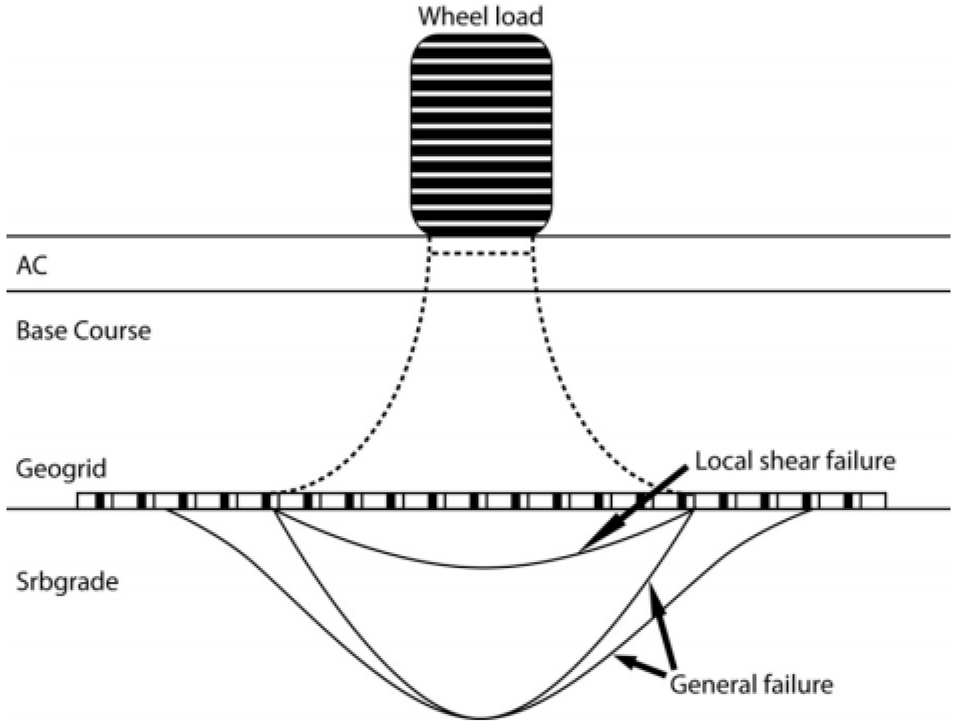

Figure 2. 4: Schematic illustration of improved bearing capacity (Perkins 2001)

Tension Membrane Mechanism

The tension membrane effect (Giroud and Noiray, 1981) develops as a result of vertical deformation creating a concave shape in the tensioned geogrid layer; this is demonstrated in Figure 2.5. The vertical component of the tension membrane force can reduce the vertical stress acting on the subgrade. Some displacement is needed to mobilize the tension membrane effect. Generally, a higher deformation is required for the mobilization of tensile membrane resistance as the stiffness of the geogrid decreases. Significant rut depth and high stiffness of the geosynthetic must be provided to initiate the membrane effect and thus to enhance the bearing capacity of the subgrade (Som and Sahu, 1999 and Gobel et al., 1994). In order for this type of reinforcement mode to be significant, there is a consensus that the subgrade CBR should be less than 3 (Barksdale et al., 1989).

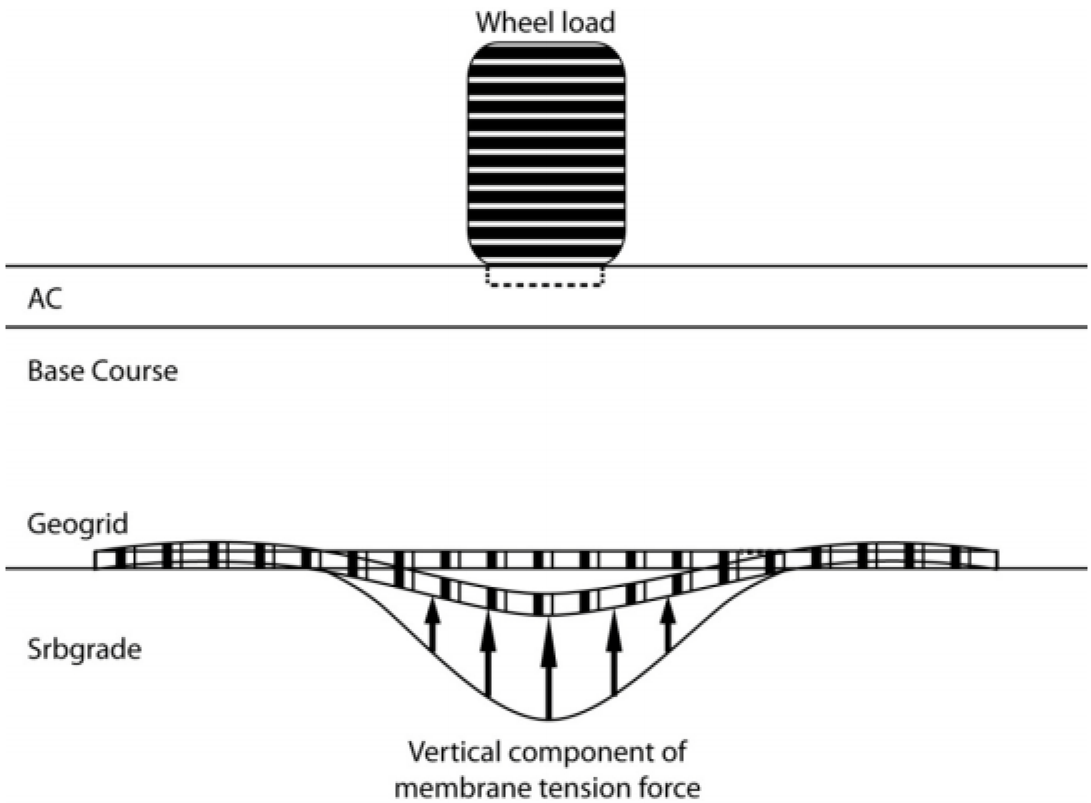

Figure 2. 5: Schematic illustration of tension membrane mechanism (Perkins 2001)

2.5. Numerical Analyses of Geosynthetic Reinforced Pavement

Several numerical studies were performed to analyze pavement sections and assess the improvements due to the geosynthetic reinforcement. Most of the numerical studies were performed using the finite element method. Different constitutive models were used to determine the model that is most capable of representing the stresses and deformations in a reinforced pavement. Table 2.1 summarizes the constitutive models to model the asphalt concrete layers, base course layers, subgrade layers, reinforcement and interface that were reported in literature to investigate reinforced flexible pavement.

Conventional plasticity models with isotropic hardening rules are well suited for the prediction of permanent strain under a single cycle of load application. Repeated application of stress to the same level as that experienced during the initial load cycle results in purely elastic behavior with no accumulation of permanent strain. Plasticity based material models with kinematic hardening rules need to predict the accumulation of permanent strain in pavement layers under the application of repeated traffic loads.

The use of plasticity models with kinematic hardening rules allows for the growth of permanent surface deformation to be better predicted. Plasticity models of this type have been available since the 1970’s (Dafalias, 1975) but have only recently been applied to pavement modeling. McVay and Taesiri (1985) described a bounding surface plasticity model that was developed and compared to results from repeated load triaxial tests.

The bounding surface concept is general and permits the inclusion of any type of formulation for a yield surface, which is taken to represent the formulation for the bounding surface.

The finite element analyses results of Barksdale et al. (1989) showed that the bearing capacity ratio value increased by increasing the stiffness of the reinforcement. Increasing the thickness of the AC or base course layers reduced the magnitude of the bearing capacity ratio. The optimal location of the reinforcement was found to be between the bottom of the base course layer and 1/3 up into the base layer.

Miura et al. (1990) performed a finite element analysis on reinforced and unreinforced pavement sections. They compared the results of the finite element analysis with the experimental measurements on similar sections. The results indicated that the prediction of finite element analysis was not in agreement with the behaviour observed in the tests. The predicted reduction in surface displacements was 5% compared to an actual displacement reduction of 35% measured by the tests.

Dondi (1994) used finite element based software package to conduct a three-dimensional finite element analysis to model the geosynthetic-reinforced pavements. The results of this study indicated that the use of the reinforcement resulted in an improvement in the bearing capacity of the subgrade layer and a reduction in the shear stresses and strains on top of it. In addition, the vertical displacements (rutting) was also reduced by 15 to 20 % due to the intrusion of geosynthetic reinforcement. With an empirical power expression, the life of the reinforced sections was estimated to be increased by a factor of 2 to 2.5 as compared to the unreinforced section.

Wathugala et al. (1996) used the finite element software package to formulate the finite element model for pavements with geogrid reinforced bases. The results of the analysis were compared with an unreinforced pavement sections at the same geometry and material properties. The comparisons indicated that the inclusion of geogrid reinforcement reduced the permanent deformations (rutting) by 20% for a single load cycle. This level of improvement was related to the flexural rigidity of the geosynthetics caused by the model presentation used by the authors (Perkins, 2001).

Leng and Gabr (2005) conducted a numerical analysis using FE software to investigate the performance of reinforced unpaved pavement sections. Their previous experimental work was used to validate the performance of the developed finite element model of the geosynthetic reinforced pavements Leng and Gabr (2002). The researchers reported that the performance of the reinforced section was enhanced as the modulus ratio of the aggregate layer to the subgrade decreased. The critical pavement responses were significantly reduced for higher modulus geogrid or better soil/aggregate-geogrid interface property.

Kwon et al. (2005) developed a finite element model for the response of geogrid reinforced flexible pavements. The results of this study indicated that the benefits of including geogrids in the granular base-subgrade interface could be successfully modeled by considering residual stresses concentrations assigned just above the geogrid reinforcement. These residual stresses were found to considerably increase the resilient moduli predicted in the base and subgrade of a pavement section modeled. In addition, the study indicated that low subgrade vertical strains were also predicted to demonstrate a lower subgrade rutting potential when residual stress concentrations were assigned in the vicinity of the geogrid.

Nazzal et al. (2010) developed a finite-element model with PLAXIS 2D software package to investigate the effect of placing geosynthetic reinforcement within the base course layer on the response of a flexible pavement structure. Finite-element analyses were conducted on different unreinforced and geosynthetic reinforced flexible pavement sections. The results of this study demonstrated the ability of the modified critical state two-surface constitutive model to predict, with good accuracy, the response of the considered base course material at its optimum field conditions when subjected to cyclic as well as static loads. The results of the finite-element analyses showed that the geosynthetic reinforcement reduced the lateral strains within the base course and subgrade layers. Furthermore, the inclusion of the geosynthetic layer resulted in a significant reduction in the vertical and shear strains at the top of the subgrade layer. The improvement of the geosynthetic layer was found to be more pronounced in the development of the plastic strains rather than the resilient strains. The reinforcement benefits were enhanced as its elastic modulus increased.

2.6. Summary of Literature Findings

Based on the above literature review, it is clearly demonstrated that geogrid base reinforcement benefits depend on a number of factors. These include: location of geogrid layer within the base course layer, base course thickness, strength/stiffness of subgrade layer, and the geometric and engineering properties of the geogrids. Studies in the literature have shown that the weaker the subgrade, the higher the percent reduction of rutting, and there was little improvement obtained for subgrades with high CBR (Cancelli and Montanelli 1999, Perkins 1999). The benefit of geogrid generally decreases with an increase in the thickness of the base course and becomes insignificant when the base course is very thick (Kinney et al. 1998, Collin et al. 1996). The location of geogrid within the base layer in the pavement system is very important to its reinforcement effectiveness (Perkins 1998, Webster 1993). The optimum location of geogrid depends on many factors, such as subgrade strength and base course thickness. For a thin base course layer, placing geogrid at the subgrade/base course interface gives better performance and that the geogrid should be placed at the upper one third of the base course layer for a thicker base course layer (Hass et al. 1988, Al-Qadi et al. 2008). However, no benefits were expected when a single layer of geogrid was placed at the midpoint or higher within the base layer for a thick base course over very soft flexible subgrades (Hass et al. 1988). Current available information does not provide clear quantifiable relationship between the performance of geogrid base reinforcement and any of the geogrid properties, such as aperture geometry, stability modulus, flexural stiffness, junction strength, and tensile modulus (Berg et al. 2000). It is believed that these properties work together to determine the performance of geogrid. Any property alone may not be enough to characterize the performance of geogrid.

Table 2. 1: finite element studies of reinforced pavements

Author	**Analysis Type**	**AC Model**	**BC Model**	**Subgrade Model**	**Reinforcement Model**	**Interface Model**
Barksdale et al. (1989)	Axi-symmetric	Isotropic Nonlinear Elastic	Anisotropic Nonlinear Elastic	Isotropic Nonlinear Elastic	Linear Elastic	Linear Elastic-Perfectly-Plastic
Miura et al (1990)	Axi-symmetric	Isotropic Nonlinear Elastic	Isotropic Nonlinear Elastic	Isotropic Nonlinear Elastic	Isotropic Nonlinear Elastic	Linear Elastic Joint element
Dondi (1994)	3D	Isotropic Nonlinear Elastic	Isotropic Drucker-Prager Model	None	Isotropic Nonlinear Elastic	Elastoplastic Mohr-Coulomb model
Whathugala et al. (1996)	Axi-symmetric	Isotropic Drucker-Prager Model	Isotropic Drucker-Prager Model	Hiss δ_0	Isotropic Von Mises	Non Isotropic Elastoplastic
Perkins (2001)	3D	Linear Elastic-Perfectly-Plastic	Bounding Surface Model	Bounding Surface Model	Orthotropic linear elastic	Elastoplastic Mohr-Coulomb model
Leng and Gabr (2001)	Axi-symmetric	None	Isotropic Drucker-Prager Model	Drucker-Prager Model	Isotropic E-P-P	Elastoplastic Mohr-Coulomb model
Kwon et al. (2005)	Axi-symmetric	Isotropic Linear Elastic	Nonlinear Elastic	Isotropic Linear Elastic	Isotropic Linear Elastic	Isotropic Linear Elastic
Abu-Farsakh et al. (2009)	Axi-symmetric	Linear Elastic-Perfectly-Plastic	Drucker-Prager Model	Drucker-Prager Model	Isotropic Linear Elastic	Fully Bonded
Nazzal et al. (2010)	Axi-symmetric	Linear Elastic-Perfectly-Plastic	Critical State	Cam-Clay	Isotropic Linear Elastic	Fully Bonded

CHAPTER THREE
MATERIALS AND METHODOLOGY

3.1. Introduction

The scope of this chapter is to build and develop a numerical model to simulate a road embankment reinforced with geogrid laid on weak soil. The description of study area was presented. Material parameter for soil profile is correlated from test result conducted by a researcher from study area. Geogrid material parameter is also presented based on standard. Constitutive models that represent the behaviour of both embankment material, geogrid and soft soil materials are decided too.

In order to build a realistic model for a road embankment reinforced with geogrid laid on soft soil, the modelling process should involve a series of challenges; including the appropriate approach for simulation, dimension of the model, mesh geometry, boundary positions, selection of parameters used in the analysis and the right choices for the constitutive model that represent the studied soil. In addition, as the FEM is an appropriate technique, it is necessary to carry out a number of preliminary checks, such as mesh sensitivity and distance to the boundary, to ensure accurate numerical analysis.

3.2. Description of study area

3.2.1. Location

The study area is located in Oromia regional state, 37km southeast of Addis Ababa and 10km northwest of Bishoftu having latitude and longitude of $08^{0}48/N$ $38^{0}54/E$ and elevation of 1950m above sea level

The road starts at Kera branching right from the Addis Ababa -to- Dire Dawa highway at an intersection in the town with coordinate of 488940.22E and 971877.281N.

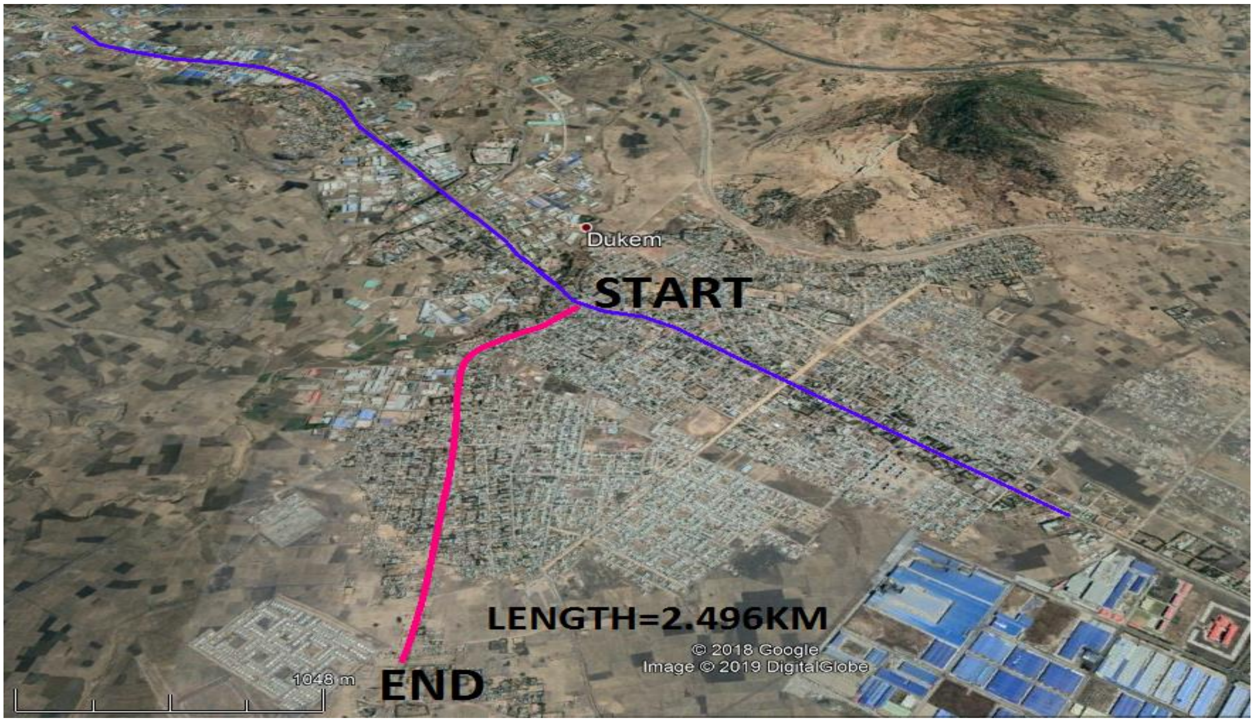

Figure 3. 1: Satellite map of study area

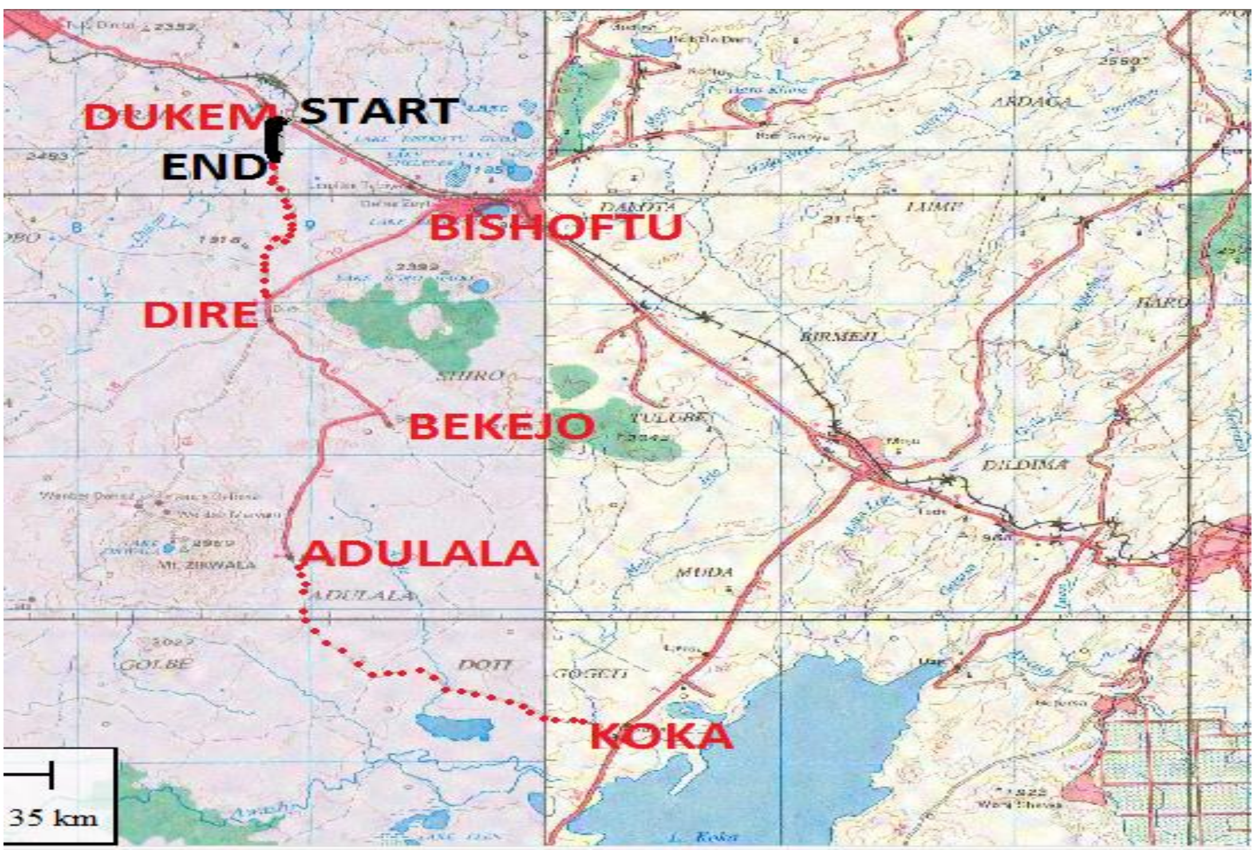

Figure 3.2: Google map of study area

3.2.2. Geology

General geological feature of study area were evaluated aided by the "geological map of Nazret (NC37-15)" with scale of 1:250000, published in 1978 by geological survey of Ethiopia

According to the geological map the geological formation of study area is covered predominantly with four type of geological formation .amongst these formation akaki basalt(scoria and spatter cone with associated basaltic lava flow), rhyolite to minor trachitic lava and pumice , ridge forming trachitic lava, lacustrine deposit cover the majority part of the project

Along the proposed asphalt road the field observation signifies that the whole stretch is covered by lacustrine deposits of black cotton soil. The lacustrine deposit composes predominantly of highly plastic silt clays.

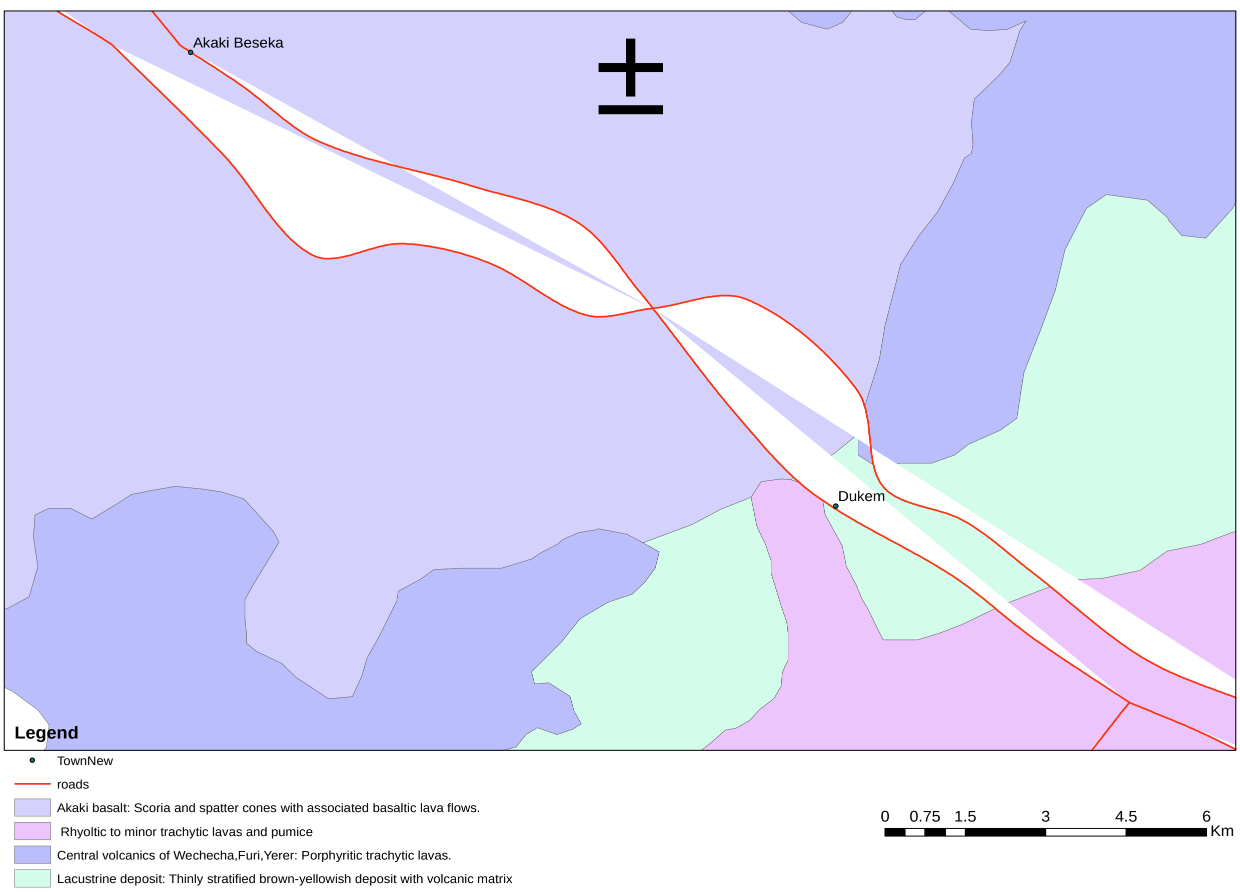

Figure 3.3: Geology of Dukem areas and esp. study area

3.3. Development of material parameter

3.3.1. Sub-grade soil

The sub-grade soil investigation is one of the basic tasks in this study it is about assessing its general suitability to be used as foundation material. The sub grade investigation carried includes soil extension survey, sampling, laboratory test, and finally interpretation of result. The samples were taken from test pits at every 500m with in 25000m.the major soil test conducted on these soil sample include classification test, modified proctor density and three point California bearing ratio (CBR) test.

Field investigation for sub-grade soils

Field and laboratory works are mainly conducted for sub-grade soil investigation. Test pitting, sampling and testing of sub-grade materials was the voluminous task. A total of six sub-grade soil samples were taken, at interval of 500m. All the samples are subjected to both classification test (Atterberg limit and Grain size analysis) and strength test (CBR and swell test). The field investigation task was aimed at assessing the actual condition of the alignment soil that includes:

- Visual sub grade soil extension survey,
- Test pitting and taking of representative soil samples.

The soil extension survey was carried out based on the observation made in the test pits excavation and by observations made on the nearby natural ground exposures along the road corridor. In general, the sub-grade soils along the route are found to be highly expansive silty clay soils. Overlying the problematic soils, there is a thin layer of granular materials for placing the existing cobble stones.

Test pit logging and sampling

Test pits with approximate radius of 50cm were dug to an average depth of 5m every 500m, staggered left and right of centerline of the road. The test pit helps in observing thickness and characteristics of the encountering soil layers and as well as in sampling of the sub grade material for the required laboratory tests. The log description is presented in the table below.

Laboratory investigation findings of sub-grade soils

After visual inspection, sub-grade materials collected from the test pits were taken to the laboratory, on which CBR and classification tests are conducted.

Generally speaking, soils with low plasticity (low liquid limit and plasticity index) and fewer fines are more stable physically and mechanically than high plastic, fine soils. A total of six samples were collected at the interval of 500m and tested for classification and CBR.

Table 3. 1: Sub-grade Soil Laboratory Test Results

No.	Station	Atterberg limit (AASHTO T89 &		Soil Classification (AASHTO M-145)	Proctor Density (AASHTO T-180)		96 hours Socked CBR Value	
		LL	PI		O.M.C (%)	Max. Dry Density (kg/m^3)	At 2.5mm	Swell (%)
1	0+000	81.5	36.5	A-7-6	27	1451	0.98	12.75
2	0+500	71.5	21.3	A-7-6	24.5	1495	0.98	11.1
3	1+000	43.5	21.0	A-7-6	23.2	1580	2.15	3.27
4	1+500	41.0	19.5	A-7-6	20.5	1640	1.37	5.47
5	2+000	72.8	34.1	A-7-6	28.5	1457	0.88	9.17
6	2+496	58.9	27.7	A-7-6	22	1448	0.88	7.59

The data from the laboratory test results (Table-3.1) reveal that the liquid limits are mainly clustered between 41 and 81. The PI values range from 19.55 to 36, depicting a property of moderately to highly plastic soil. The classification test showed that these soils fall into A-7-6, as per AASHTO soil classification system, indicating a poor material requiring improvement.

In addition to the AASHTO soil classification tests, the 4 days soaked CBR tests were performed on the soil samples to determine the sub-grade shear strengths. Wherever a soil with a CBR value of less than 3% is occurring within the design depth, it should be replaced with a better material having a good bearing strength. Analysis of the laboratory 4-days soaked CBR at 95% MDD and percent swell values performed on samples collected from the existing road bed indicates that the material have a CBR value within the range of 0.88% to 2.15% and swell value of 3.27% to 12.75% as measured after the four days soaked CBR specimen.

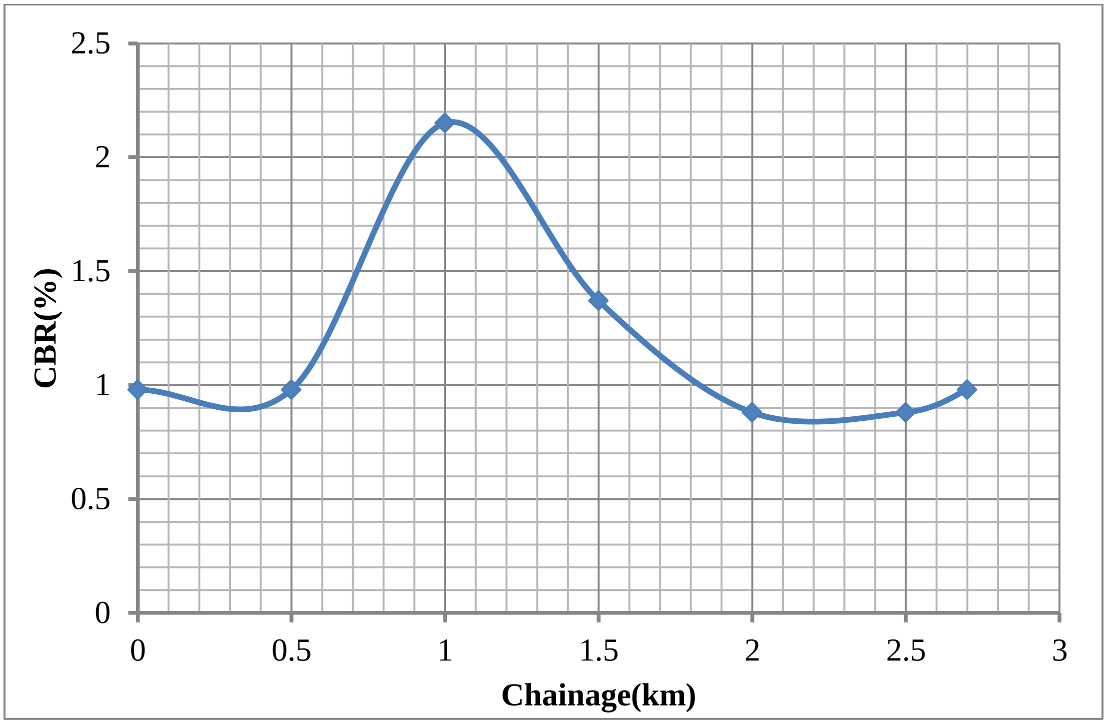

Figure 3. 4: CBR Distribution of Subgrade Samples along the route

The reasonable selection on the study plot was examined based on the CBR (i.e. the minimum subgrade strength). Further correlation on engineering properties of soil sub-grade was performed for the chosen study plot (i.e. station 2+000 minimum subgrade strength).

Basic geotechnical properties

The general properties required for simulating the soil material as per Mohr Coulomb model mainly includes: bulk unit weight (γ, kN/m^3), saturated unit weight (γsat, kN/m^3), the at-rest coefficient of horizontal soil stress (K_o)…etc. The bulk unit weight (γsat, kN/m^3) of the cohesive soil has calculated (Eq. 3.1) by using the index property correlation recommended by Carter and Bentley (2016). Table A-3 in the appendix

$$\gamma_{sat} = \gamma_d(1 + w) \quad [3.1]$$

$$K_o = 1 - sin\varphi \quad [3.2]$$

Strength Characteristics

The strength characteristics required for simulating the soil material as per Mohr Coulomb model mainly includes: effective cohesion (c', kN/m^2), effective angle of internal friction (ϕ', ^{o}), initial angle of dilatancy (ψ, ^{o})…etc.

A relationship between effective shear strength and plasticity index for remoulded clays has been established by Gibson (1953), as indicated in Eq. 3.3.

$$\phi' = 0.085PI^{1.4} - 0.75PI + 31.9 \quad [3.3]$$

The effective cohesion value (c') had empirically correlated to effective friction angle (ϕ'), as recommended by (Look, 2007) Table A-4 in the appendix.

Stiffness Characteristics

The elastic deformation parameters of the soil material required as per Mohr Coulomb model includes: Young's modulus (E) and Poisson's ratio (ν).

Typical values for Young's modulus and Poisson's ratio of clay materials (after Gordon, 1978) was correlated and presented in Appendix A-5

3.3.2. Embankment

Basic geotechnical properties

The general properties required for simulating the soil material as per Mohr Coulomb model mainly includes: bulk unit weight (γ, kN/m^3), saturated unit weight (γsat, kN/m^3), the at-rest coefficient of horizontal soil stress (K_o)…etc. The bulk unit weight (γsat, kN/m^3) of the cohesive soil has calculated (Eq. 3.1) by using the index property correlation recommended by Carter and Bentley (2016). Appendix A-6

$$\gamma_{sat} = \gamma_d(1 + w) \quad [3.4]$$

$$K_o = 1 - sin\varphi \quad [3.5]$$

Strength Characteristics

The strength characteristics required for simulating the soil material as per Mohr Coulomb model mainly includes: effective cohesion (c', kN/m^2), effective angle of internal friction (ϕ', ^{o}), initial angle of dilatancy (ψ, ^{o})…etc.

A relationship between effective shear strength and plasticity index for granular soils has been established by Stark and Eid (1997), Appendix A-7 as indicated in Eq. 3.6.

$$\phi' = 43 - 10 \log PI \qquad [3.6]$$

The effective cohesion value (c') of cohesion less soil is recommended to be zero, while A nominal value for c = 1kPa is adopted to ensure numerical stability.

Stiffness Characteristics

The elastic deformation parameters of the soil material required as per Mohr Coulomb model includes: Young's modulus (E) and Poisson's ratio (ν).

The stiffness parameter (Young's modules,E) has been correlated with CBR value based on the poisons ratio (after Elsa Eka Putri *et. al,* 2012)

$$E = 863.82 * CBR\ (kPa) \quad \text{at } \nu=0 \qquad [3.7]$$

$$E = 840.53 * CBR\ (kPa) \quad \text{at } \nu=0.3 \qquad [3.8]$$

$$E = 751 * CBR\ (kPa) \quad \text{at } \nu=0.4 \qquad [3.9]$$

Typical values for Young's modulus and Poisson's ratio of clay materials (after Gordon, 1978) was correlated and presented in Appendix A-8

Table 3. 2: subgrade and embankment materials

Soil Parameter	Subgrade		Embankment	Unit
	Layer - I	Layer - II		
Material model	MC	MC	MC	-
Depth	0.00 - 2.50	2.50 - 5.00	-	(m)
Type of material behaviour	Undarined	Undarined	Drained	-
Bulk unit weight (γ)	18.4	19.1	20.2	kN/m3
Saturated unit weight (γsat)	18.4	19.1	20.2	kN/m3
Over-consolidation ratio	1	1	1	-
Poisson's ratio (ν)	0.35	0.35	0.3	-
Young's modulus (E)	1000	2000	4000	kN/m2
Cohesion (Cref)	13	17	1	kN/m2
Friction angle (ϕ')	18	22	34	º
Dilatancy angle (ψ)	0	0	4	º
Lateral earth coefficient K_0	0.69	0.63	0.44	-

3.3.3. Asphalt concrete (AC) Layer

In this study, the linear elastic model was used to describe the behaviour of asphalt concrete (AC) layer. Pavement properties used after (Jacobs..M,Frunt.M, and rering (2016)

Table 3.3. Pavement material properties

Pavement Properties	Asphalt Concrete	unit
EA	1.29E+06	kN/m
EI	1.07E+05	kNm^2/m
W	2.2	kN
ν	0.15	-

3.3.4. Geogrid

A linear elastic model was used to describe the behaviour of geogrid material since the induced strain in the geogrid is very small (<1%) and is considered within the linear elastic range of the geogrid layer. Five types of geogrid with different equivalent elastic modulus were used in the finite element analysis to investigate the effect of geogrid tensile strength on pavement response and performance. A summary of these properties are shown in Table 3.4. Material property of geogrid after Jie Gu, 2011.

Table 3. 4: Geogrid material properties (after Jie Gu, 2011).

Geogrid type	Reference Name	Elastic Modulus [kPa]	Area [m]	EA [kN/m]
Geogrid Type I**	GGI	585,100	0.06	35,000
Geogrid Type II**	GGII	860,000	0.06	52,000
Geogrid Type III**	GGIII	950,000	0.06	57,000

**Parameters from the manufactures

3.3.5. Traffic loading

The loading model in this study included applying gravity loads in the first load step of the analysis, then applying loading representative of a 80kN single axle wheel loading, which is the standard load known as equivalent single axle load (ESAL) recommended by ERA (2013).

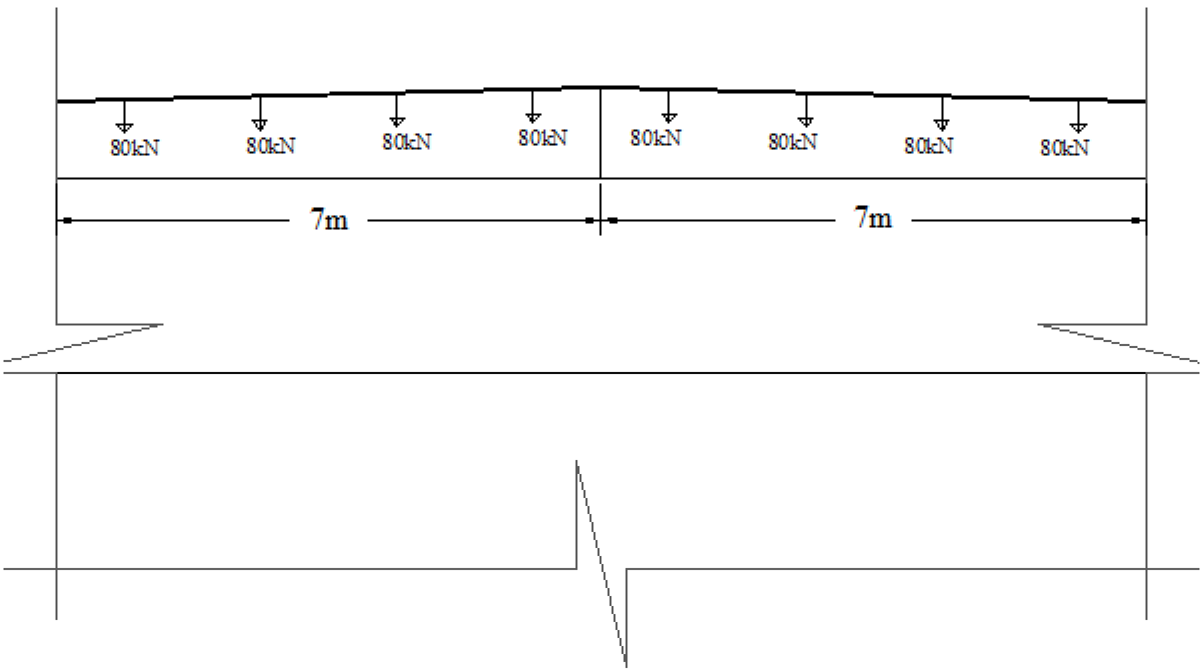

Figure 3. 5: Layout of traffic loading as per ERA manual 2013.

Converting the applied point traffic loading (ESAL of 80kN) into working linear distributed load:

$$P_d = \frac{\sum F}{x} = \frac{4*80}{7} = 45.71 \approx 50kN/m^2 \qquad [3.10]$$

3.4. Model development

3.4.1. Preliminary checks to ensure accurate numerical analysis

The accuracy of the finite element model depends not only on the level of sophistication of the material model, but also on the boundary condition of the domain, on the number and type of the elements in to which the domain is discretized and other modeling issues.

Influence of distance to boundary

External boundaries are an artificial representative of real forces, extensions and conditions that define the solution of a finite element model. It is not possible to include real natural extension of a mass of soil or some events applied on it, so finite element code (PLAXIS 2D) enables the user to substitute the reaction of these extensions and events as a restraint, displacements and forces at the boundary. Consequently, the user can quantify these effects and assign them to the studied model with minimum effect on the accuracy of this model. Positions of boundary restraints can significantly affect finite element simulation results. Since the generated reaction forces and displacement in these boundaries can influence the impact of the applied forces on the zones of interest. So to avoid any restriction that reflected on the accuracy of the finite element model, a user should select the location of this boundaries to be sufficient distant from any zone of interest, but at the same time the user should consider them not to be exceedingly far, costing more time in the analyzing process (Ammari, and Clarke, 2016).

The sensitivity analysis was carried out for side boundary as the bottom is depend on soil profile it is stiff enough at 5m deep.

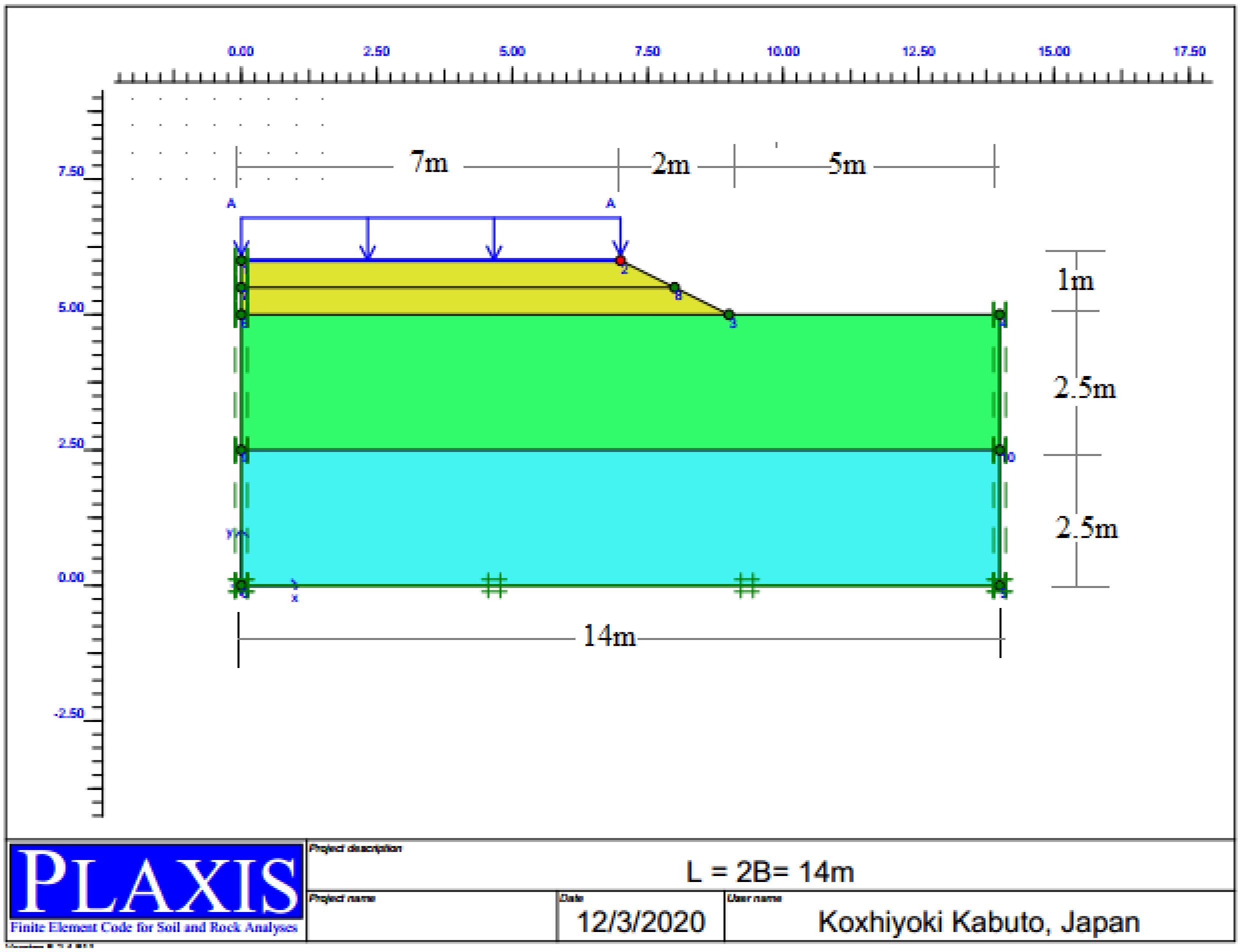

Figure 3. 6: Layout of soil profile

The location of distance to the boundary from the footing center ranged from 2B-12B (Killen, 2012).

The sensitivity analysis was conducted on selected 7m road cross-section the vertical displacement was measured at point A, B, C where A is below the embankment; B is between soft clay and stiff clay; and C is at the toe of slope.

The accuracy of relevant boundary distance is determined by comparing the normalized error for vertical displacement (u_y) at a selected point where the side boundary is located at a distance xB against that of 12B.

Normalized error for vertical displacement, $u_y = \left(\frac{u_{y\,(xB)} - u_{y\,(12B)}}{u_{y\,(12B)}}\right)$

Where: $u_{y\,(xB)}$ - is vertical displacement at the selected point for the case of side boundary is located at (xB) m from the center of the roadway.

$u_{y\,(12B)}$ - is vertical displacement at the selected point for the case of side boundary is located at (12B) m from the center of the roadway.

The flowchart outlining the steps taken to ensure accurate numerical analysis for boundary distance is shown in Figure 3.3.

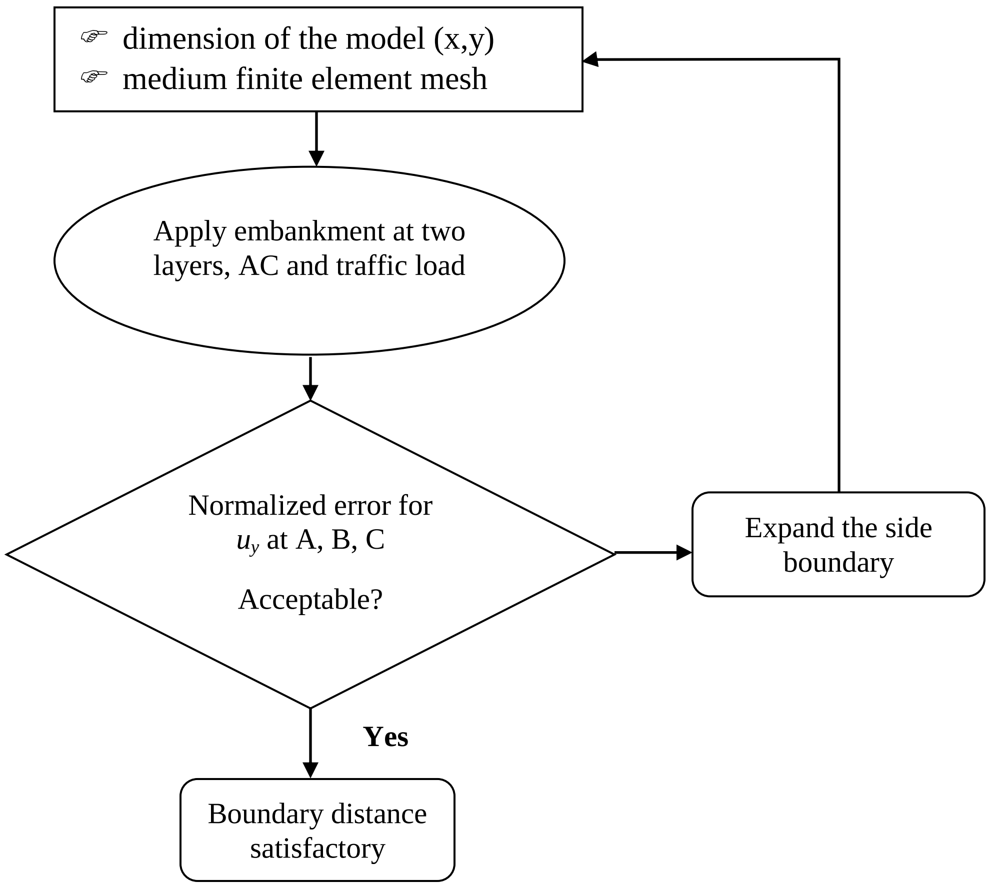

Figure 3. 6: Flowchart outlining preliminary analysis checks for boundary distance

Table 3. 3: Influence of the distance to boundary upon the Vertical displacement of a 7 m road cross-section

Distance to boundary	**Vertical displacement, u_y (mm)**				**Normalized error (%)**			
(B = footing width)	Point A	Point B	Point C	Extreme Uy,max	Point A	Point B	Point C	Extreme
2B	206.14	188.51	8.50	206.14	1.41	1.11	19.17	1.41
4B	205.83	188.58	10.00	205.83	1.56	1.08	4.93	1.56
6B	206.09	188.75	10.10	206.09	1.44	0.99	3.99	1.44
8B	209.70	191.04	10.72	209.70	0.29	0.21	1.90	0.29
10B	209.00	190.38	10.39	209.00	0.04	0.14	1.23	0.04
12B	209.09	190.64	10.52	209.09	0.00	0.00	0.00	0.00

Table 3. 4: Influence of the distance to boundary upon the horizontal displacement of a 7 m road cross-section

Distance to boundary	**Horizontal displacement, u_x (mm)**				**Normalized error (%)**			
(B = footing width)	Point A	Point B	Point C	Extreme, Ux,max	Point A	Point B	Point C	Extreme
2B	0.00	0.00	37.79	56.37	0.00	0.00	2.95	2.18
4B	0.00	0.00	37.58	56.23	0.00	0.00	2.40	1.93
6B	0.00	0.00	37.19	56.13	0.00	0.00	1.34	1.74
8B	0.00	0.00	36.70	55.17	0.00	0.00	0.00	0.00
10B	0.00	0.00	36.70	55.45	0.00	0.00	0.00	0.51
12B	0.00	0.00	36.70	55.17	0.00	0.00	0.00	0.00

Table 3. 5: Influence of the distance to boundary upon the effective stress of a 7 m road cross-section

Distance to boundary	**Effective stress , σ_{yy} (kN/m2)**	**Normalized error (%)**
(B = footing width)	Extreme	Extreme
2B	163.59	1.08
4B	163.08	0.77
6B	163.02	0.73
8B	161.95	0.07
10B	161.80	0.03
12B	161.84	0.00

It appears that positioning the boundary closer than 2B to the center of the footing induces more Vertical displacement (i.e. around 19%) in the road embankment. The distance to the boundary from the center of the footing is conservatively chosen at 4B for all the subsequent FEA in which the vertical displacement is quite low (maximum error is less than 5%, which is negligible normalized error).

3.4.2. Mesh sensitivity analysis

The influence of the number of elements upon the accuracy of the finite element model was investigated by conducting a mesh sensitivity analysis. Mesh sensitivity analysis was conducted for a reasonably selected 4B boundary distance from the center where the accuracy of medium and fine meshes are compared against the very fine (v_f) meshes.

The vertical displacement (u_y) was examined for the mesh sensitivity analysis as the settlement performance of the geogrid reinforced road embankment is the one of focus of this thesis. u_y was measured at the points A, B and C, where A is below the embankment; B is between soft clay and stiff clay; and C is at the toe of slope (Table 3.7).

The accuracy of medium and fine meshes is determined by comparing the normalized error for vertical displacement (u_y) against very fine meshes.

Normalized error for vertical displacement, $u_y = \left(\frac{u_{y,vf} - u_y}{u_{y,vf}}\right)$

Where: u_y - vertical displacement at the selected point for the medium and fine meshed elements

$u_{y,vf}$ - is vertical displacement at the selected point for very fine meshed elements

In addition to checking convergence of displacement with an increasing number of elements, the mesh was also checked for discontinuities at inter-element boundaries. Discontinuities typically occur in regions of rapid changes of stress and strain, i.e. beneath the edge of embankment, and can be overcome by refining the mesh in these regions.

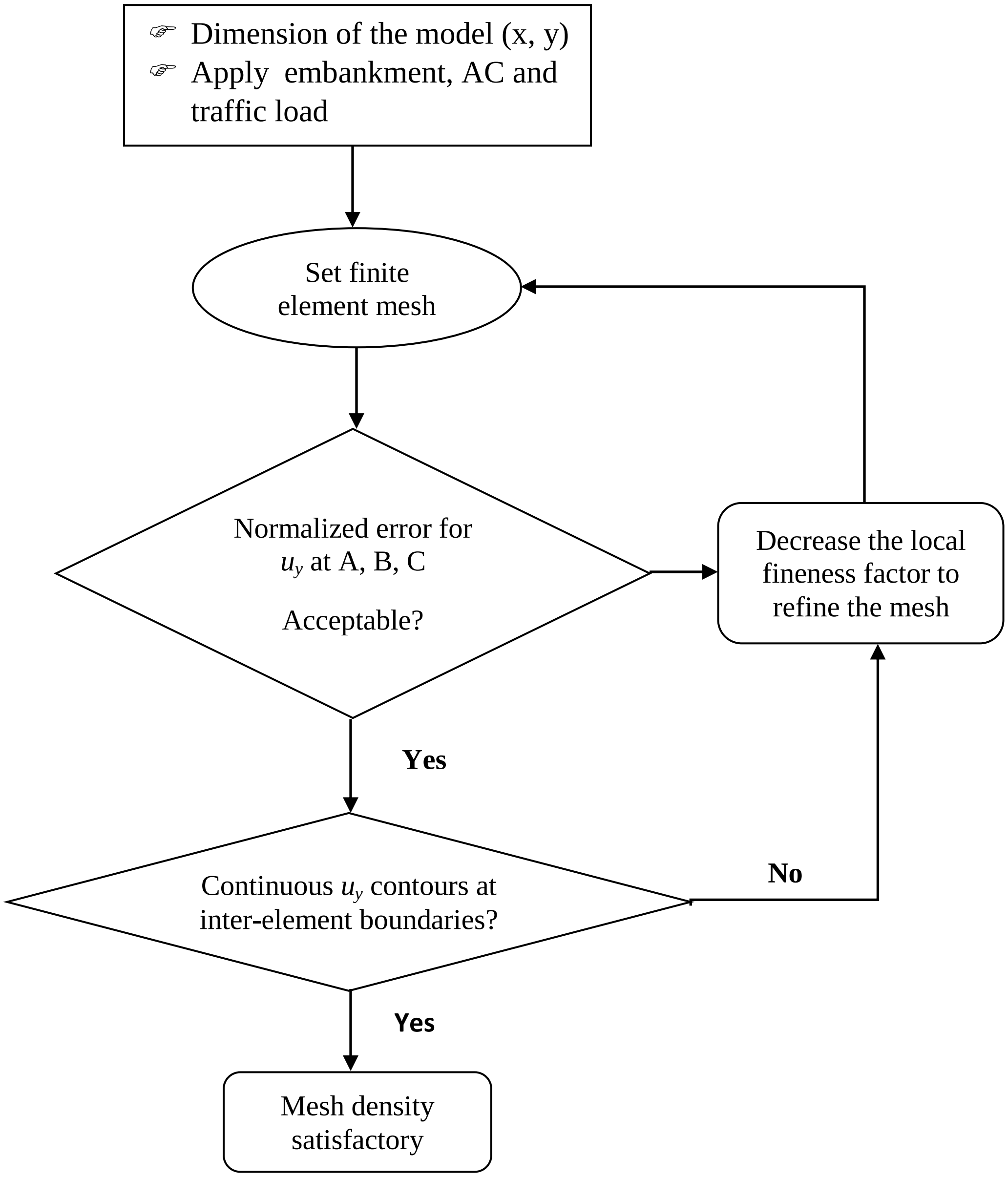

Figure 3. 7: Flowchart outlining preliminary analysis checks for mesh density

The number of elements used for each mesh and the normalized error for the vertical displacement is shown in Table 3.4. It is clear that the values for medium and fine meshes are converging towards the very fine mesh and also the normalized error between the fine and very fine meshes for the vertical displacement is quite low (maximum error is no greater than 5%).

Table 3. 6: Influence of the mesh sensitivity on the vertical displacement at points A, B and C

Mesh	**Vertical displacement, u_y (mm)**				**Normalized error (%)**			
	A	B	C	Extreme Ux,max	A	B	C	Extreme
Coarse	209.70	190.95	10.68	209.70	2.0	1.3	7.0	2.0
Medium	207.83	189.58	10.60	207.83	1.1	0.6	6.1	1.1
Fine	206.44	188.95	10.14	206.44	0.4	0.3	1.6	0.4
Very fine	205.57	188.48	9.98	205.57	0.0	0.0	0.0	0.0

Table 3. 7: Influence of the mesh sensitivity on the horizontal displacement at points A, B and C

Mesh	**Horizontal displacement, u_x (mm)**				**Normalized error (%)**			
	A	B	C	Extreme Ux,max	A	B	C	Extreme
Coarse	0.00	0.00	37.69	56.46	0.0	0.0	0.7	0.6
Medium	0.00	0.00	37.58	56.23	0.0	0.0	0.4	0.2
Fine	0.00	0.00	37.41	56.02	0.0	0.0	0.0	0.0
Very fine	0.00	0.00	37.43	56.11	0.0	0.0	0.0	0.0

Table 3. 8: Influence of the mesh sensitivity on the extreme effective stress

Mesh	**Effective tress , σ_{yy} (kN/m2)**	**Normalized error (%)**
	Extreme	Extreme
Coarse	161.87	1.12
Medium	163.08	0.39
Fine	163.52	0.12
Very Fine	163.71	0.00

3.4.3. Modeling of geogrid-soil interface

Interface elements are available in PLAXIS 2D Foundation to model the interaction between smooth and rough surfaces i.e. between geogrid and soil. Interface elements can simulate gap and slip displacements, which are normal and parallel to the interface, respectively. The loss of strength at the interface is modeled with a reduction factor (R_{inter}), which relates the interface strength to the soil strength through friction angle (ϕ) and cohesion (c):

$$c_i = R_{inter} c_{soil} \qquad [3.11]$$

$$tan\varphi_i = R_{inter} tan\varphi_{soil} \leq tan\varphi_{soil} \qquad [3.12]$$

To modeling soil geogrid interaction, interface element has been used at the contact point of soil and geogrid. R_{intr} parameter has been used for definition shear strength between soil and reinforcement. According to Bergado and Teerawattanasuk (2008), R_{intr} has been considered as 0.9 (R_{intr} = 0.9).

3.5. Numerical simulation of geogrid reinforced road embankment

Numerical simulation were performed to know the performance of road embankment when reinforced with geogrid of different stiffness

3.5.1. Geometric modeling

The various configuration of road embankment analyzed was out lined in the following section. The soil profile, which was computed in section 3.2 was adopted for all of the subsequent FEA. The 1 m high of embankment and 7m width road with slope of 1:1.5, 1:2, 1:3 is selected for this analysis , the traffic loading of 50 kPa ,which was considered based on the recommendation of ERA manual 2013 was adopted for all subsequent FEA. The geogrid supposed to reinforce the road embankment was inculsed in different layers and the parametric study was done in order to decide preferable reinforcement layer. It was also considered that three-geogrid type was adapted for simulation, and consequently studied based on their stiffness characteristics. The layout of geometric modeling of road embankment suited for simulation is illustrated below in Figure 3.8.

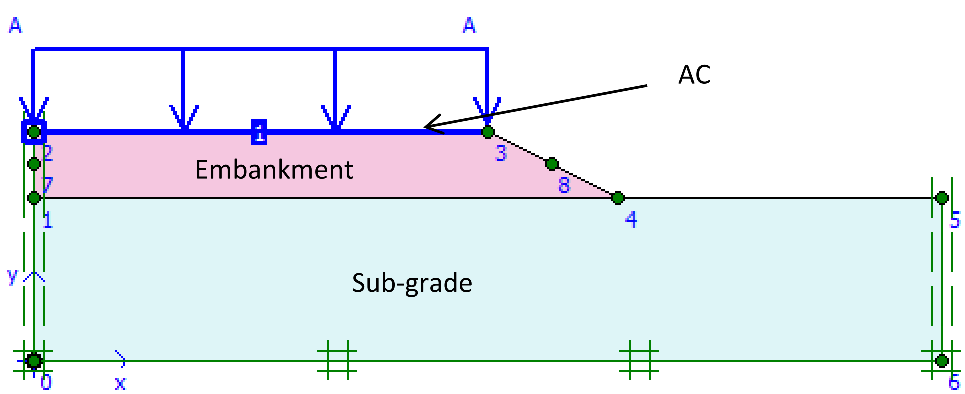

Figure 3. 8: The layout of road embankment

3.5.2. The theoretical framework of numerical simulation

The FE code PLAXIS 2D version 8.6 was used for the plane strain model. This code automatically generates the finite element mesh using triangulation procedure. The apparent subgrade soil, embankment and geogrid were modeled as continuum element using 15-node wedge elements for 2D plane strain code.

All of the subsequent FEA were performed using a small strain formulation and a staged construction process was modeled. Every model in PLAXIS 2D, before the beginning of any calculation phase, starts with the initial phase. The initial phase consists of the soil clusters only in which not all other structural parts are activated. Therefore, this stage calculates the stresses and deformations due to the soil clusters only by means of gravity loading. The undrained behavior is not considered for the initial phase because, in the this phase, the stresses from the self-weights are considered to have occurred for a long period of time making the development of excess pore water pressures irrelevant. Therefore in the initial phase, the option "ignore undrained behavior is selected". For the other phases, this option is not selected, as it is needed to consider the excess pore water pressures during construction and at the end of all loading phases. The embankment construction consists of two phases, each taking 30 days. After the first construction phase, a consolidation period of 725days (Equation 3.13) was introduced to allow excess pore pressures to dissipate. After the second construction phase, another construction period of 725 days was introduced. The geodrid material is "wished-in-place" at preferred position. Then after the pavement material replaced by plate was constructed. And finally traffic loading of 50kN/m^2 was introduced. Hence, a total of four calculation phases have to be defined.

Time rate of consolidation after embankment construction at each phase was considered as equivalent representative of *in-situ* compaction.

$$T_v = {c_v t}/{H_{dr}^2} \quad [3.13]$$

The site compaction in this equivalently defined in this work as a time required for 90% of compaction, where for U of 90%, T_v = 0.848 (Braja M. Das, 2000). Coefficient of consolidation correlated with index properties of the material:

$$C_v = {0.0245}/{(LL + PL)} - 0.0003 \quad [3.14]$$

Hence, $0.848 = {(9.58 * 10^{-4} cm^2/\text{sec}) * t_{90}}/{(50cm)^2} \rightarrow t_{90} = 2.61 * 10^6 sec = 725 days$

The surface wearing (asphalt concrete) construction assumed to be done within 30days. The design period of the urban road is 20years as per ERA manual (2013). Hence, the time predefined for the loading application on the road is days of 20years, which is 7300days.

In any non-linear analysis where a finite number of calculation steps are used, there will be some drift from the exact solution. To limit this drift, tolerated error option is available in PLAXIS 2D. The tolerated error used in these runs for all phases except for few phases is 0.01. A tolerated error of 0.01 was suggested for most type of calculations. A tolerated error of 0.01 means the computed value differs from the exact solution by maximum of 1%. Therefore, this error is considered to be within safe and working limits. The maximum iterations that this version of PLAXIS 2D allows is 100. The default value is 50 iterations. Therefore, this value has worked and has resulted in convergence of the results of all phases.

3.5.3. FEM Matrix

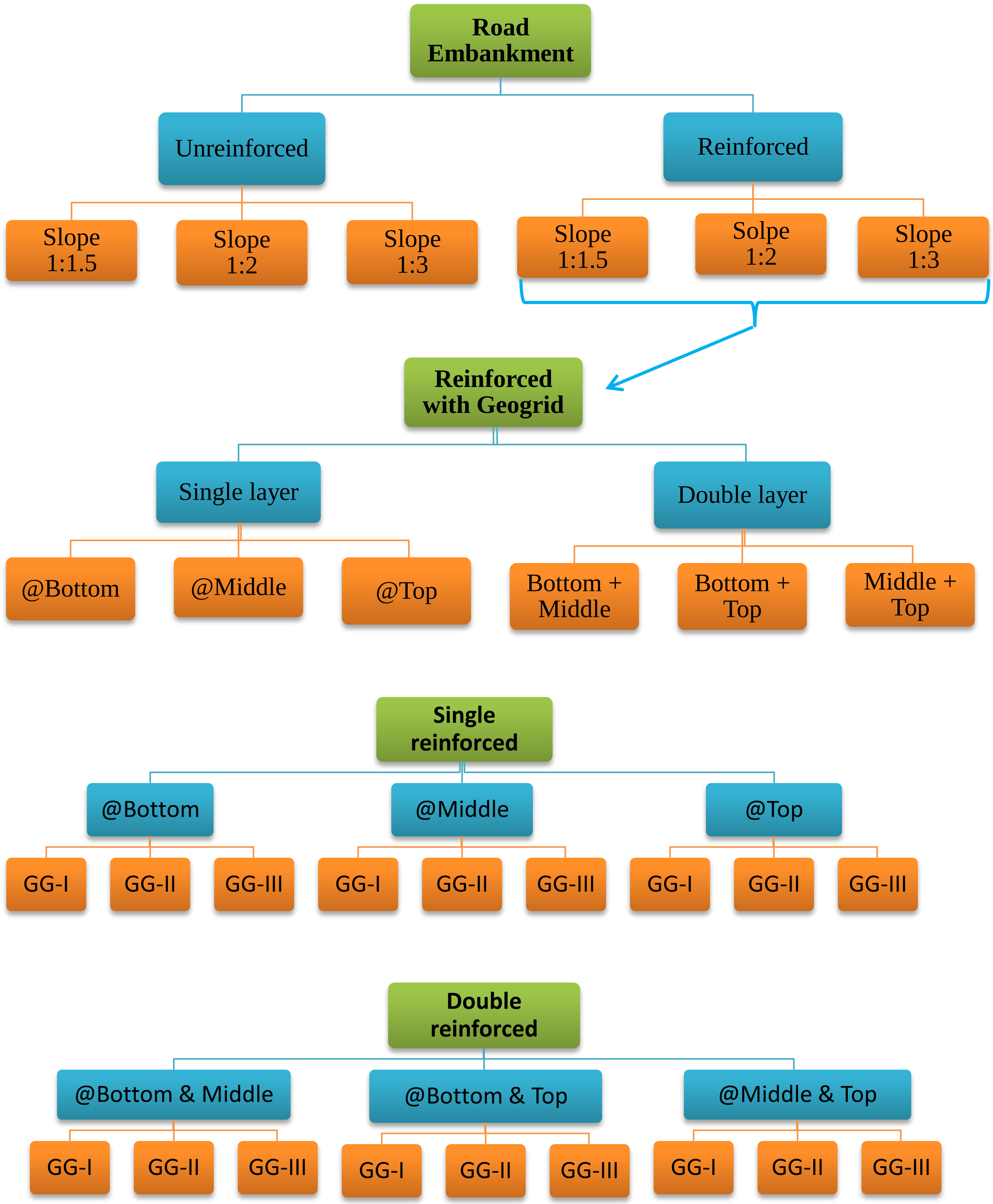

Figure 3. 9: Schematic illustration of FEM matrix

CHAPTER FOUR

RESULTS OF FEA AND DISCUSSION

4.1. Introduction

A series of 57 FEA were conducted using PLAXIS 2D to figure out the vertical and horizontal displacement reduction of road embankment laid on soft soil with various configurations. As described previously that the main focus of this study is to verify the effectiveness of geogrid in road embankment and to develop better understanding of the behavior in weak clay soils. The parametric study mainly relied on the settlement performance of geogrid reinforced road embankment at working load levels (i.e. traffic load).

This chapter scopes a detail result of analysis, influence of key design parameters, validation of the result of FEA and also the discussion of results.

4.2. Detail Results of Finite Element Analysis

The subsequent FEA were conducted using PLAXIS 2D code to examine the effect of key design parameters upon the performance of geogrid reinforced road embankment. Finite element analyses were conducted on unreinforced and reinforced embankment over laid on silty clay to evaluate the influence of various factors affecting the performance of strip footing on reinforced studied soils.

The factors included in this study are: side slope, geogrid application layer and type of geogrid and number of reinforcement layer. For each case, the load-deformation curve, obtained from the finite element simulation, was used to determine lateral deformation, vertical settlement and effective stress of the road embankment.

Table 4.1 demonstrates the summary of the finite element analyses result acquired from PLAXIS 2D plain strain code for both unreinforced and reinforced road embankment at slope of 1:1.5. The outputs obtained from the model are the extreme value of horizontal displacement, vertical displacement and effective stress of each model.

Table 4. 1: The results of FEA of a road embankment at slope of 1:1.5.

Slope V:H	Reinforcement	Reinforcement Layer		Parametric results		
		Layer	at	Horizontal displacement [mm]	Vertical displacement [mm]	Effective mean stress [kN/m^2]
1:1.5	Unreinforced	-	-	56.03	207.79	163.46
	Reinforced with GG-I	Single	Bottom	34.03	140.48	144.09
			Middle	39.24	146.28	144.07
			Top	41.05	148.15	143.79
		Double	Bottom + Middle	32.53	135.66	142.20
			Bottom + Top	32.67	135.38	142.17
			Middle +Top	37.75	140.69	142.13
	Reinforced with GG-II	Single	Bottom	30.26	126.27	139.20
			Middle	35.38	131.54	139.16
			Top	37.30	133.61	138.88
		Double	Bottom + Middle	28.85	121.53	137.30
			Bottom + Top	28.93	121.21	137.29
			Middle +Top	33.89	125.94	137.22
	Reinforced with GG-III	Single	Bottom	26.96	113.07	134.32
			Middle	31.67	117.13	134.27
			Top	33.55	118.99	133.96
		Double	Bottom + Middle	25.15	109.70	132.54
			Bottom + Top	25.64	107.65	132.35
			Middle +Top	30.19	111.46	132.33

As shown in the Figure 4.1, the sample output view of the model. Figure 4.2, 4.3 and 4.4 illustrates the interpreted result of reinforcement vs extreme horizontal displacement, vertical displacement and effective stress of road embankment laid on soft soil at side slope of 1:1.5 respectively.

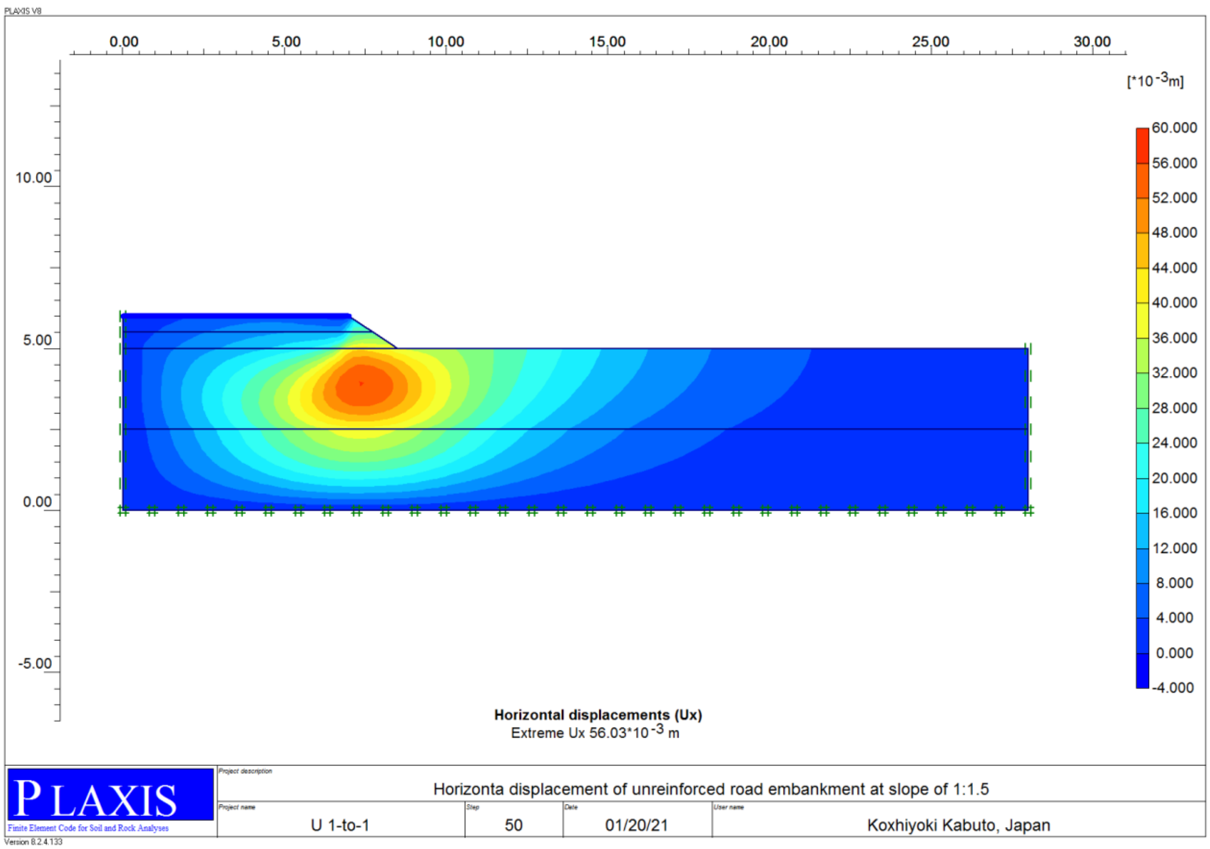

Figure 4. 1: PLAXIS 2D output view (Sample) of horizontal displacement [mm] of unreinforced road embankment at slope of 1:1.5.

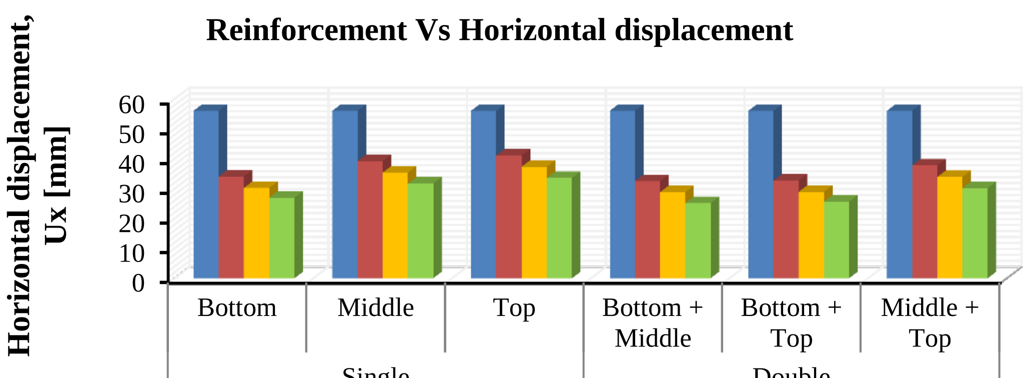

	Bottom	Middle	Top	Bottom + Middle	Bottom + Top	Middle + Top
	Single			Double		
Unreinforced	56	56	56	56	56	56
GG-I	34	39	41	33	33	38
GG-II	30	35	37	29	29	34
GG-III	27	32	34	25	26	30

Reinforcement

Figure 4. 2: PLAXIS 2D output of horizontal displacement [mm] at slope of 1:1.5.

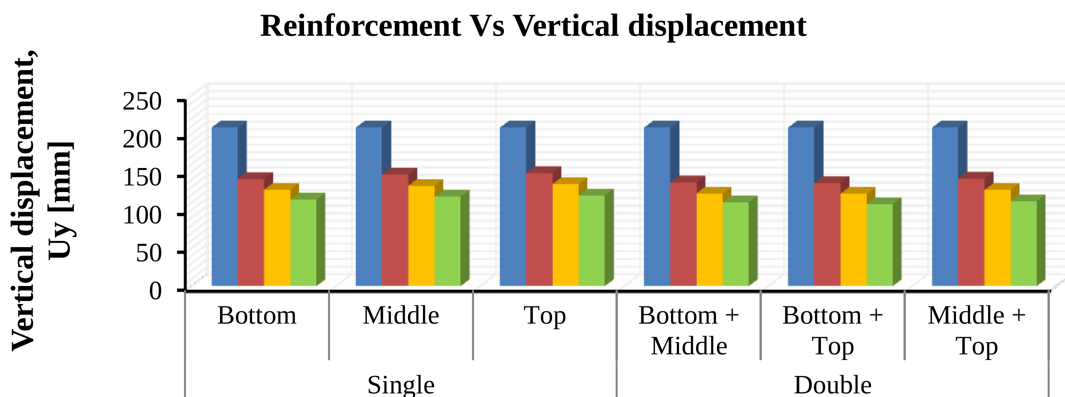

	Bottom	Middle	Top	Bottom + Middle	Bottom + Top	Middle + Top
Unreinforced	208	208	208	208	208	208
GG-I	140	146	148	136	135	141
GG-II	126	132	134	122	121	126
GG-III	113	117	119	110	108	111

Reinforcement

Figure 4. 3: PLAXIS 2D output of vertical displacement [mm] at slope of 1:1.5.

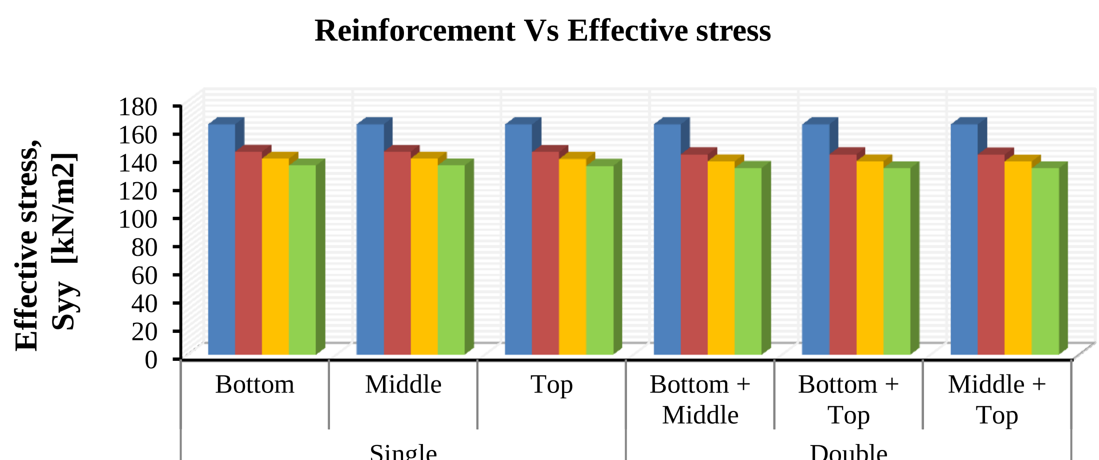

	Bottom	Middle	Top	Bottom + Middle	Bottom + Top	Middle + Top
Unreinforced	163	163	163	163	163	163
GG-I	144	144	144	142	142	142
GG-II	139	139	139	137	137	137
GG-III	134	134	134	133	132	132

Reinforcement

Figure 4. 4: PLAXIS 2D output of effective stress [kN/m^2] at slope of 1:1.5.

Table 4.2 summarizes the FEA results attained from modelling for both unreinforced and reinforced road embankment at slope of 1:2. The outputs obtained from the model are the extreme value of horizontal displacement, vertical displacement and effective stress of each model.

Table 4. 2: The results of FEA of a road embankment at slope of 1:2.

Slope V:H	**Reinforcement**	**Reinforcement Layer**		**Parametric results**		
		Layer	**at**	**Horizontal displacement [mm]**	**Vertical displacement [mm]**	**Effective mean stress [kN/m^2]**
1:2	Unreinforced	-	-	56.02	206.44	163.52
	Reinforced with GG-I	Single	Bottom	26.70	114.36	134.34
			Middle	31.21	117.92	134.34
			Top	33.14	119.41	134.03
		Double	Bottom + Middle	25.29	109.39	132.46
			Bottom + Top	25.40	109.12	132.43
			Middle +Top	29.79	112.25	129.47
	Reinforced with GG-II	Single	Bottom	22.72	101.60	129.60
			Middle	27.50	102.99	129.44
			Top	29.41	104.56	129.11
		Double	Bottom + Middle	21.83	95.04	127.59
			Bottom + Top	21.90	94.78	127.56
			Middle +Top	26.35	96.14	127.50
	Reinforced with GG-III	Single	Bottom	20.03	86.24	124.61
			Middle	23.97	88.43	124.54
			Top	25.73	89.62	124.19
		Double	Bottom + Middle	18.74	81.17	122.73
			Bottom + Top	18.78	80.94	122.71
			Middle +Top	22.54	82.68	122.60

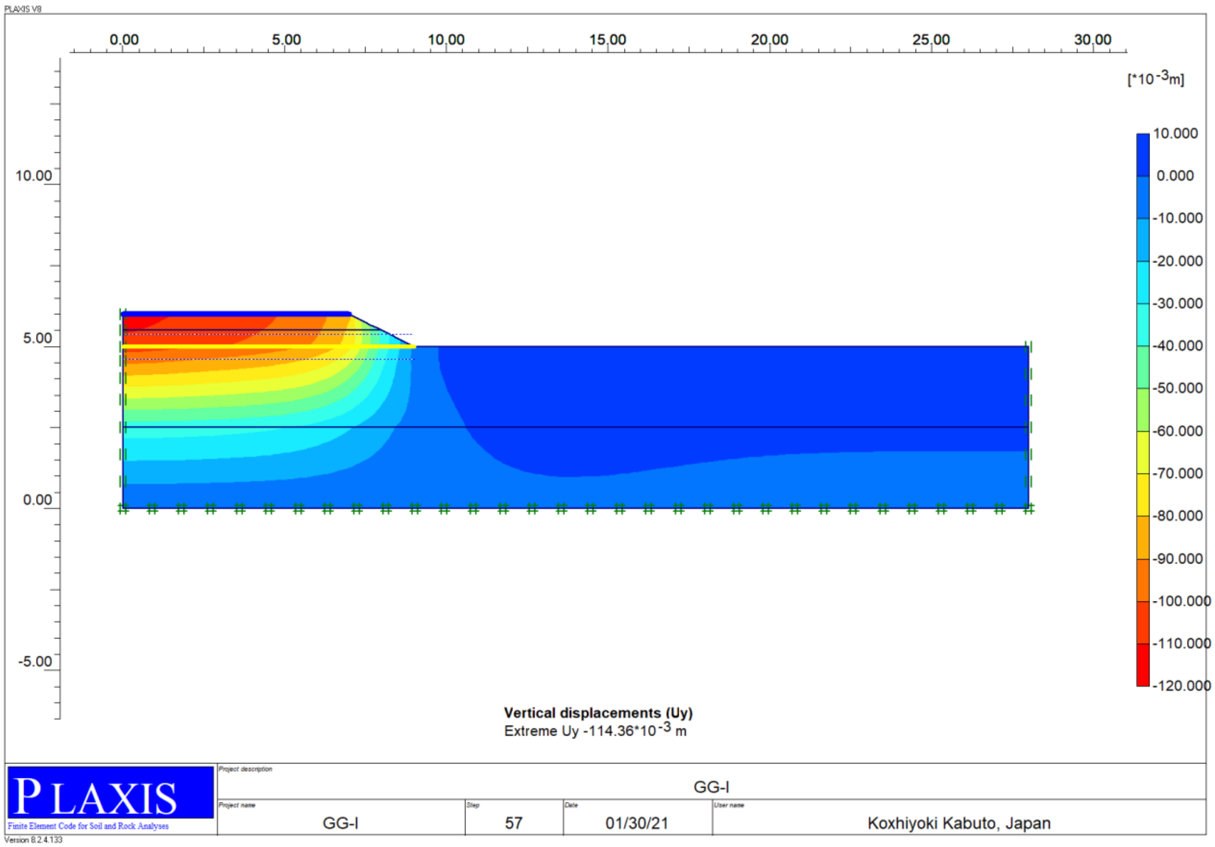

Figure 4. 5: PLAXIS 2D output view (Sample) of vertical displacement [mm] of single layer reinforced road embankment at slope of 1:2.

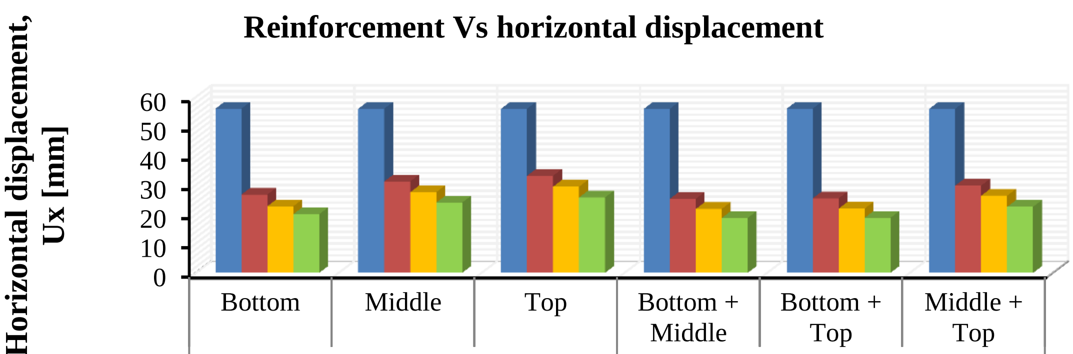

	Bottom	Middle	Top	Bottom + Middle	Bottom + Top	Middle + Top
	Single			Double		
Unreinforced	56	56	56	56	56	56
GG-I	27	31	33	25	25	30
GG-II	23	27	29	22	22	26
GG-III	20	24	26	19	19	23

Reinforcement

Figure 4. 6: PLAXIS 2D output of horizontal displacement [mm] at slope of 1:2.

Reinforcement Vs Vertical displacement

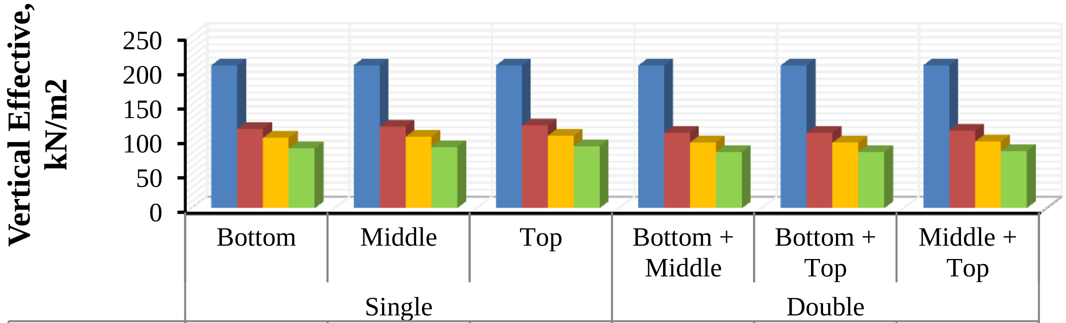

	Bottom	Middle	Top	Bottom + Middle	Bottom + Top	Middle + Top
	Single			Double		
Unreinforced	206	206	206	206	206	206
GG-I	114	118	119	109	109	112
GG-II	102	103	105	95	95	96
GG-III	86	88	90	81	81	83

Reinforcement

Figure 4. 7: PLAXIS 2D output of vertical displacement [mm] at slope of 1:2.

Reinforcement Vs Effective stress

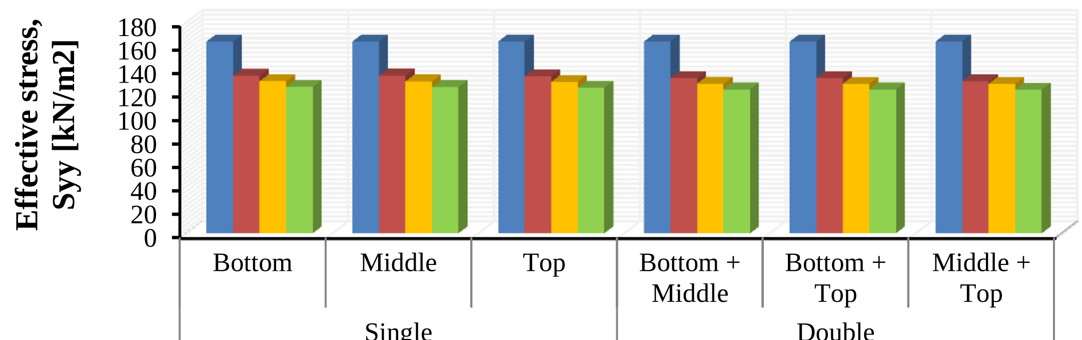

	Bottom	Middle	Top	Bottom + Middle	Bottom + Top	Middle + Top
	Single			Double		
Unreinforced	164	164	164	164	164	164
GG-I	134	134	134	132	132	129
GG-II	130	129	129	128	128	127
GG-III	125	125	124	123	123	123

Reinforcement

Figure 4. 8: PLAXIS 2D output of effective stress [kN/m^2] at slope of 1:2.

Figure 4.5, 4.6, 4.7 and 4.8 outlines the sample output view of the model the interpreted result of reinforcement vs extreme horizontal displacement, vertical displacement and effective stress of road embankment laid on soft soil at side slope of 1:2 respectively.

Table 4.2 presents the FEA results detected from modelling for both unreinforced and reinforced road embankment at slope of 1:3. The outputs obtained from the model are the extreme value of horizontal displacement, vertical displacement and effective stress of each model.

Table 4. 3: The results of FEA of a road embankment at slope of 1:3.

Slope V:H	**Reinforcement**	**Reinforcement Layer**		**Parametric results**		
		Layer	**at**	**Horizontal displacement [mm]**	**Vertical displacement [mm]**	**Effective mean stress [kN/m^2]**
1:3	Unreinforced	-	-	54.95	206.76	163.60
	Reinforced with GG-I	Single	Bottom	25.17	114.66	134.38
			Middle	29.88	117.99	134.44
			Top	32.22	119.38	134.11
		Double	Bottom + Middle	23.82	109.53	132.51
			Bottom + Top	23.94	109.38	132.47
			Middle +Top	28.47	112.29	132.49
	Reinforced with GG-II	Single	Bottom	21.54	101.84	129.47
			Middle	26.27	102.98	129.53
			Top	28.56	104.55	129.20
		Double	Bottom + Middle	20.46	95.10	127.63
			Bottom + Top	20.53	94.78	127.60
			Middle +Top	24.90	97.27	127.59
	Reinforced with GG-III	Single	Bottom	18.62	86.28	124.64
			Middle	22.86	86.28	124.63
			Top	24.93	89.58	124.28
		Double	Bottom + Middle	17.60	81.08	122.77
			Bottom + Top	17.34	81.73	122.86
			Middle +Top	21.52	82.46	122.69

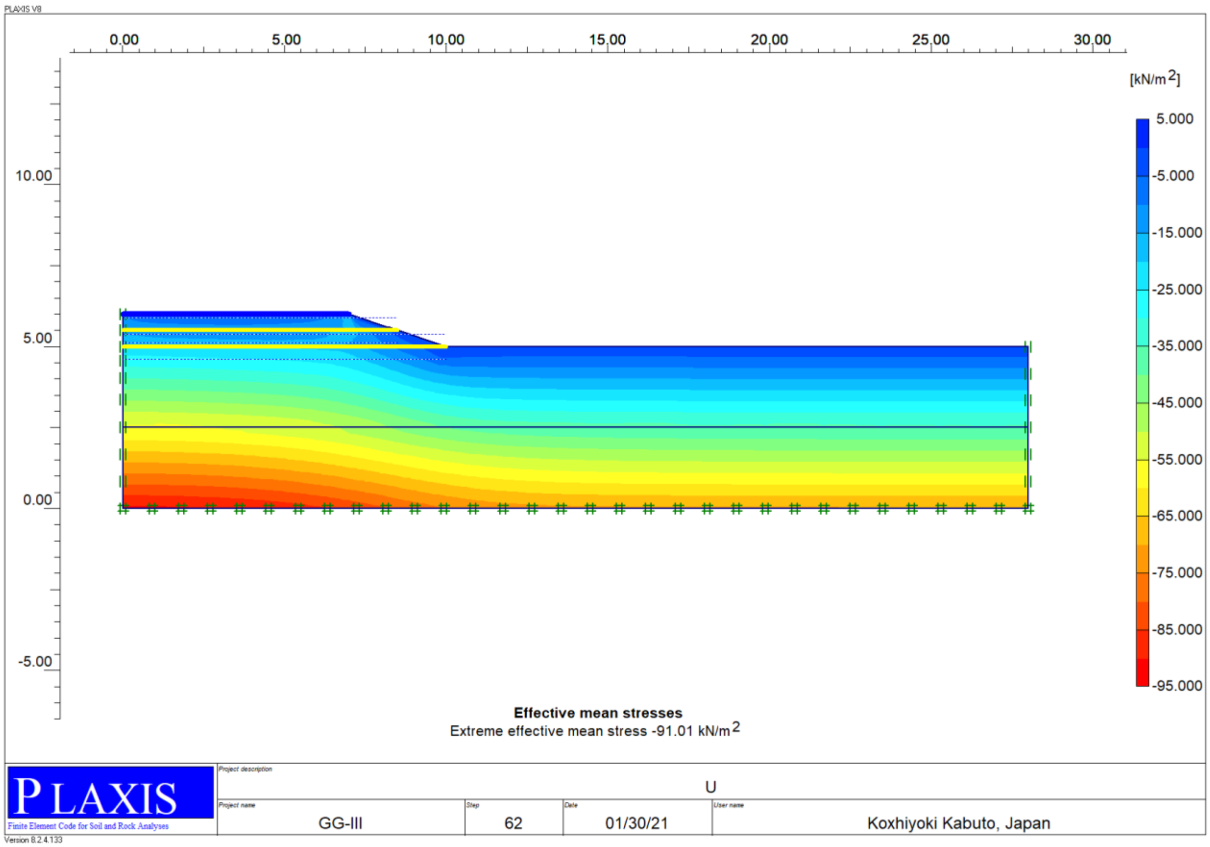

Figure 4. 9: PLAXIS 2D output view (Sample) of effective stress [kN//m^2] of double layer reinforced road embankment at slope of 1:3.

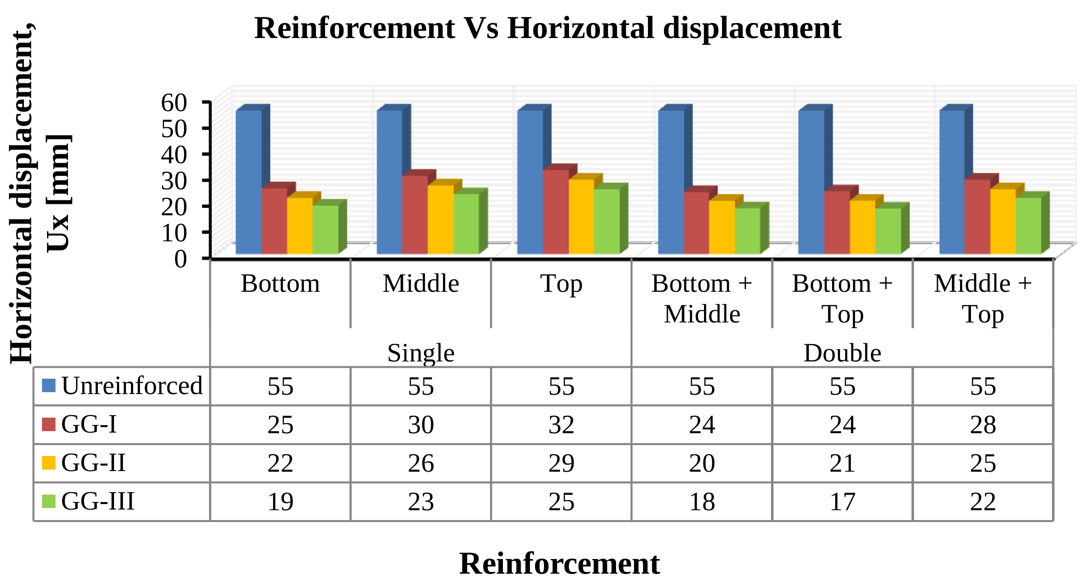

	Bottom (Single)	Middle (Single)	Top (Single)	Bottom + Middle (Double)	Bottom + Top (Double)	Middle + Top (Double)
Unreinforced	55	55	55	55	55	55
GG-I	25	30	32	24	24	28
GG-II	22	26	29	20	21	25
GG-III	19	23	25	18	17	22

Figure 4. 10: PLAXIS 2D output of horizontal displacement [mm] at slope of 1:3

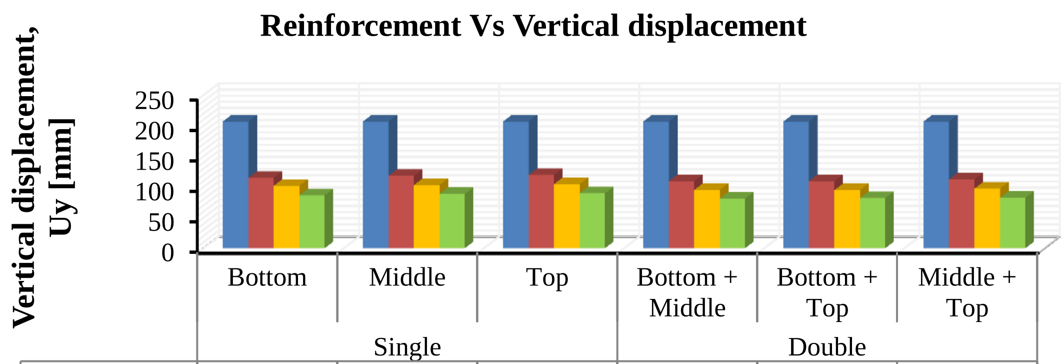

	Bottom	Middle	Top	Bottom + Middle	Bottom + Top	Middle + Top
	Single			Double		
Unreinforced	207	207	207	207	207	207
GG-I	115	118	119	110	109	112
GG-II	102	103	105	95	95	97
GG-III	86	88	90	81	82	82

Reinforcement

Figure 4. 11: PLAXIS 2D output of vertical displacement [mm] at slope of 1:3.

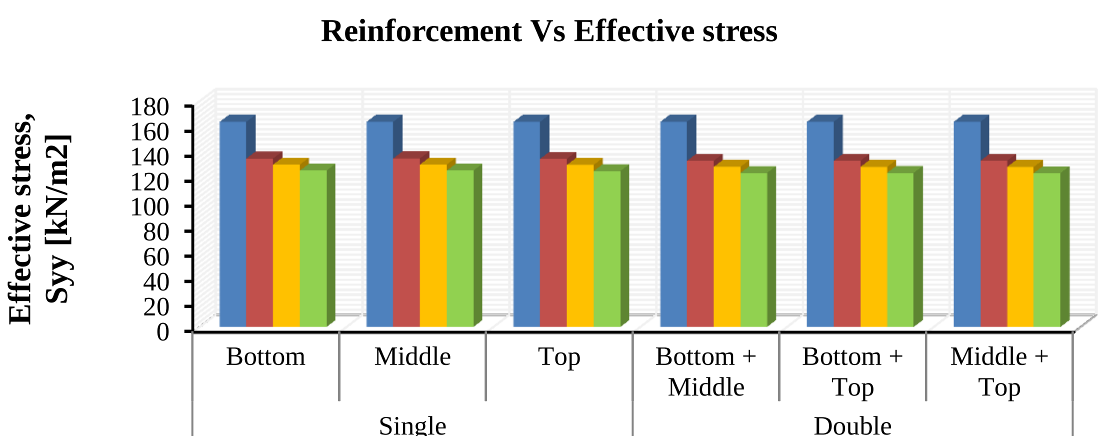

	Bottom	Middle	Top	Bottom + Middle	Bottom + Top	Middle + Top
	Single			Double		
Unreinforced	164	164	164	164	164	164
GG-I	134	134	134	133	132	132
GG-II	129	130	129	128	128	128
GG-III	125	125	124	123	123	123

Reinforcement

Figure 4. 12: PLAXIS 2D output of effective stress [kN/m^2] at slope of 1:3

Figure 4.9, 4.10, 4.11 and 4.12 outlines the sample output view of the model the interpreted result of reinforcement vs extreme horizontal displacement, vertical displacement and effective stress of road embankment laid on soft soil at side slope of 1:3 respectively.

4.3. Parametric study

The key design parameters that might affect the performance of road embankment addressed in this study include: side slope of the embankment, layering position of reinforcement and the type of geogrid used to reinforce the road embankment.

(i) Effect of side slope

The side slope of the embankment determines the lateral stability of the road structure. As dictated in the Figure 4.13 -to- 18, the influence of side slope selected as per ERA 2013 manual to model the road embankment are 1:1.5, 1:2 and 1:3. In this FE modelling the determinants used to present the influence of side slope up on the road embankment performance are vertical settlement, horizontal displacement and effective stress.

a) With respect to horizontal displacement (lateral deformation)

The influence with respect to the horizontal displacement for the single and double-layered reinforcement is shown in Figure 4.13 and 4.14 respectively. In the figure 4.13 and 4.14, the result indicates that the horizontal displacement decreases with the steeper the side slope.

b) With respect to vertical displacement (settlement)

The influence with respect to the vertical displacement for the single and double-layered reinforcement is shown in Figure 4.15 and 4.16 respectively. As dictated in the figure, the result indicates that the vertical displacement decreases with the steeper the side slope.

c) With respect to effective stress

The influence with respect to the effective stress for the single and double-layered reinforcement is shown in Figure 4.17 and 4.18 respectively. As dictated in the figure, the result indicates that the effective stress decreases with the steeper the side slope.

The stability of the slope is an important aspect in embankment construction. The result reflects that the gentle the slope, the reduced the deformation and settlement. From the graph, you imagine that the failure criteria are all reduce frequently when you move from 1:1.5 to 1:2 and gently from 1:2 to 1:3. Based on this result we may decide that from three ERA recommended side slopes the more efficient one to design safe and economic geogrid reinforced road embankment.

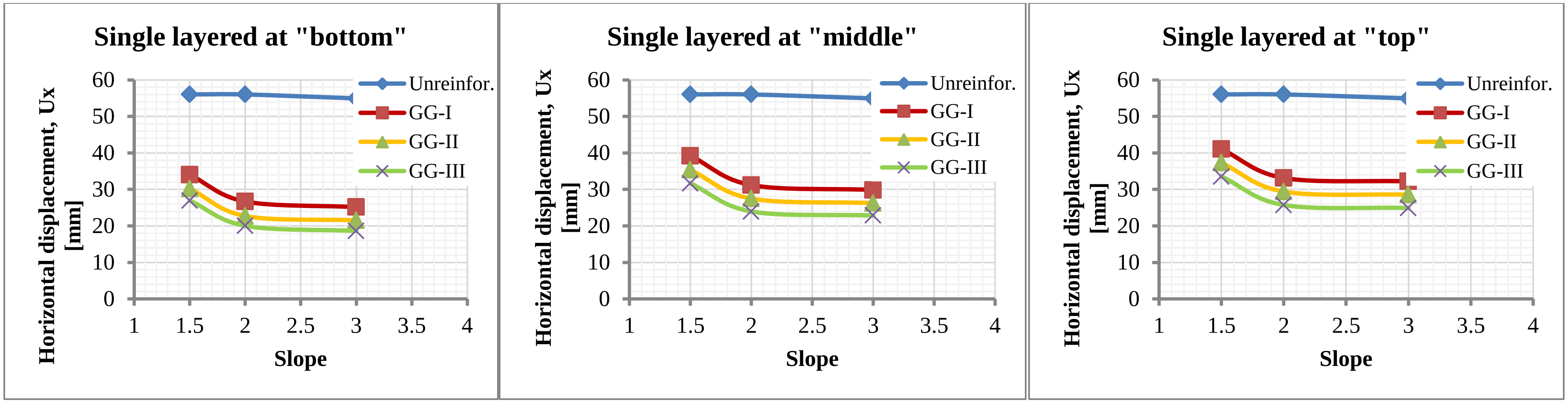

(i) (ii) (iii)

Figure 4. 13: Horizontal displacement Vs Side slope for *single-layered* at (i) “bottom”, (ii) “middle” and (iii) “top” reinforcement

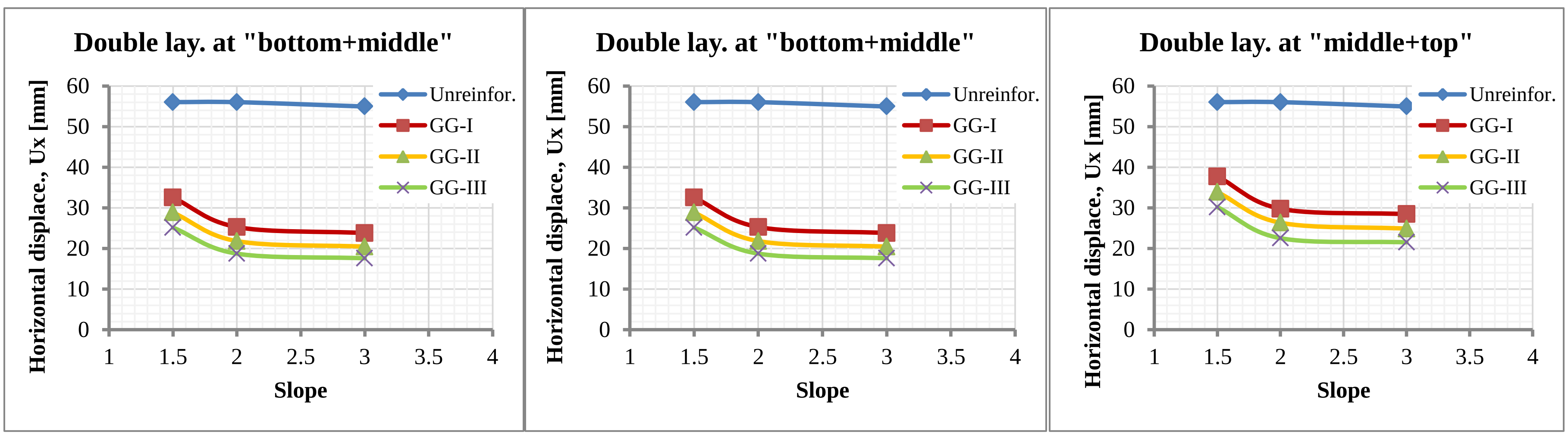

(i) (ii) (iii)

Figure 4. 14: Horizontal displacement Vs Side slope for *double-layered* at (i) “bottom”, (ii) “middle” and (iii) “top” reinforcement

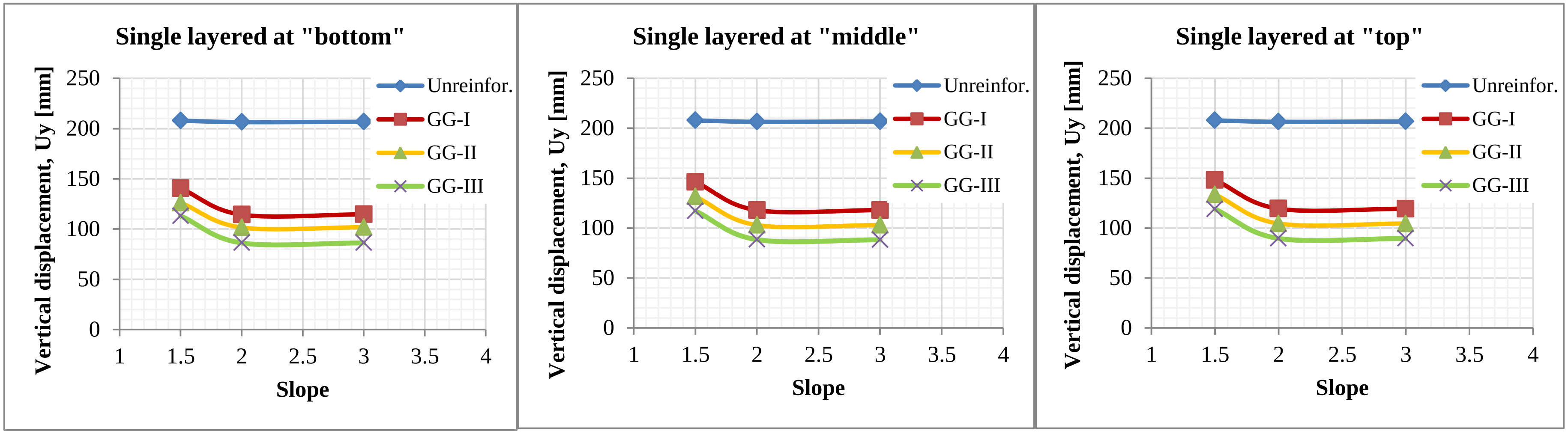

(i) (ii) (iii)

Figure 4. 15: Vertical displacement Vs Side slope for *single-layered* at (i) “bottom”, (ii) “middle” and (iii) “top” reinforcement

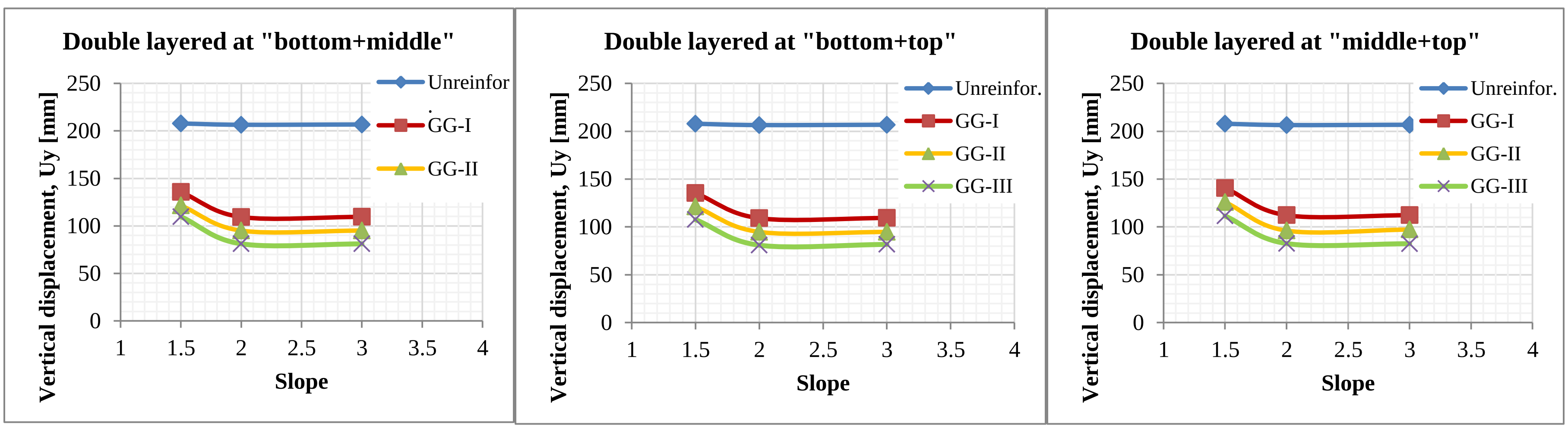

(i) (ii) (iii)

Figure 4. 16: Vertical displacement Vs Side slope for *double-layered* at (i) “bottom”, (ii) “middle” and (iii) “top” reinforcement

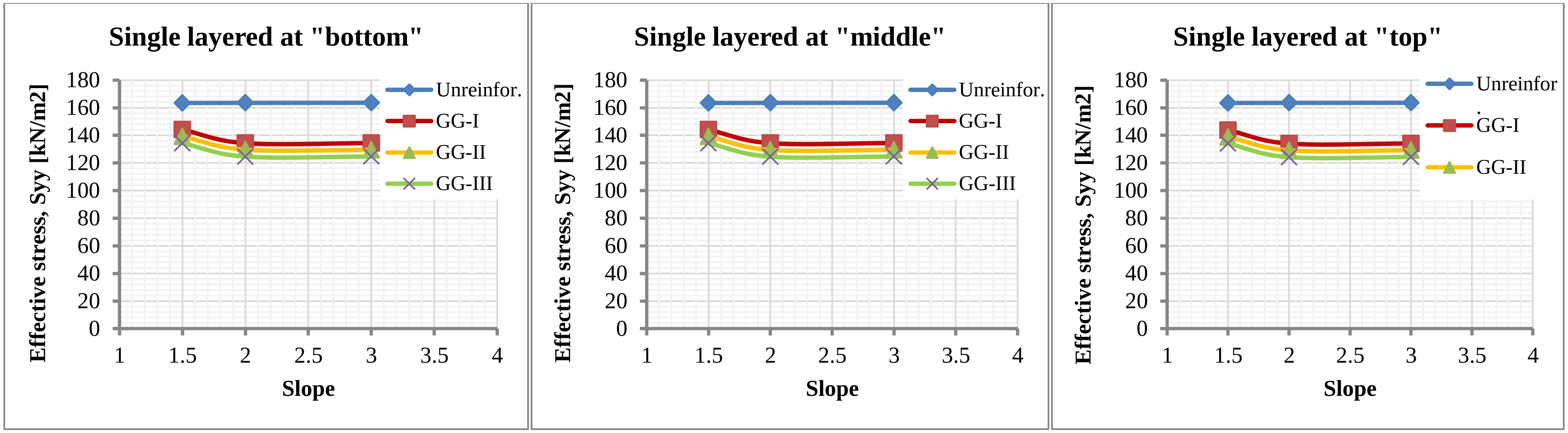

(i) (ii) (iii)

Figure 4. 17: Effective stress Vs Side slope for *single-layered* at (i) “bottom”, (ii) “middle” and (iii) “top” reinforcement

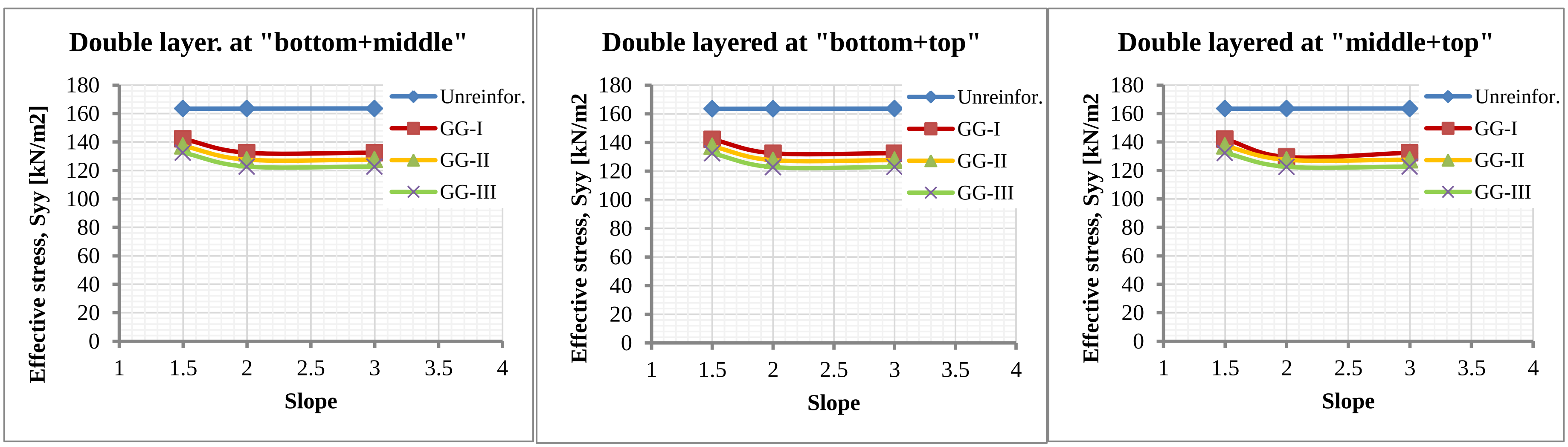

(i) (ii) (iii)

Figure 4. 18: Effective stress Vs Side slope for *double-layered* at (i) “bottom”, (ii) “middle” and (iii) “top” reinforcement

(ii) Effect of location of geogrid material

Considering the influence of geogrid reinforcement position applied in the road embankment was figured out below. In this FE modelling the determinants used to present the effect of layer in which geogrid reinforced up on the road embankment performance are vertical settlement, horizontal displacement ad effective stress.

a) With respect to horizontal displacement

As outlined in the figure below the influence of reinforcing position to model the road embankment are applied at “bottom”, “middle” and “top” of the embankment for the single-layered reinforcement and at “bottom + middle”, “bottom + top” and “middle + top” of the embankment for the double-layered reinforcement. The effect of reinforcing position with respect to the horizontal displacement for the single-layered and double-layered is shown in Figure 4.19.

In the Figure 4.19, the result indicates that the bottom-layered reinforcement may reduce more horizontal displacement than that of middle-layered and top-layered reinforcement.

b) With respect to vertical displacement

The influence of reinforcing position with respect to the vertical displacement for the single and double-layered reinforcement at their respective application layer is shown in Figure 4.20. As illustrated in the figure, the result indicates that the bottom-layered reinforcement may slightly reduce vertical displacement than that of middle-layered and top-layered reinforcement.

c) With respect to effective stress

The influence of reinforcing position with respect to the effective stress for the single and double-layered reinforcement at their respective application layer is shown in Figure 4.21. As dictated in the figure, the result illustrates that the bottom-layered reinforcement may slightly reduce effective than that of middle-layered and top-layered reinforcement.

This reflects that when the geogrid is applied at the bottom of the embankment (i.e. above the soft soil) it may highly influence the performance of road embankment.

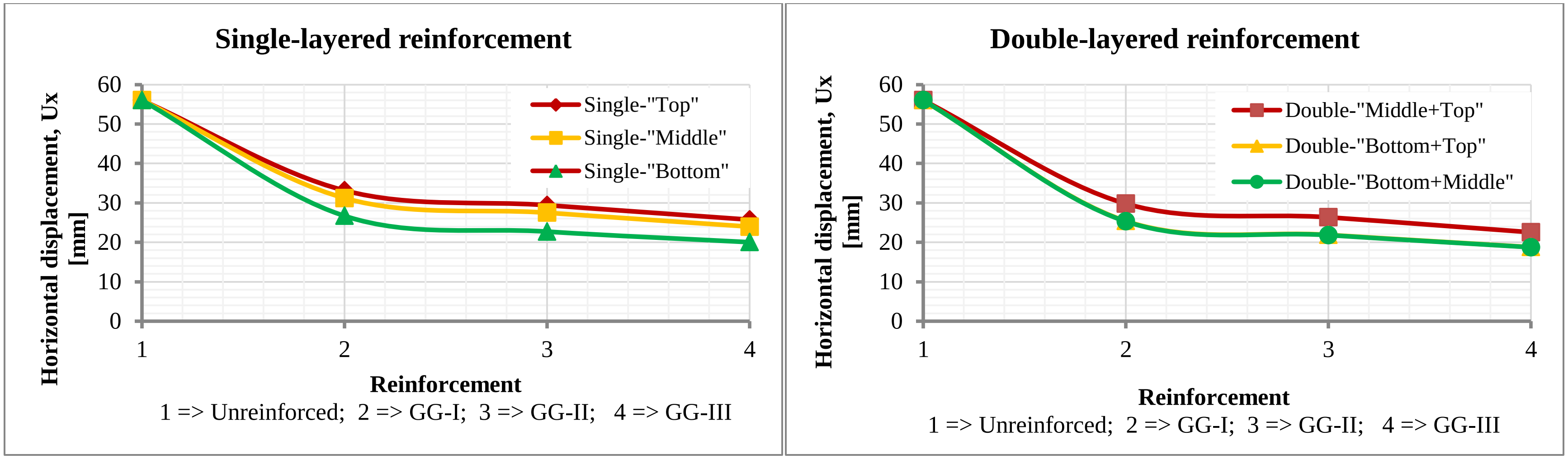

(i) (ii)

Figure 4. 19: Horizontal displacement Vs Reinforcement for *single-layered* and *double-layered* reinforcement

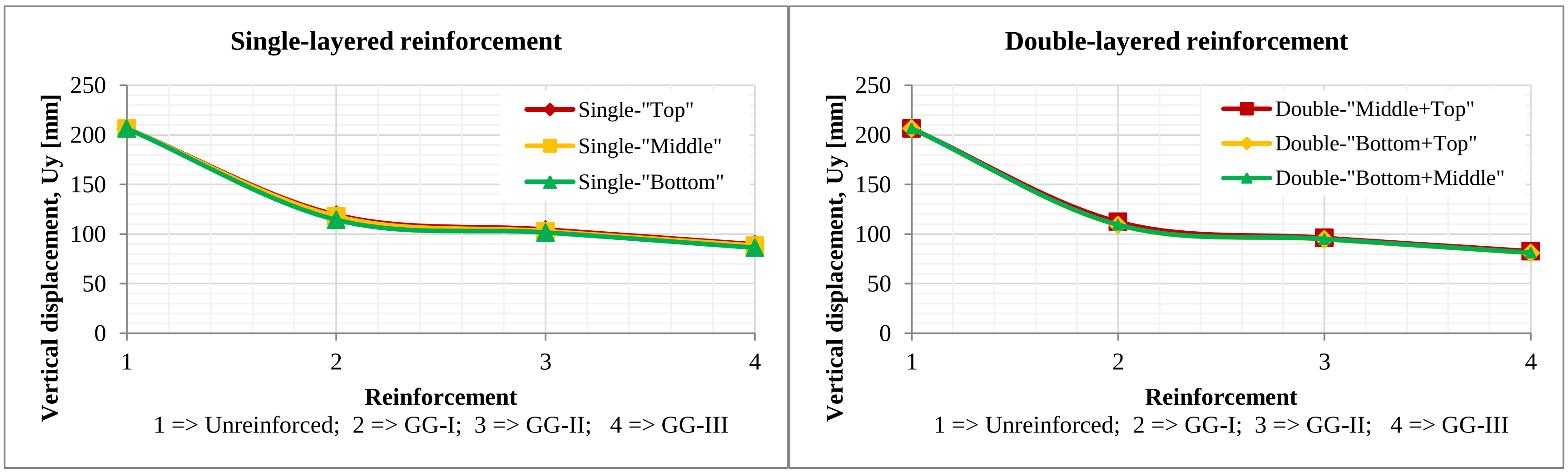

(i) (ii)

Figure 4. 20: Vertical displacement Vs Reinforcement for (i) *single-layered* and (ii) *double-layered* reinforcement

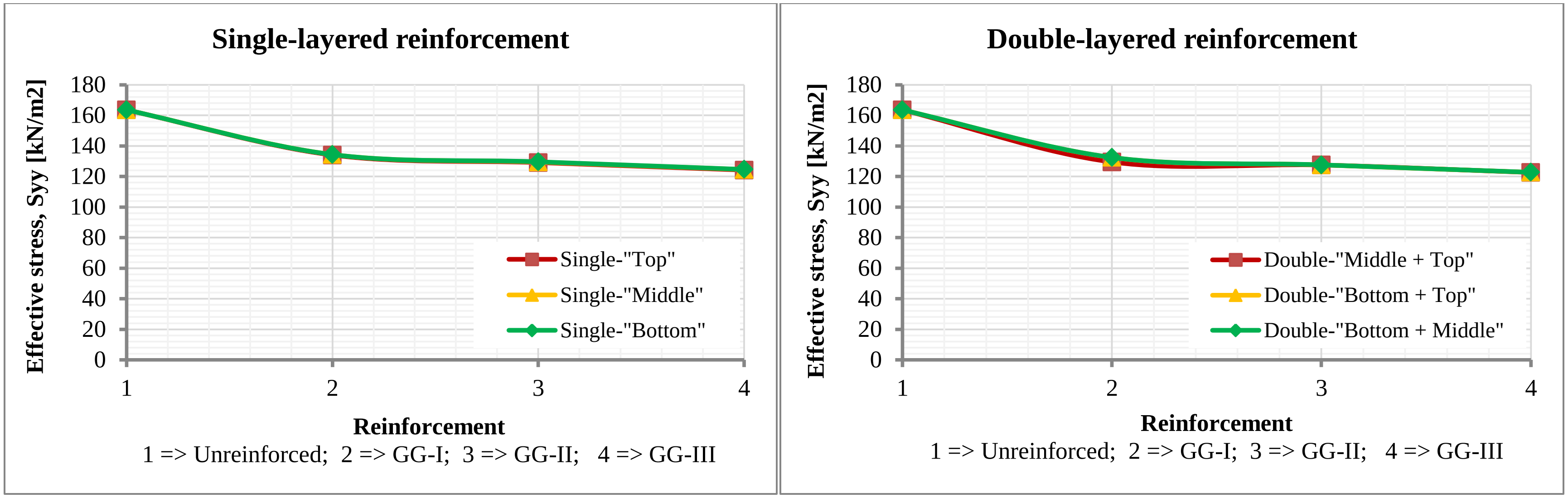

(i) (ii)

Figure 4. 21: Effective stress Vs Reinforcement for (i) *single-layered* and (ii) *double-layered* reinforcement

(iii) Effect of Geogrid Type and Number of Reinforcement Layers

Considering the influence of type of geogrid reinforcement and number of layer applied in the road embankment was figured out below. The types of geogrid used in this study are: type I (GG-I), type II (GG-II) and type III (GG-III). And also the number of reinforcement layer used are: no reinforcement, single layered-reinforcement and double layered reinforcement. In this FE modelling the determinants used to present the effect of layer in which geogrid reinforced up on the road embankment performance are vertical settlement, horizontal displacement ad effective stress.

a) With respect to horizontal displacement

The influence of type of geogrid and number of layer is shown in Figure 4.22(i). In the Figure 4.22 (i), the result indicates that the type III (GG-III) geogrid reinforcement is more convenient than the rest two in reducing lateral strains.

b) With respect to vertical displacement

The influence of reinforcing position with respect to the vertical displacement for the single and double-layered reinforcement at their respective application layer is shown in Figure 4.20. As illustrated in the figure, the result indicates that the bottom-layered reinforcement may slightly reduce vertical displacement than that of middle-layered and top-layered reinforcement.

c) With respect to effective stress

The influence of reinforcing position with respect to the effective stress for the single and double-layered reinforcement at their respective application layer is shown in Figure 4.21. As dictated in the figure, the result illustrates that the effective stress decreases with the increment of side slope.

This reflects that when the geogrid is applied at the bottom of the embankment (i.e. above the soft soil) it may highly influence the performance of road embankment.

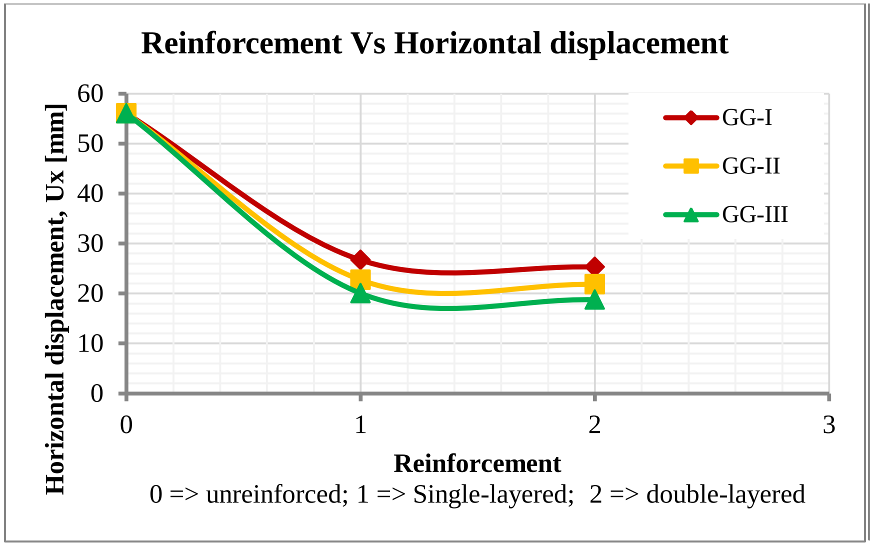

(i)

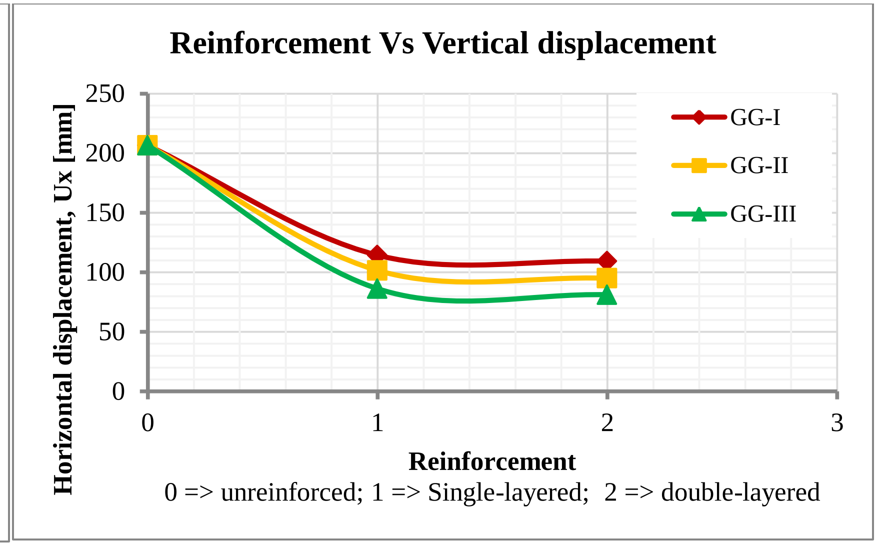

(ii)

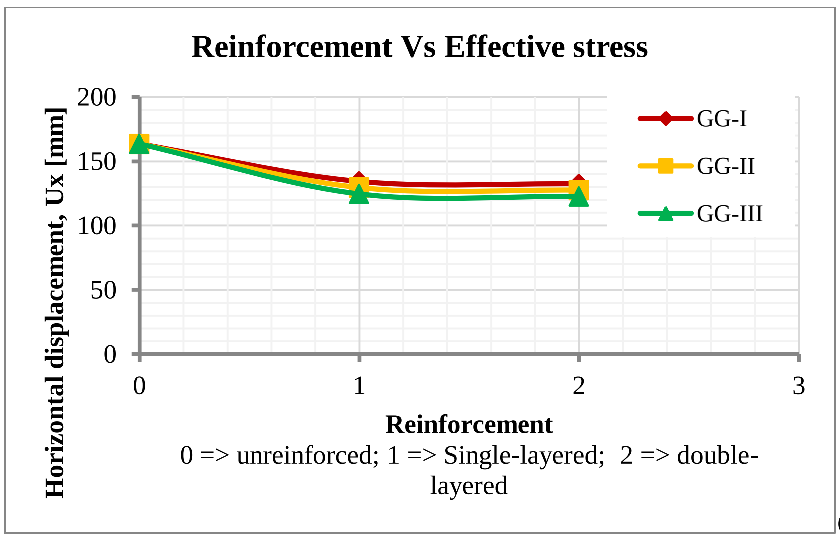

GG-I: - type I geogrid, GG-II: - type II geogrid, GG-III: - type III geogrid

(iii)

Figure 4. 22: Reinforcement Vs (i) *Horizontal displacement*, (ii) *Vertical displacement* and (ii) *Effective stress*

4.4. Validation of Finite Element Analysis

The FEM is a powerful investigative tool which has many advantages over laboratory experiments and large scale field tests. However, the FEM is still an approximate technique which idealises real-life situations into a set of continuum components and adopts constitutive models to simulate soil behavior. As a result, it is necessary to validate the output of the FEM to ensure that the real-life situation is accurately modelled.

In order to verify the suitability of the adopted material models for the soil, geogrids, and geogrid-soil interaction, finite element analyses were first checked against the results from laboratory model tests for geogrid reinforced road embankment on silty clay subgrade soil reported by Chen (2007). The model used in the laboratory were steel plates with dimensions of 150 mm x 150 mm x 25 mm (length x width x height), and the model tests were conducted in a 1.5 m long, 0.9 m wide and 0.9 m deep steel box. The geogrid used has an equivalent thickness of 1mm and an elastic modulus of 3700 kPa. Figures 4.23(i) and 4.24(ii) show the comparison between the finite element analyses and the laboratory model tests for unreinforced and one-layer geogrid reinforced road embankment on silty clay subgrade soil.

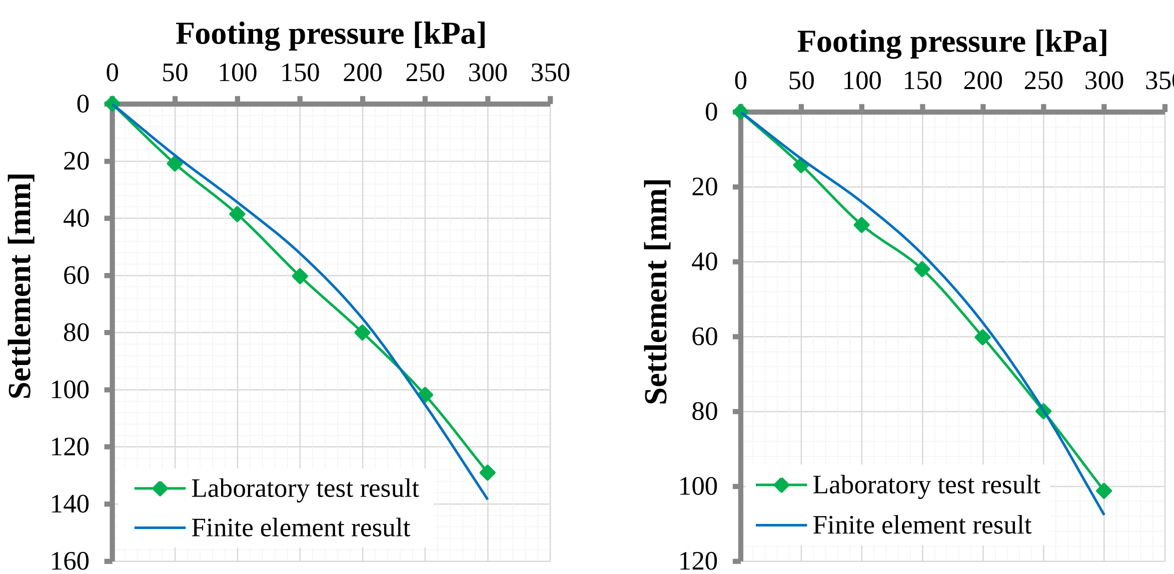

Figure 4. 23: the comparison between the finite element analyses and the laboratory model tests for (i) Unreinforced embankment soil (ii) Geogrid-reinforced embankment soil

As can be seen, the finite element analyses have a reasonable agreement with the results of model tests, although there are some discrepancies between them that are less remarkable near the soil's ultimate bearing pressure. Therefore, the developed finite element model can be used with confidence to perform parametric study to evaluate the effect of different variables and parameters contributing to the performance of reinforced road embankment.

4.5. Discussion

A series of two-dimensional FEA were undertaken to examine the influence of key design parameters upon the performance of geogrid reinforced road embankment. The road embankment simulated in 2D FEA code with different side slope, geogrid layer placement and type of geogrid standard applied with respect to the determinants like lateral deformation (horizontal displacement), settlement (vertical displacement) and effective stress was analysed.

The study mainly focused on the deformation performance of road embankment, as the design of foundations on weak soils usually governed by settlement scenarios rather than bearing capacity criteria due to its high compressibility. Hence, the settlement performance of geogrid reinforced road embankment at working load levels of upmost importance.

Relying on the parametric study the geogrid reinforced road embankment with side slope of 1:2, a single layered type III geogrid placed at the bottom of the embankment is selected and recommended as the most efficient combination of the rest all.

As clearly illustrated before the performance of geogrid reinforced road embankment for efficient combination with respect to lateral deformation is that the horizontal displacement of reinforced embankment was reduced around one-third of unreinforced one (i.e. reduction factor is 36%). It was demonstrated that there is also a significant reduction in settlement when the ground is reinforced with the convenient combination of geogrid reinforcement factors. The vertical displacement of the reinforced embankment was reduced by 42% of untreated one.

Reinforcement under an embankment can be used to reduce vertical and horizontal displacement but in general it is more effective in reducing horizontal displacement. The reduction in displacements obtained is a function of the shear strength and depth of the soft clay layer.

The reinforcement improves the resistance to shear stress and hence improves the stability of the embankment (Sae-Tia et al., 1999). In addition, they may reduce excessive and differential settlement and lateral deformation (Latha et al., 2006).

CHAPTER FIVE

CONCLUSIONS AND RECOMMENDATIONS

5.1. Conclusions

In this study a serious of 10 preliminary checks for sensitivity analyses and 57 subsequent FEA were conducted and the extreme values of horizontal displacement, U_x, vertical displacement, U_y and effective stress, σ_{yy}, of each model was obtained to figure out the non-dimensional parameter so called reduction factor which reflects the extent of performance of geogrid-reinforced embankment with respect to that of unreinforced one.

Based on the results of the numerical modeling analysis of geogrid-reinforced bases in flexible paved road embankment, the following conclusions can be drawn:

- ☞ Relying on the parametric study the geogrid reinforced road embankment with side slope of 1:2, a single layered type III geogrid placed at the bottom of the embankment selected and recommended as the most efficient combination of the rest all.
- ☞ The performance of geogrid reinforced road embankment for efficient combination with respect to lateral deformation is that the horizontal displacement of reinforced embankment was reduced around one-third of unreinforced one (i.e. reduction factor is 36%). Thus, the geogrid reinforcement of base course layer results in reducing the lateral strains within the base course and subgrade layers.
- ☞ The significant reduction in settlement when the ground is reinforced with the convenient combination of geogrid reinforcement factors. The vertical displacement of the reinforced embankment was reduced by 42% of untreated one.
- ☞ Reinforce under an embankment can be used to reduce vertical and horizontal displacement but in general it is more effective in reducing horizontal displacement. The reduction in displacements obtained is a function of the shear strength and depth of the soft clay layer.

5.2. Recommendations

Based on the findings of the present study, it is evident that further research in this field can yield practical and valuable result. Hence, future studies should focus on:

- Using the finite element model for the reinforced road embankment to simulate a full-scale geogrid reinforced approach slab embankment and compare the finite element results with field measurements from monitoring instrumental embankments.
- The effects of some key design parameters have been addressed in detail. But there are still other influential points to be touched especially width ratio effects, variability of material stiffness and strength characteristics, and effect of pavement structures.

REFERENCES

Abramson, L. W., Lee, T. S., Sharma, S., & Boyce, G. M. (2001). *Slope stability and stabilization methods*. John Wiley & Sons

Abu-Farsakh, M., Sharma, R., Chen, Q., & Yoon, S. (2009). Analytical modeling of geogrid reinforced soil foundation. *Geotextiles and Geomembranes*, *27*(1), 63-72.

Al-Qadi, I. L., Dessouky, S. H., Kwon, J., & Tutumluer, E. (2008). Geogrid in flexible pavements: validated mechanism. *Transportation Research Record*, *2045*(1), 102-109.

Ammari, K. ; Clarke, B. (2016). Predicting the Effect of Vibro Stone Column Installation on Performance of Reinforced Foundations. *World Academy of Science, Engineering and Technology, International Science Index 110, International Journal of Civil, Environmental, Structural, Construction and Architectural Engineering*, 0(2), 111 - 117.

Anderson, P., & Killeavy, M. (1989). Geotextiles and Geogrids: cost effective alternate materials for pavement design and construction. In *Geosynthetics, Conference, 1989, San diego, California, USA* (Vol. 2).

Bakhtiar, O. A. (2012). *Performance of embankment on Bamboo-geotextile composite reinforced soft clay* (Doctoral dissertation, Universiti Teknologi Malaysia).

Barksdale, R. D., Brown, S. F., and Chan, F., 1989. "Potential benefits of geosynthetics in flexible pavement systems", *National Cooperative Highway Research Program Report No. 315*, Transportation Research Board, National Research Council, Washington, DC, USA, 56 p.

Bender, D. A., & Barenberg, E. J. (1978). Design and behavior of soil-fabric-aggregate systems. *Transportation Research Record*, (671).

Berg, R. R., Christopher, B.R., and Perkins, S.W. 2000. "Geosynthetic reinforcement of the aggregate base course of flexible pavement structures." GMA White paper II, Geosynthetic material Assoiation, Roseville, MN, USA, 130 p.

Bergado, D. T., & Teerawattanasuk, C. (2008). 2D and 3D numerical simulations of reinforced embankments on soft ground. *Geotextiles and Geomembranes*, *26*(1), 39-55.

Bhattacharyya, S. K. (2009). *Highway embankment design in Bangladesh* (Doctoral dissertation, University of Birmingham).

Cancelli, A., & Montanelli, F. (1999). *In-ground test for geosynthetic reinforced flexible paved roads* (No. Volume 2)

Carter, M., & Bentley, S. P. (2016). *Soil properties and their correlations*. John Wiley & Sons.

Chai, J. C., & Miura, N. (2002). Traffic-load-induced permanent deformation of road on soft subsoil. *Journal of geotechnical and geoenvironmental engineering*, *128*(11), 907-916.

Collin, J. G., Kinney, T. C. and Fu, X., 1996. “Full Scale Highway Load Test of Flexible Pavement Systems with Geogrid Reinforced Base Courses”, *Geosynthetics International*, Vol. 3, No.4, pp. 537-549.

Dafalias, Y. F., & Popov, E. P. (1975). A model of nonlinearly hardening materials for complex loading. *Acta mechanica*, *21*(3), 173-192.

Dondi, G., 1994. “Three-dimensional finite element analysis of a reinforced paved road.” Proceedings of the Fifth International Conference on Geotextiles, Geomembrane and Related Products, Singapore, pp. 95-100.

Good Look, B. (2007). *Hand book of geotechnical investigation and design.* UK, Londo: Taylor and Francis.

Giroud, J. P., & Noiray, L. (1981). Geotextile-reinforced unpaved road design. *Journal of geotechnical and geoenvironmental engineering*, *107*(ASCE 16489).

Gu, J. (2011). Computational modeling of geogrid reinforced soil foundation and geogrid reinforced base in flexible pavement.

Indraratna, B., Lackenby, J., McDowell, G., & Christie, D. (2007). Effect of confining pressure on ballast degradation and deformation under cyclic triaxial loading. *Géotechnique*, *57*(6), 527-536.

Killeen, M. (2012). Numerical modelling of small groups of stone columns. *Phd Thesis, National University of Ireland, Galway*.

Khan, S. A., & Abbas, S. M. (2014). Numerical modelling of highway embankment by different ground improvement techniques. *Int J Innovative Res Adv Eng*, *1*(10), 350-356.

K. Kiran, J.Mohan (2016). A study on ground improvement techniques for pavement construction. *International Journal of Advanced Research in Science and Engineering*. *Vol.5 (10).*

Kumar, S., Puri, V. K., Das, B. M., & Devkota, B. C. (2000). Geotechnical Properties of Fly Ash and Lime- Fly Ash Stabilized Coal Mine Refuse. *Electronic Journal of Geotechnical Engineering*, *5*, 4.

Kwon, J., Kim, M., & Tutumluer, E. (2005). Interface modeling for mechanistic analysis of geogrid reinforced flexible pavements. In *Advances in pavement engineering* (pp. 1-15).

Latha, G. M and Somwanshi, A., 2009. “Bearing capacity of square footings on geosynthetic reinforced sand” Geotextiles and Geomembranes 27, pp. 281–294.

Leng, J. and Gabr, M, 2002. “Characteristics of Geogrid-Reinforced Aggregate under Cyclic Load,”*Journal of Transportation Research Board*, No. 1786, National Research Council, Washington, D.C., pp. 29-35.

Leng, J., Gabr, M. A., 2005, “Numerical Analysis of Stress-deformation Response in Reinforced Unpaved Road Sections”, Geosynthetics International, Vol.12, No.2, pp.111-119.

McVay, M. C. and Taesiri, Y., 1985. “Cyclic Behavior of Pavement Base Materials”, *Journal of Geotechnical Engineering*, Vol. 111, No. 1, pp.1-17.

Miura, N., Sakai, A., Taesiri, Y., Yamanouchi, T. and Yasuhara, K. 1990. “Polymer grid reinforced pavement on soft clay grounds”, *geotextiles and geomembranes*, Vol. 9, No. 1, pp. 99-123.

Molenaar, A. A. A., Houben, L. J. M., & Alemgena, A. A. (2003). Estimation of maximum strains in road bases for pavement performance predictions. In *Maintenance and Rehabilitation of Pavements and Technological ControlInstituto dos Estrados de Portugal, Auto-Estrados de Norte, SA, Galp Engeria, Monte and Monte, SA*.

Nazzal, M. D., Tao, M., Mohammad, L. N., Zhang, Z., & Wu, Z. (2010). Application of shakedown theory in characterizing traditional and recycled pavement base materials. *Journal of Transportation Engineering*, *136*(3), 214-222.

Perkins, S. W., Ismeik, M. and Fogelsong, M. L., 1999. "Influence of Geosynthetic Placement Position on the Performance of Reinforced Flexible Pavement Systems," Proceedings of the Conference Geosynthetics ‘99, Boston, MA, USA, Vol. 1, pp. 253-264.

Perkins, S. W., 1999a. "Mechanical Response of Geosynthetic Reinforced Pavements," *Geosynthetics International, Industrial Fabrics Association International, Roseville, MN.*

Perkins, S. W., 2001. “Mechanistic-empirical modeling and design model development of geosynthetic reinforced flexible pavements”, Montana Department of transportation, Helena, Montana, Report No. FHWA/MT-01-002/99160-1A.

Putri, E. E., Rao, N. S. V. K., & Mannan, M. A. (2012). Evaluation of modulus of elasticity and modulus of subgrade reaction of soils using CBR test. *Journal of Civil Engineering Research*, *2*(1), 34-40.

Qiu, J., Huurman, M., Jacobs, M., Woldekidan, M., & Frunt, M. (2016). Towards sustainable horizontal asphalt recycling. In *Proc., 4th Chinese-European Workshop on Functional Pavement Design, Delft, The Netherlands*.

Sae-Tia, W., Kouda, M., & Kusakabe, O. (1999). Deformation and Stability of Unreinforced and Reinforced Embankment on Soft Clay. *GEOTECHNICAL ENGINEERING*, *30*(2).

Som, N., & Sahu, R. B. (1999). Bearing capacity of a geotextile-reinforced unpaved road as a function of deformation: a model study. *Geosynthetics International*, *6*(1), 1-17.

Stark, T. D., & Eid, H. T. (1997). Slope stability analyses in stiff fissured clays. *Journal of Geotechnical and Geoenvironmental Engineering*, *123*(4), 335-343.

Wathugala, G. W., Huang, B., and Pal, S., 1996. “Numerical simulation of geosynthetic reinforced flexible pavement”, *Transportation Research Record 1534*, Transportation Research Board, national Research Council, Washington, DC, USA, pp.58-65.

APPENDICES

Appendix A: Data Collection and Correlation

A-1. Laboratory test data collected

Table A-1: Laboratory test data collected for subgrade soil

No.	Station	Atterberg limit (AASHTO T89 & 90)		Soil Classification (AASHTO M-145)	Proctor Density (AASHTO T-180)		96 hours Socked CBR Value (AASHTO T-193)	
		LL	PI		O.M.C (%)	Max. Dry Density (kg/m3)	At 2.5mm	Swell (%)
1	0+000	81.5	36.5	A-7-6	27	1451	0.98	12.75
2	0+500	71.5	21.3	A-7-6	24.5	1495	0.98	11.1
3	1+000	43.5	21.0	A-7-6	23.2	1580	2.15	3.27
4	1+500	41.0	19.5	A-7-6	20.5	1640	1.37	5.47
5	2+000	72.8	34.1	A-7-6	28.5	1457	0.88	9.17
6	2+496	58.9	27.7	A-7-6	22	1448	0.88	7.59

Table A-2: Laboratory test data collected for Embankment soil

Atterberg limit (AASHTO T89 & 90)		Soil Classification (AASHTO M-145)	Proctor Density (AASHTO T-180)	
LL	PI		O.M.C (%)	Max. Dry Density (kg/m3)
34.6	7.8	A-7-6	23.2	1668

A-2. Data correlated

Table A - 3: Correlation of basic geotechnical properties for subgrade soil

Depth [m]	Soil type	*w*[%]	ρd [kN/m3]	γd [kN/m3]	γunsat [kN/m3]	γsat [kN/m3]
0 - 2.50	Soft Clay	28.5	1457	14.3	18.4	18.4
2.50 - 5.00	Stiff Clay	23.2	1580	15.5	19.1	19.1

Table A - 4: Correlation of strength characteristics for Subgrade soil

Depth [m]	Soil type	LL	PI	ϕ'	c'
0 - 2.50	Soft Clay	72.8	34.05	18	13
2.50 - 5.00	Stiff Clay	43.5	21.00	22	17

Table A - 5: Correlation of basic stiffness characteristics for Subgrade soil

Depth [m]	Soil type	c'min	c'max	c'	Emin	Emax	E'	E_l
0 - 2.50	Soft Clay	10	20	13	2,000	7,000	3,620	1,000
2.50 - 5.00	Stiff Clay	10	20	17	2,000	7,000	5,590	2,000

Table A - 6: Correlation of basic geotechnical properties for Embankment soil

Material type	Soil type	*w*[%]	ρd [kN/m3]	γd [kN/m3]	γ [kN/m3]	γsat [kN/m3]
Drained	Sand	23.2	1668	16.4	20.2	20.2

Table A - 7: Correlation of strength characteristics for Embankment soil

Station	Soil type	LL	PI	ϕ'	ϕ'min	ϕ'max	c'min	c'max	c'
Drained	Sand	34.6	7.81	34	15	25	10	20	1

Table A - 8: Correlation of Stiffness characteristics for Embankment soil

Material type	Soil type	CBR [%]	ν	E'	E_l
Drained	Granular	12.71	0.3	10,680	4,000

Table A - 11: Geogrid material properties (Jie Gu, 2011)

Geogrid type	**Reference Name**	**Elastic Modulus [kPa]**	**Area [m]**	**EA [kN]**
Geogrid Type I	GGI	585,100	0.06	35,000
Geogrid Type II	GGIII	860,000	0.06	52,000
Geogrid Type III	GGV	950,000	0.06	57,000

Appendix B: PLAXIS 2D Foundation Input

B-1. Subgrade and Embankment material input parameters

Table B - 1: Summary of subgrade and embankment materials

Soil Parameter	Subgrade		Embankment	Unit
	Layer - I	Layer - II		
Material model	MC	MC	MC	-
Depth	0.00 - 2.50	2.50 - 5.00	-	(m)
Type of material behaviour	Undarined	Undarined	Drained	-
Bulk unit weight (ɣ)	18.4	19.1	20.2	kN/m3
Saturated unit weight (ɣsat)	18.4	19.1	20.2	kN/m3
Over-consolidation ratio	1	1	1	-
Poisson’s ratio (***v***)	0.35	0.35	0.3	-
Young's modulus (E)	1000	2000	4000	kN/m2
Cohesion (Cref)	13	17	1	kN/m2
Friction angle (Φ’)	18	22	34	º
Dilatancy angle (Ψ)	0	0	4	º
Lateral earth coefficient K0	0.69	0.63	0.44	-

B-2. AC Pavement material input parameters

Table B - 2: Pavement material properties

Pavement Properties	Asphalt Concrete	unit
EA	1.29E+06	kN/m
EI	1.07E+05	kNm2/m
W	2.2	kN
V	0.15	-

B-3. Geogrid input parameters

Table B - 3: Geogrid material properties (Jie Gu, 2011)

Geogrid type	Reference Name	Elastic Modulus [kPa]	Area [m]	EA [kN]
Geogrid Type I	GGI	585,100	0.06	35,000
Geogrid Type II	GGIII	860,000	0.06	52,000
Geogrid Type III	GGV	950,000	0.06	57,000

Appendix C: PLAXIS 2D Foundation Output

C-1. The results of FEA of a road embankment at slope of 1:1.5

Table C - 1: The results of FEA of a road embankment at slope of 1:1.5.

Slope V:H	Reinforcement	Reinforcement Layer		Parametric results		
		Layer	at	Horizontal displacement [mm]	Vertical displacement [mm]	Effective mean stress [kN/m^2]
1:1.5	Unreinforced	-	-	56.03	207.79	163.46
	Reinforced with GG-I	Single	Bottom	34.03	140.48	144.09
			Middle	39.24	146.28	144.07
			Top	41.05	148.15	143.79
		Double	Bottom + Middle	32.53	135.66	142.20
			Bottom + Top	32.67	135.38	142.17
			Middle +Top	37.75	140.69	142.13
	Reinforced with GG-II	Single	Bottom	30.26	126.27	139.20
			Middle	35.38	131.54	139.16
			Top	37.30	133.61	138.88
		Double	Bottom + Middle	28.85	121.53	137.30
			Bottom + Top	28.93	121.21	137.29
			Middle +Top	33.89	125.94	137.22
	Reinforced with GG-III	Single	Bottom	26.96	113.07	134.32
			Middle	31.67	117.13	134.27
			Top	33.55	118.99	133.96
		Double	Bottom + Middle	25.15	109.70	132.54
			Bottom + Top	25.64	107.65	132.35
			Middle +Top	30.19	111.46	132.33

C-2. The results of FEA of a road embankment at slope of 1:2

Table C - 2: The results of FEA of a road embankment at slope of 1:2.

Slope V:H	Reinforcement	Reinforcement Layer		Parametric results		
		Layer	at	Horizontal displacement [mm]	Vertical displacement [mm]	Effective mean stress [kN/m^2]
1:2	Unreinforced	-	-	56.02	206.44	163.52
	Reinforced with GG-I	Single	Bottom	26.70	114.36	134.34
			Middle	31.21	117.92	134.34
			Top	33.14	119.41	134.03
		Double	Bottom + Middle	25.29	109.39	132.46
			Bottom + Top	25.40	109.12	132.43
			Middle +Top	29.79	112.25	129.47
	Reinforced with GG-II	Single	Bottom	22.72	101.60	129.60
			Middle	27.50	102.99	129.44
			Top	29.41	104.56	129.11
		Double	Bottom + Middle	21.83	95.04	127.59
			Bottom + Top	21.90	94.78	127.56
			Middle +Top	26.35	96.14	127.50
	Reinforced with GG-III	Single	Bottom	20.03	86.24	124.61
			Middle	23.97	88.43	124.54
			Top	25.73	89.62	124.19
		Double	Bottom + Middle	18.74	81.17	122.73
			Bottom + Top	18.78	80.94	122.71
			Middle +Top	22.54	82.68	122.60

C-3. The results of FEA of a road embankment at slope of 1:3

Table C - 3: The results of FEA of a road embankment at slope of 1:3.

Slope V:H	Reinforcement	Reinforcement Layer		Parametric results		
		Layer	at	Horizontal displacement [mm]	Vertical displacement [mm]	Effective mean stress [kN/m^2]
1:3	Unreinforced	-	-	54.95	206.76	163.60
	Reinforced with GG-I	Single	Bottom	25.17	114.66	134.38
			Middle	29.88	117.99	134.44
			Top	32.22	119.38	134.11
		Double	Bottom + Middle	23.82	109.53	132.51
			Bottom + Top	23.94	109.38	132.47
			Middle +Top	28.47	112.29	132.49
	Reinforced with GG-II	Single	Bottom	21.54	101.84	129.47
			Middle	26.27	102.98	129.53
			Top	28.56	104.55	129.20
		Double	Bottom + Middle	20.46	95.10	127.63
			Bottom + Top	20.53	94.78	127.60
			Middle +Top	24.90	97.27	127.59
	Reinforced with GG-III	Single	Bottom	18.62	86.28	124.64
			Middle	22.86	86.28	124.63
			Top	24.93	89.58	124.28
		Double	Bottom + Middle	17.60	81.08	122.77
			Bottom + Top	17.34	81.73	122.86
			Middle +Top	21.52	82.46	122.69